INVESTIGATION OF ION EXCHANGE RESINS:

UNDERSTANDING FOULING MECHANISMS AND

DEVELOPMENT OF NOVEL APPLICATIONS

By

SATISH I. KURIYAVAR

Bachelor of Science in Chemistry
University of Mumbai
Mumbai, INDIA
1995

Master of Science in Analytical Chemistry
University of Pune
Pune, INDIA
1997

Submitted to the Faculty of the
Graduate College of the
Oklahoma State University
in partial fulfillment of
the requirements for
the Degree of
DOCTOR OF PHILOSOPHY
July, 2006

INVESTIGATION OF ION EXCHANGE RESINS:

UNDERSTANDING FOULING MECHANISMS AND

DEVELOPMENT OF NOVEL APPLICATIONS

Dissertation Approved:

Dr. Allen Apblett

Dr. Nicholas Materer

Dr. LeGrande Slaughter

Dr. Gary L. Foutch

Dr. A. Gordon Emslie
Dean of the Graduate College

ACKNOWLEDGEMENTS

I wish to express my sincere appreciation and gratitude to my thesis advisor, Dr. Allen Apblett for his supervision, constructive guidance, inspiration and patience during the entire course of this research. My sincere appreciation extends to my other committee members Dr. Nicholas Materer, Dr. Gary Foutch and Dr. LeGrande Slaughter, whose guidance, assistance and support has been very valuable to me during this investigation. I would like to thank Dr. Iob and Dr. Berlin for their support and encouragement and valuable discussions. I would like to thank Dr. Warren Ford for his suggestions, discussions and financial aid for attending National ACS Meetings through Oklahoma Nanonet. I would like to express my gratitude to Terry Colberg and Phoebe Doss for their assistance with SEM ad TEM images.

I would like to express my sincere gratitude to all my members of Apblett Research Group and my colleagues at Chemistry Department for their suggestions, encouragement and support during this study. I would like to thank Dr. B.P.Kiran who has helped me tremendously at professional and personal levels.

I would also like to give my special thanks to my mother, my sisters, brother and all my family members for their strong encouragement at times of difficulty, unconditional love and understanding throughout the whole period. I wish to thank Vladimira Sykova for her help and encouragement at various levels during this work.

I would like to acknowledge the Chemistry Department and Oklahoma EPSCoR for financial support during this research study.

TABLE OF CONTENTS

III. SYNTHESIS OF NANOMETRIC AGGREGATES OF IRON, ZINC, NICKEL, AND ALUMINUM OXIDE FROM ION EXCHANGE RESINS

IV. SPHERICAL AGGREGATES OF NANOPARTICULATE IRON AND ZINC OXIDE FOR ARSENIC REMEDIATION

LIST OF TABLES

Table **Page**

LIST OF SCHEMES

Scheme **Page**

LIST OF FIGURES

CHAPTER I

INTRODUCTION

Ion exchange process is one of the oldest phenomenons, which has been mentioned as early as in the times of Aristotle. However, its description in modern scientific terminology has been attributed to soil scientists H.S. Thompson and J.T. Way in the mid-nineteenth century. Since then, ion exchange process has been studied and its application in various fields has grown by leaps and bounds. The utilization of ion exchange technology by wide range of industries has grown rapidly since its introduction in the early 20th century [1]. Numerous applications of this technology include: water treatment [2], reagents purification [3], purification of cane, maize, and sugars in sugar industry [4], biological recovery including purification [5], solvent purification [6], catalysis [7], pharmaceuticals [8], and heavy metal ion remediation [9]. Ion exchange resins play a pivotal role in water treatment plants throughout the globe. With the development of new technologies in fabrication, and environmental and health concerns, the requirement for cleaner and purer water/solvents has gained the highest priority.

An ion exchange reaction can be defined as the reversible exchange of ions between a solid phase and a solution phase wherein the ion exchanger is insoluble in the solution medium. It can be represented as shown in Figure 1.1.

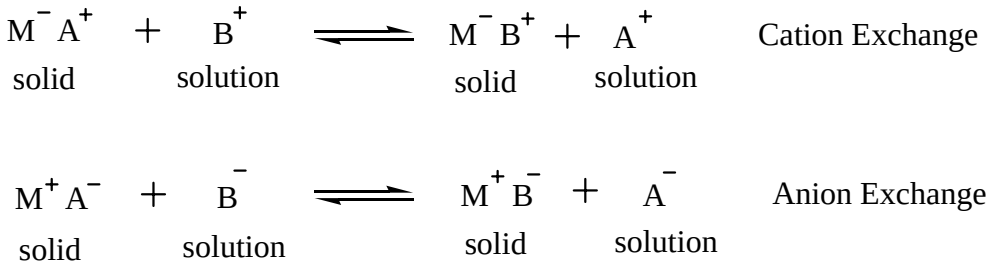

Figure 1.1: Ion exchange process

The main fact in this process is that charge neutrality is preserved at all times in both phases by exchanging counter ions in equivalent amounts. The ion exchange capacity of an ion exchanger is a measure of its total content of exchangeable ions, which can be expressed in terms of micro moles per gram or micro moles per liter of the exchangeable ions. There has been lot of development in terms of synthesis of ion exchange materials. The fundamental requirements for such materials are:

a) An inert host structure allowing diffusion of hydrated ions in a hydrophilic matrix
b) The host structure must carry a fixed ionic charge
c) Controlled and effective ion exchange capacity
d) Physical stability in terms of mechanical strength and resistance to attrition.

The synthesis of ion exchange resins is focused at obtaining a material that is three-dimensional, cross-linked matrix of hydrocarbon chains containing fixed ionic groups. Monomeric organic electrolytes have been polymerized in order to form cross-linked network. Also, non ionic monomers have been used to synthesize cross-linked matrix, in which the fixed ionic groups are then introduced. A variation to this method is to introduce ionic groups while the polymerization is still in progress. The resin should be

insoluble, but able to swell to a certain extent. Highly cross linked polymers can not swell properly. Therefore, the polymerization must be carried out in such a way that appropriate amount of cross links are formed.

In 1935, Adams and Holmes recognized the ion exchange properties of a cation exchanger formed by the condensation product of phenol and formaldehyde. Although this material was an extremely weak cation exchanger, it led to the synthesis of the first high performance ion exchange resins. They solved the problem by choosing anionic and cationic groups with higher acid and base strengths. Today cation exchangers with fixed ionic groups of different acid strengths are synthesized. The most commonly used strong acid resins are made with stronger sulfonic acid groups ($-SO_3H$) and weak acid resins with carboxylic acid groups (-COOH). Most of the present ion exchange resins are addition copolymers prepared from vinyl monomers. These polymers have a higher chemical and thermal stability as compared to the condensation polymers. This method has an added advantage that the degree of cross-linking, and particle size of the resins are more readily adjusted. The most important resins of this type are cross-linked polystyrenes which have been treated with sulfuric acid or chlorosulfonic acid in order to incorporate sulfonic acid groups. [10,11,12,13] Divinylbenzene is used as a cross-linking agent. The reaction is shown below in figure 1.2.

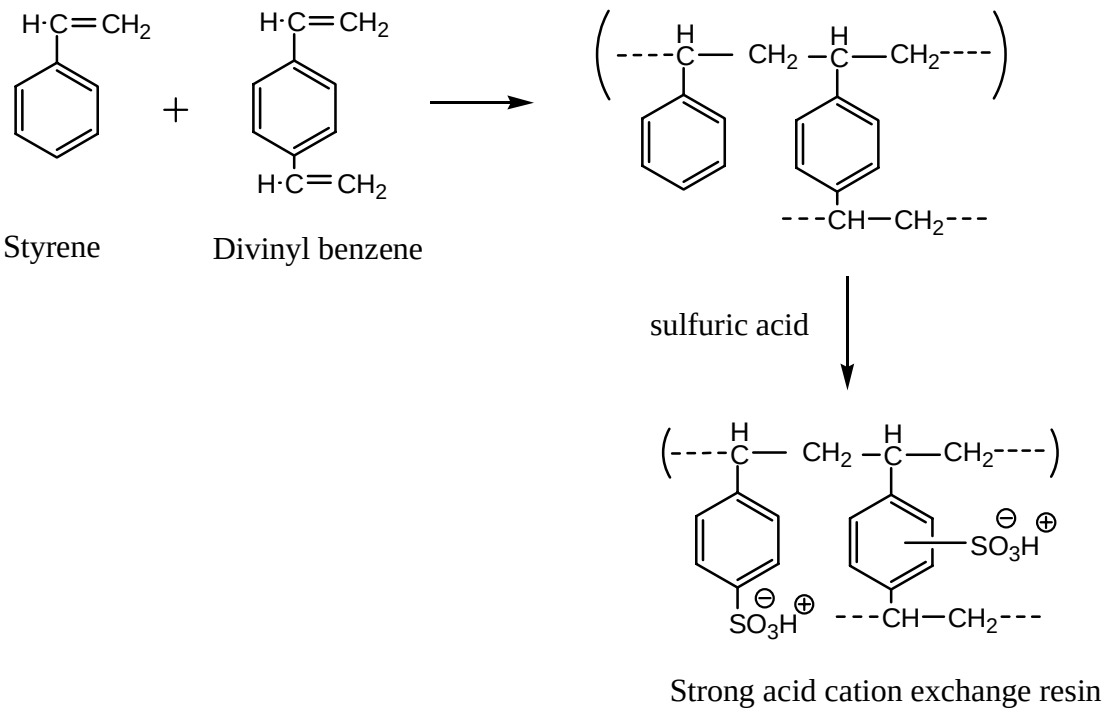

Figure 1.2: Synthesis of strong cation exchange resin

Instead of pure divinylbenzene, mixture of different divinylbenzene isomers (40-55%) and ethylstyrene (45-60%) is used in the industries. Therefore, ethylstyrene is also incorporated into the resin matrix to certain extent. The degree of cross-linking is adjusted by varying the amount of divinylbenzene content. Generally, cation exchange resins prepared by this method contain 8-12 % of divinylbenzene. Resins with lower divinylbenzene content swell strongly and are soft and gelatinous, whereas resins with high divinylbenzene content cannot swell and are tough and mechanically more stable.

The copolymer beads are using Pearl Polymerization technique.[14,15] The monomers without the inhibitors are mixed along with a polymerization catalyst such as benzoyl peroxide. It is also possible to use partially polymerized monomer instead of pure monomer. The mixture is then added to thoroughly agitated aqueous solution kept at

85-100°C. The mixture forms small suspended droplets. This suspension is stabilized by the addition of stabilizers such as gelatin, polyvinyl alcohol, sodium oleate, sodium methacrylate, magnesium silicate, etc. This will help in preventing the agglomeration of the droplets in the solution. The size of the droplet can be manipulated by varying the type of stabilizers used, the viscosity, and the agitation. The polymer obtained is in the form of fairly uniform spherical shiny beads. Their size can be varied between 1 μm to 2 mm without major difficulties.

The sulfonation process is relatively simple and easy if proper precautions are taken. Sulfonation progresses from outer shells toward the center of the particles and is accompanied by considerable swelling and heat generation due the exothermic nature of the reaction. During the process, some of the beads might crack due to the strain exerted on the resin matrix. This is avoided by allowing the beads to swell prior to sulfonation in solvents such as toluene, nitrobenzene, methylene chloride or trichloroethane.[12,13] Sulfonation process results in practically complete mono-sulfonation of all benzene rings including those of the divinylbenzene and ethylstyrene components depending upon the reaction time. However, double substitution does not occur under the above mentioned conditions. This was proved by chemical analyses, which showed that the sulfonation process stops when on the average one group is introduced per benzene ring.[11] Sulfonation is not the only way of introducing fixed ionic groups into cross-linked polystyrene. Polystyrene cation exchangers have also been prepared using phosphonic, phosphinic, and arsenic acid groups.

Anion exchangers were also covered in the patents by Adam and Holmes, which contained weak base amino groups such as $–NH_3^+$ and $R_2NH_2^+$.[13] Later on, anion

exchange resins with strong-base quaternary ammonium groups were prepared with $N^{+}(CH_3)_3$ etc. In the beginning ion exchange resins were condensation polymers, which were replaced by more stable addition polymers. However, the strong base anion exchange resins cannot compete with cation exchange resins with respect to their chemical and thermal stability, and resin life. The first anion exchange resins were prepared by condensation process from aromatic amines such as m-phenylenediamine with formaldehyde. [13] Condensation polymers suffered from the fact that the cross-linking and base strength are dependant on each other since the amino groups take part in the condensation process. However, in case of the addition polymers the degree of cross-linking can be adjusted in a relatively simple and reproducible way without affecting the base strength of the ionic groups. Most of the important anion exchange resins are made from cross-linked styrene by pearl polymerization technique as explained earlier. Also, variety of styrene derivatives have been used along with different cross-linking agents.[13] The synthesis of anion exchange resin is shown in Figure 1.3. The basic group can be introduced in the polymer matrix by different methods. Generally, anion exchange resins are prepared by chloromethylation of polystyrene beads, which are then treated with ammonia or primary, secondary, or tertiary alkyl amines.

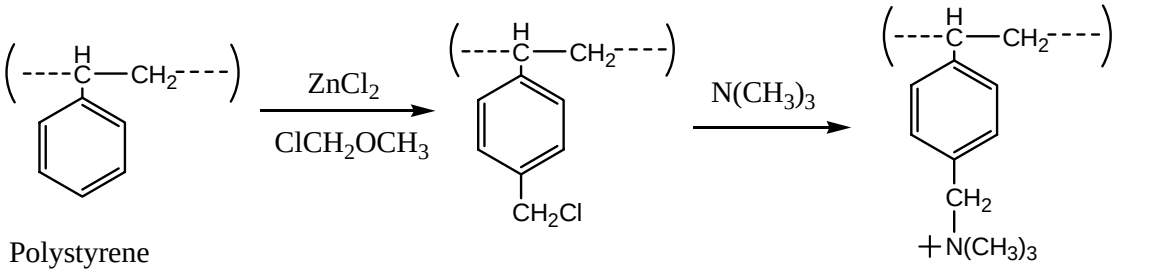

Figure 1.3: Synthesis of strong base anion exchange resin

The reaction with a tertiary amine yields a strong base anion exchange resin containing quaternary ammonium groups. In order to obtain uniform degree of chloromethylation and cross-linking, the beads are swollen in chloromethylether before the reaction is initiated by the addition of the catalyst.[13,16] If failed to do so, it will result in higher degree of substitution in the outer shell as compared to the center of the bead. The anion exchange capacity of the resin can be adjusted to certain extent by altering the reaction time and thereby changing the degree of chloromethylation. The quaternization of chloromethylated resins using tertiary alkyl amines is relatively simple and takes place quantitatively. Any alkyl amine can be used for this process, however, bulky amines are avoided due to hindrances, which prohibit their movement inside the cross-linked resin beads. The reaction with an amine in the aqueous phase is facilitated by swelling the resin beads in dioxane, which acts as a swelling agent. One of the important aspects for this research is that relatively monodisperse spherical particles are prepared as mentioned above.

One major application of particular interest to this study is condensate polishing at nuclear power plants. The basic design of a nuclear power plant is shown in Figure 1.4. The main idea is to use the heat generated by nuclear fission in the reactor nuclear fuel to heat the primary coolant circulated in the closed primary circuit. High pressure is used to keep the primary coolant in the liquid state at very high temperatures. In the secondary circuit (or water-steam circuit) steam is generated, which is used to rotate the turbines. The primary and secondary circuits are separated from each other by steam generators in order to keep secondary circuit and the turbines free of any radioactivity.

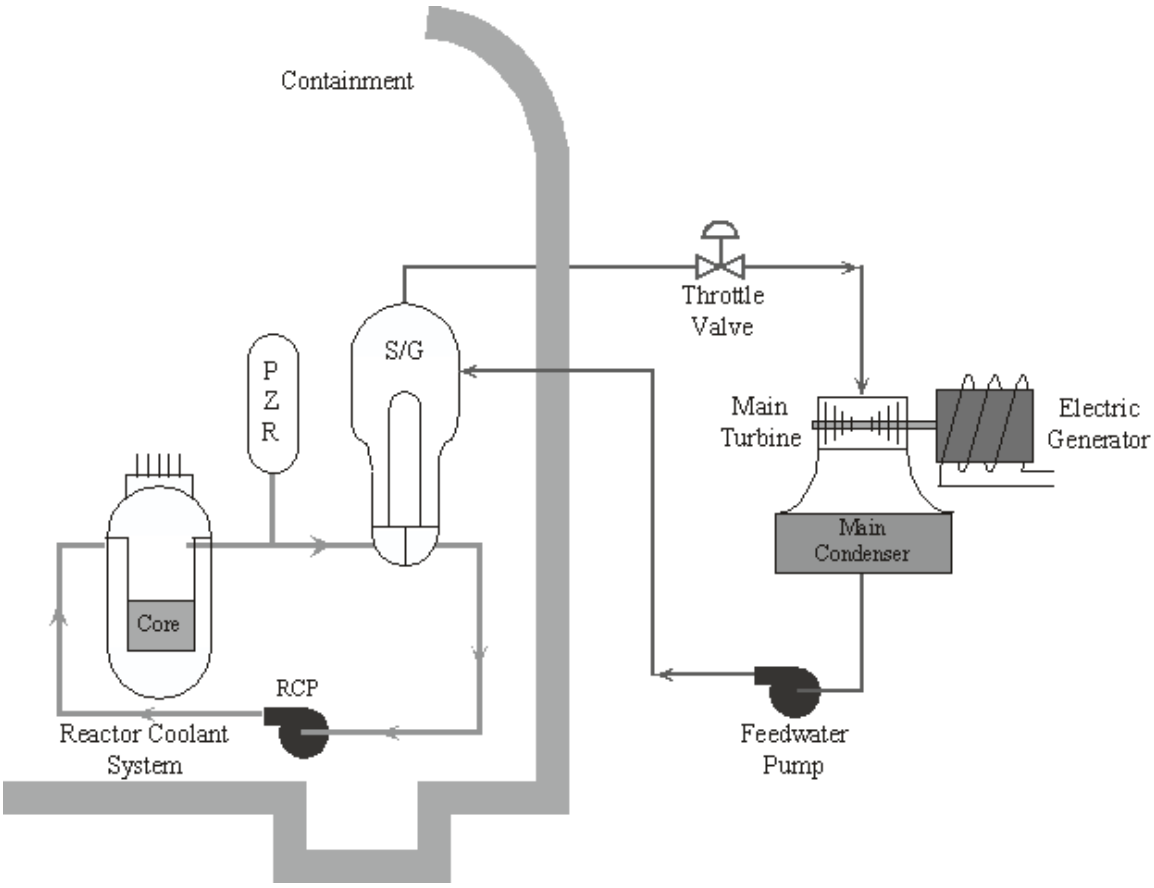

Figure 1.4: Pressurized water reactor scheme [17]

Ultra pure water is used in the secondary circuit to generate saturated steam for use in the steam plant. This high level of water purity is essential in order to prevent corrosion and deposition of inorganic contaminants on the steam generator tubing. This is due to the fact that there is a high rate of evaporation occurring in the steam generators and that can induce concentration of impurities and cause the risk of corrosion. Improving operating efficiency and maximizing the component life without having to replace equipment parts is highly essential. Most of the cases of power plant shutdowns are due to impurities and other problems directly related to corrosion and cost a plant millions of dollars. The high purity and insignificant amount of ions present in ultrapure water causes it to quickly

dissolve even trace amounts of contaminants and atmospheric gases, especially CO_2, which ionizes in the water to form carbonic acid. This gives the ultrapure water some acidity, which is inherently responsible for corrosion problems. These problems often force unscheduled and extended outages for maintenance, repairs works, loss of power, and revenue losses due to downtime of the plant. This makes it very important for an increased understanding of properties of ultrapure water and water chemistry of the pressurized water reactors to avoid any tragedies.

A very high purity of water can be achieved by using condensate polishing, which is an ion exchange process used to remove traces of ionic impurities present in water by passing it through series of cation and anion exchange resin columns along with mixed bed resin columns. The use of regenerated mixed bed demineralizers for condensate polishing dates back to early 1950's. Apart from the capital investment for a power plant, the operating cost of the plant is an essential factor in determining its feasibility of power generation. The cost of resin replacement at a rate of 20% per year would be almost 35-40% of the total annual operating cost of the plant. This does not include additional losses incurred due to downtime of the plant[18]. The condensate polishing process must deal with impurities that arise inside the steam system, leaks, and corrosion[19]. Apart from all these economic factors, one more major issue, which comes with any nuclear power plant is accidents and their effects on environment and mankind. Accidents such as Three Mile Island, Middletown, PA and Chernobyl, Ukraine are grim reminders of the risks involved with these power plants. The main concerns would be the risk of release of radioactive materials into the atmosphere, meltdown of the nuclear core, and risk of cancer and birth defects in exposed people. However, the cost of evacuation and

radioactive waste clean-up can be a big hurdle in itself. The accident at Chernobyl was the direct result of design flaws in the power plant's cooling system, which might have caused the uncontrollable power surge that led to the destruction. According to the Ukrainian Ministry of Health, more than 3 million people are registered as direct victims of Chernobyl. Since the accident, more than 330,000 people have been relocated away from the radiation contaminated sites. However, the magnitude of the accident is evident from the clean up cost that reached hundreds of billions of dollars over two decades. The government of Belarus has already spent a total of $13 billion on Chernobyl from 1991 to 2003. It has estimated the losses over 30 years at $235 billion[20].

The worst commercial nuclear accident on the US soil occurred at the Three Mile Island reactor in Middletown, PA in 1979. The initial investigations reported equipment failure compounded by human mistakes that led to a loss of coolant and partial core meltdown. The plant was built at a cost of $700 million and had been on-line for just 90 days. More than one hundred thousands living near the plant had to be evacuated during this crisis. The accident spewed radioactive gases and water into the atmosphere[21]. In order to defuel the facility, $1 billion was spent almost immediately. Three months of nuclear power production at Three Mile Island has cost close to $2 billion in construction and cleanup bills. [22] The evidence shows that the trouble started somewhere in the condensate polisher system. Due to some unknown reasons the polisher outlet valves were forced to close. This demonstrates the importance of smallest error around condensate polishing system cannot be taken lightly. Thus, the problems encountered with the condensate system and condenser vacuum played a key role in the whole incident, which exponentially arose within a short period of time[23]. Keeping such

mishaps in mind, the US nuclear capacity is projected to decline from 9.1 GW in 1994 to between 61.4 and 76.0 GW by the end of 2015[21].

These accidents prove that it is absolutely essential that the corrosion problem be taken seriously and combated at all costs. This also puts pressure on the condensate polishing process itself since it is the backbone of the processes for keeping the impurities and corrosion products at bay. It is a proven fact that hydronium ions are the main cause in accelerating corrosion process especially at elevated temperature and pressure conditions. The root of the problem in ultrapure water is dissolved $CO_{2,}$ which leads to the formation of dissociated carbonic acid in small quantities making the water acidic. To prevent the water from becoming acidic, pH control agents are usually added to the water. Numerous compounds have been used but most have failed for one reason or the other. Ethanolamine is commonly used today but it causes serious problems with the ion exchange resin performance. This investigation sought to determine how ethanolamine fouls ion exchange resins and to identify an alternate amine that would perform well in nuclear power plants.

Beyond nuclear power plants another important application of ion exchange resins is waste water and drinking water purification. The use of metal loaded ion exchange resins to prepare spherical aggregates of nanometric metal oxides was explored. The intention was to use the excellent monodispersity and morphology of the ion exchange resin beads to generate ceramic replicas with perfect size and shape for water treatment. Such materials would be expected to be useful in a variety of catalytic and remediation operations. This investigation focused on their use for removal of arsenic from water.

One more objective of the proposed research was to develop magnetic ion exchange beads that could be used to accelerate the water purification process. That is to create materials that could be dispersed in water and rapidly removed by magnetic filtration after toxic metals had been adsorbed. Such materials would also be amenable to remote manipulation by magnetic field in instances where human exposure must be avoided, e.g. for radioactive metal separation. Two applications were explored, removal of uranium from drinking water and dyes from waste water. Uranium is a common contaminant in ground water and is damaging to people because of its chemical toxicity, particularly to kidneys. Treatment of effluent from the textile industry is a challenging issue. The severity of the problem arises due to the presence of variety of dyes in water that can undergo chemical and biological changes, deprive plants and aquatic species of their valuable oxygen and thereby damaging the ecological system. Dyes and their degradation products can also be toxic and carcinogenic. Therefore, their discharge into environment is highly undesirable and there are various technologies developed in order to adsorb them from the waste systems [24, 25,26,27,28,29,30,31]. Activated charcoal and other high surface area inorganic spheres have been tested and utilized so far. Magnetic nanometric spheres could be used for this problem making the removal of dyes efficient and rapid.

References

1. Greig, J.A. *Ion exchange at the millennium.* Imperial College Press: London, UK, 2000.
2. McGarvey, F.X.; Fisher, S.A. *Desalination* **1986**, *59*, 403-24.
3. Gorshkov, V.; Muraviev, D.; Warshawsky, A. *Solvent Extr. Ion Exch.* **1998**, *16*, 1-73.
4. Madsen, R. F.; Nielsen, W. K.; Winstrom-Olsen, B. *Sugar J.* **1978**, *41*, 15-19.
5. Gonzalez, M. I.; Alvarez, S.; Riera, F.A.; Alvarez, R. *Ind. Eng. Chem. Res.* **2006**, 45, 3243-3247.
6. Anon. *IP.com Journal* **2003**, *3*, 13.
7. Yadav, G.D.; Lande, S.V. *Org. Process Res. Dev.* **2005**, *9*, 288-293.
8. Abdekhodaie, M. J.; Wu, X.Y. *Biomaterials* **2006**, *27*, 3652-3662.
9. Vilensky, M.Y.; Berkowitz, B.; Warshawsky, A. *Environ. Sci. Technol.* **2002**, *36*, 1851-1855.
10. Abrams, I. M. *Ind. Eng. Chem.* **1956**, *48*, 1469-1972.
11. Pepper, K.W. *J. Appl. Chem.* **1951**, *1*, 124-132.
12. Wheaton, R.M.; Harrington, D.F. *Ind. Eng. Chem.* **1952**, *44*, 1796-1800.
13. Helfferich, F. *Ion exchange.* Dover Publications: New York, 1995.
14. Hohenstein, W.P.; Mark, H. *J. Polymer Sci.* **1946**, *1*, 127-145.
15. Winslow, F. H., Matreyek, W. *Ind. Eng. Chem.* **1951**, *43*, 1108-1112.
16. Pepper, K.W.; Paisley, H.M.; Young, M.A. *J. Chem. Soc.* **1953**, 4097-4105.
17. U.S. Nuclear Regulatory Commission. Pressurized water reactor. http://www.nrc.gov/reactors/pwrs.html.

18. Salem, E.; LaTerra, T. *Ultrapure water* **2000**, *17*, 30-35.

19. Anon. *Power* **1993**, *137*, 77-82.

20. Green Facts. Scientific facts on the Chernobyl nuclear accident. http://www.greenfacts.org/chernobyl/index.htm.

21. Notable nuclear accidents.http://core.ecu.edu/soci/juskaa/soci3222/nuclear.htm.

22. Gateway Ukraine.www.brama.com.

23. Earths. Sabotage at Three Mile Island? http://www.earths.net/oct23-oct29_01.htm.

24. Mak, S-Y.; Chen, D-H. *Dyes Pigm.* **2004**, *61*, 93-98.

25. Ruthven, D.M. *Principles of adsorption and adsorption processes;* John Wiley & Sons: New York, NY, 1984.

26. McKay, G. *Use of adsorbents for the removal of pollutants from wasterwaters;* CRC Press: Boca Raton, FL, 1995.

27. Kannan, N.; Sundaram, M.M. *Dyes Pigm.* **2001**, *51*, 25-40.

28. Yu, Y.; Zhuang, Y.Y.; Wang, Z.H. *J. Colloid Interface Sci.* **2001**, *242*, 288-93.

29. Hirata, M.; Kawasaki, N.; Nakamura, T.; Matsumoto, K.; Kabayama, M.; Tamura, T.; Tanada, S. *J Colloid Interface Sci.* **2002**, *254*, 17-22.

30. Ghosh, D.; Bhattacharyya, K.G. *Appl. Clay Sci.* **2002**, *20*, 295-300.

31. Lee, C.K.; Low, K.S.; Chung, L.C. *J Chem. Tech. Biotechnol.* **1997**, *69*, 93-99.

CHAPTER II

INVESTIGATION INTO ION EXCHANGE RESIN FOULING MECHANISM

Introduction

Originally trisodium phosphate was used in the secondary cycle of pressurized water reactors as an anti-scaling agent as early as the late 1970's. This was, however, discarded after the phosphate was identified as the source of wastage attack on the steam generator tubings. By the early 1980's, most plants had already started the use of volatile amines to control corrosion throughout the steam cycle by maintaining an adequately alkaline pH. Their treatments consisted of ammonia for pH control and hydrazine for oxygen removal. The understanding at that time was to reduce the solubility of iron by maintaining pH at or above 9 in the absence of any oxygen[1]. Since then, there has been a lot of effort put into finding an ideal compound or amine, which would fit the requirements. The most fundamental selection criteria for an amine are: its ability to combat corrosion by being a strong base, low volatility with a good water-steam partition coefficient close to 1, and thermal decomposition yielding only non-harmful products. The volatility of the amines determines their distribution pattern in the secondary system. Highly volatile amines will stay in the steam phase as opposed to the water phase. This results in very little protection for wet steam areas, which are highly prone to

flow-accelerated corrosion. An amine with low relative volatility will tend to distribute with the water phase. More of the amine is carried into the wet steam phase, which results in higher pH and better protection in these areas. However, amines with low relative volatilities will result in a lower pH in the condensate and low-temperature feed water sections. This brings us to the fact that some of the plants have started approaching mixed amine treatment wherein addition of a small quantity of ammonia or another amine is used to increase the condensate pH [2]. Apart from these primary requirements, there are other economic aspects such as low cost, availability, concentration required for achieving the desired pH, and rate of consumption/thermal decomposition in deoxygenated water at higher operating temperatures. Last but not least, the amine's safety and environmental impact issues are also of importance. Safety deals with storage, handling, and transportation issues. Environmentally, the parent amine and its decomposition products should not be toxic or carcinogenic. Optimally, the amine is a commonly used one that has extensive physical and chemical data coming from long-term studies and experience. In general, all of the amines that are used for secondary system pH control are essentially weak bases. Their dissociation constant K_b is highly temperature dependent. The most commonly used amines are ethanolamine, morpholine, and ammonia. In the beginning, ammonia proved to be most widely used pH control agent but became less popular due to its high volatility. There are several other amines, which can be categorized as advanced or alternative amines that were considered for the replacement of ammonia [3].

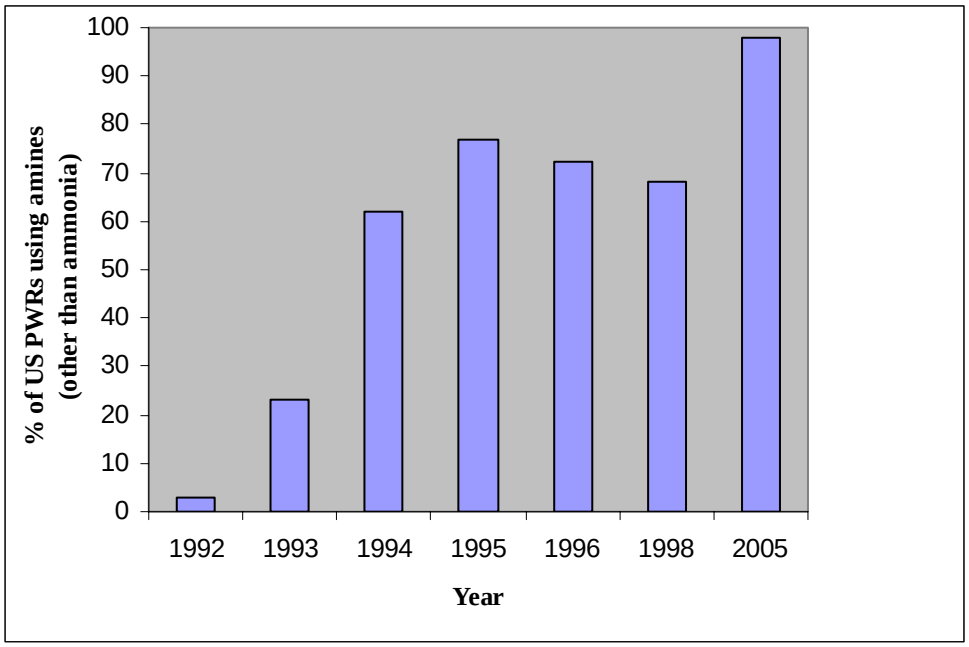

Figure 2-1: Usage of advanced amines in US pressurized water reactors (PWR's) [4]

An increase in the use of advanced amines in US pressurized water reactors is shown in Figure 2-1. According to a survey, their use has increased drastically in the recent years, which is indicated by the fact that more than 90% of the pressurized water reactors in the US have turned to advanced amines. All the way up to the mid 1980's, ammonia was the most widely used pH control agent. It has numerous advantages, such as ease of implementation, well known characteristics, experience in handling, absence of harmful decomposition products, low cost, and ease of its availability in bulk. However, ammonia suffered from one main problem, which was its partitioning between water-steam at higher temperatures. Ammonia also displays a marked decrease in its basicity at the elevated temperatures in the steam cycle. These factors reduced its effectiveness for arresting corrosion at elevated temperatures. There was also a problem of ammonia corrosion and formation of soluble copper-ammonia complexes if the pH is

above 9.2. It also required frequent regeneration of condensate polishers. This has led to a serious accident, which occurred due to corrosion of a pipe in the Surry US plant in 1986. Therefore, ammonia use as a pH control agent was restricted to only plants without copper alloys and without condensate polishers in continuous operation.

After ammonia, the next choice was morpholine. It has been satisfactorily used in pressurized water reactors in the US, France, and several other countries since 1984. The changes in dissociation constant versus temperature were less pronounced as compared to ammonia. This means the alkalinity decrease when temperature increases is less in the case of morpholine than it is for ammonia. Also, mopholine's distribution coefficient between steam and water is close to 1 giving a constant concentration over all of the steam-water system. This was not possible with ammonia due to its very high volatility. That made it difficult to keep the concentration of ammonia in liquid drains at a sufficiently high level. However, morpholine also suffered from several disadvantages over the long run. The molar concentration required to achieve alkaline pH values was higher than it was for ammonia. This led to an increase in organic compounds in the condensate. The decomposition of morpholine at elevated temperatures generated species such as organic acids, acetates, and formates. The decomposition steps of morpholine are hydrolysis followed by oxidation. These produced organic ions in the secondary loop in pressurized water reactors. Interestingly, laboratory studies and operating experience did not reveal any direct relationship between corrosion effects and the organic acids observed in the pressurized water reactors. However, their presence even in low concentrations interfered with the conductivity measurements, a key on-line monitoring technique for secondary system overall contamination [2].

Ethanolamine was first used in a full scale test at the Catawba1 Nuclear Station in early 1992 [5]. At least 17 US pressurized water reactors had switched to ethanolamine and 30 more plants were in the process of implementing the change by 1994. One of the main advantages of ethanolamine is the lower molar concentration needed, as compared to morpholine, to get the target pH at operating temperature. Another important issue with ethanolamine is its higher thermal stability, which induces a lower concentration of organic acids especially when compared with morpholine. Overall lower operating cost, increased length of run of condensate polishers, reduced frequency of resin regeneration, and lower amounts of nitrogen compounds being released into the atmosphere are some of the advantages of switching to ethanolamine. As shown in the Figure 2-2, more than 90% of the pressurized water reactors in the US had switched to this amine by the end of 2005.

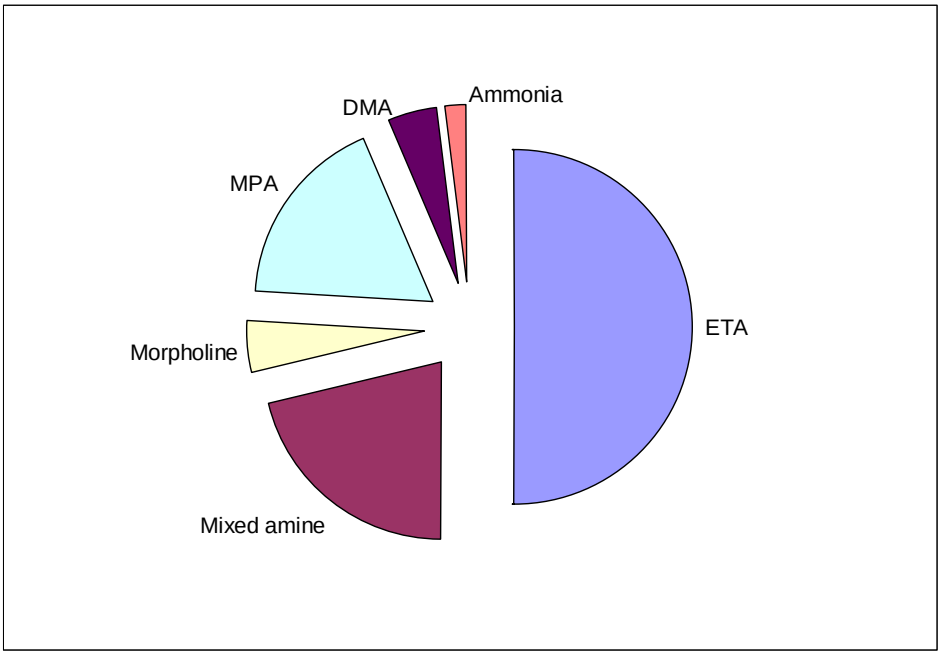

Figure 2-2: Distribution of amines used in US pressurized water reactors in 2005 [4]
(ETA=ethanolamine, MPA=3-methoxypropylamine, DMA=dimethylamine)

Theoretically, cation and anion exchange resins are capable of remaining in service for up to 20 years and 4 years, respectively [6]. Organic materials are the most common fouling agents found in industry. Generally, anion exchange resins are more sensitive to fouling and lose their service life along with their regeneration capabilities. Fouling of the resins causes lower quality of treated water and increased frequency of regeneration, along with concomitant downtime of the condensate polishers. Capacity loss of anion exchange resin has been linked to a variety of organic compounds, the most common of which are humic and fulvic acids, and inorganic compounds, such as silica [7]. The effectiveness of regeneration of a resin is commonly determined by measure of the Mass Transfer Coefficient. This is based on the kinetics of the ion exchange process at very low concentration. Loss of Mass Transfer Coefficient essentially implies resin fouling and loss of regeneration capacity. The resin may need to be replaced depending upon the severity of the problem.

When using ethanolamine, some plants began noticing increased sulfur levels in their steam generators. The origin of the sulfate was eventually traced to polisher resins. This was attributed to the residual sulfates remaining from the sulfuric acid regeneration of the anion resins as well as desulfonation of the cation exchange resin, which has sulfonate functional groups [8]. Also, the anion exchange resin must not be performing properly since even the slightest amount of sulfate release should have been taken care by anion exchange resins. The high purity requirement of the water makes it absolutely essential that even the tiniest amount of ionic leakage from resin be avoided. The regeneration processes employ sodium hydroxide and sulfuric acid and even with thorough rinsing there is a small quantity of ions left on the resins. This is generally taken

care of by using proper mixed resin beds. Both, cation and anion exchange resins must work properly in order to deliver high purity water. In the mid 1990's, higher sulfate levels were observed in several pressurized water reactors in the US. This was correlated with a quantifiable loss in Mass Transfer Coefficient values of anion exchange resins. All the affected plants were using ethanolamine as their pH control agent so it was hypothesized to damage the anion resins capacity to exchange sulfate ion. Fouled resins showed a tendency towards sulfate leakage. [9]

Clearly, the nuclear power industry has a pressing need for a pH control agent that is highly effective for corrosion protection and is compatible with the condensate polishing system. In order to find such a material, it is imperative to understand the injurious interaction of ethanolamine with the ion exchange resins and the fouling mechanism. Therefore, the main objectives of this research study were to:

1. Investigate the hypothesized fouling mechanism of ion exchange resins
2. Determine the effect of fouling on resin performance
3. Gain better understanding of the structural interaction of ethanolamine with the resin
4. Investigate structurally similar alternative amines and find a suitable candidate to replace ethanolamine in pressurized water reactors.

In order to study the fouling mechanisms under conditions similar to that used in the plants, two approaches were investigated. The first method utilized mixed bed resin columns at fixed temperature in order to mimic nuclear power plant conditions. In the

second, pH control agents were treated with resins in a closed environment, which comprised the batch test experimentation.

Experimental

The resins used were: Dowex 650H-form cation resin and Dowex 550 OH-form anion resin obtained from Aldrich chemicals, and Amberjet anion and cation resins obtained from Rohm and Haas (all resins were used as obtained). Ethanolamine, 2-methoxyethylamine, 2-methylaminoethanol, 2-dimethylaminoethanol, and 5-aminopentanol were purchased from Aldrich chemicals and were used without any further purification. Chemical analysis was done after extraction of organics from resin samples using HPLC-grade methylene chloride from Acros Organics.

Column Experiments:

Column experimentation provided a direct method to observe and test the hypothesis that contaminants/degradation products that may be migrating from cationic to anionic resins. The column methodology utilized a set up that allowed such transport of species from cationic to anionic resins. The schematic of the experimental set up is shown in Figure 2-3. This part of the investigation was carried out in Dr. Foutch's lab by Dr. Jaehyun Lee in the Department of Chemical Engineering at Oklahoma State University. Water containing the appropriate concentration of a pH control agent was circulated in a closed loop through a column of mixed bed ion exchange resin. The flow system came to equilibrium, in which the resin was saturated with amine within a few hours. The apparatus consisted of four large columns contained mixed beds of ion

exchange resins connected to four centrifugal pumps. The temperature was controlled by separate temperature controllers dedicated to individual columns. A nitrogen purge served the purpose of minimizing the oxygen content in the solution, which was checked using a dissolved oxygen probe/meter. The design of this apparatus reduced the interference of unwanted organic compounds, which might leach from materials of the tubing and the pump. Experiments were run at 60°C for 28 days with samples of the solution and resin being taken at an interval of 14 and 28 days. These resin and aqueous samples were then subjected to chemical analysis using methods described below.

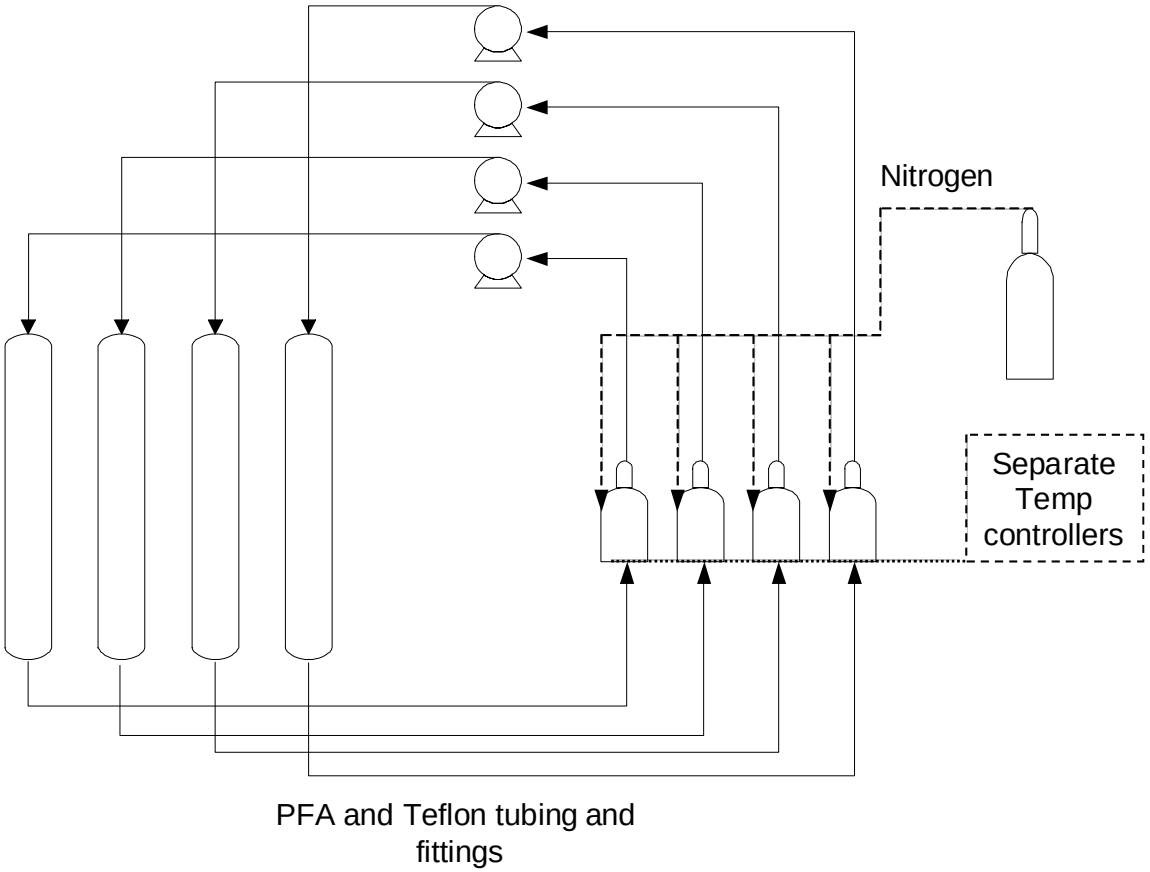

Figure 2-3: Schematic of mixed bed column experiment [10]

Batch Experiments:

Batch tests consisted of exposing ion exchange resins to a variety of pH control agents in a sealed glass bottle with Teflon-lined caps at 60°C. Samples were drawn at intervals of 14 and 28 days in order to mimic column experiments. The concentration of pH control agents used was set high at 1000 ppm in order to accelerate chemical reactions between the pH control agent and the resins. Before use, the Dowex 650 cation resin was converted to ethanolamine form by reaction with excess ethanolamine at room temperature. For each type of resin, 5.0 g of anionic resin, 5.0 g of cationic resin, and 5.0 g of mixed resin 1:1 by volume were used in separate experiments. An ethanolamine blank consisted of the 1000 ppm ethanolamine solution without any added resin. The same approach was used while scaling up the batch experiments, in which 2L bottles were used with 100 g of resin with 150 ml of 0.0164 M (equivalent to 1000 ppm ethanolamine) pH control agent. After 28 days at 60°C, the aqueous solution above the resins was tested for pH (pH electrode), oxygen concentration (dissolved oxygen probe), and conductivity.

The resin samples from the column experiments were extracted with HPLC- grade methylene chloride and the resulting solutions were analyzed using GC/MS on a Hewlett Packard GCD-1800A instrument. The compounds were identified by matching their mass spectra to the National Institute of Standards and Technology (NIST) database. An external standard of dodecane was used for quantitative analysis of the compounds. Their concentration and identification were used to understand the pathways of resin degradation mechanism. Two different extraction procedures were used for each

resin, a neutral extraction for uncharged organics followed by an acidic extraction for organic acids.

Neutral extraction of cation/anion resins:

The resin samples were weighed (approx. 10-15 g) and placed in 100 ml glass bottles with Teflon-lined caps. Then a known weight of HPLC-grade methylene chloride (approx. 30-35 g) was added to each of these bottles. The bottles were sealed and set on a roller mill for 12 hours. The methylene chloride layers were then separated using a pasture pipette and collected in a clean dry beaker. The extracts were then dried over anhydrous magnesium sulfate and were then transferred to an evaporative concentrator where they were reduced to a volume of 0.5-1.0 ml at 45°C. The concentrated methylene chloride solutions were then collected in a pre-weighed, clean, and dry 2 ml conical glass vials where their final mass was recorded. The vials were then sealed with Teflon-lined caps and were refrigerated until GC/MS analysis. The spent resin samples were then stored for subsequent acidic extraction.

Acidic extraction of cation/anion resins:

The weighed resin samples (approx. 10-15 g) from the neutral extraction were transferred to clean, dry 100 ml glass bottles with Teflon-lined caps. The samples were treated with 6 ml of concentrated analytical grade hydrochloric acid. Then a known weight of HPLC-grade methylene chloride (approx. 30-35 g) was added to each of these bottles. The bottles were sealed and set on a roller mill for 12 hours in order to extract organic compounds from the resins. The methylene chloride layer was then separated

from hydrochloric acid layer using a pasture pipette and collected in a clean dry beaker. The extracts were dried over anhydrous magnesium sulfate and were transferred to an evaporative concentrator. The volume of the extracts was reduced to 0.5-1.0 ml at 45°C. The concentrated methylene chloride solutions were then collected in a pre-weighed 2 ml conical glass vials where their final masses were recorded. The vials were then sealed with Teflon-lined caps and were refrigerated until GC/MS analysis was performed.

The aqueous solutions were extracted using the same procedure as described above, which is under both neutral and acidic conditions. All Mass Transfer Coefficient measurements were performed in Dr. Foutch's lab by Dr. Jaehyun Lee. During this investigation, Dowex 650C strong cation exchange resin and Dowex 550A strong anion exchange resin obtained from Aldrich were used without any pretreatment. A variety of new alternative pH control agents were tested as replacements for ethanolamine. These were chosen by blocking the two reactive functional groups that are present on ethanolamine, i.e. the amine ($-NH_2$) and alcohol (-OH) groups. The hydrogen atoms on these groups were replaced by methyl groups ($-CH_3$). The structure of these alternative pH control candidates are as shown in Figure 2-4. It was anticipated that one or more of these compounds would cause less fouling than ethanolamine and that the results could indicate, which part of the ethanolamine molecule is responsible for detrimental interactions with the ion exchange resins.

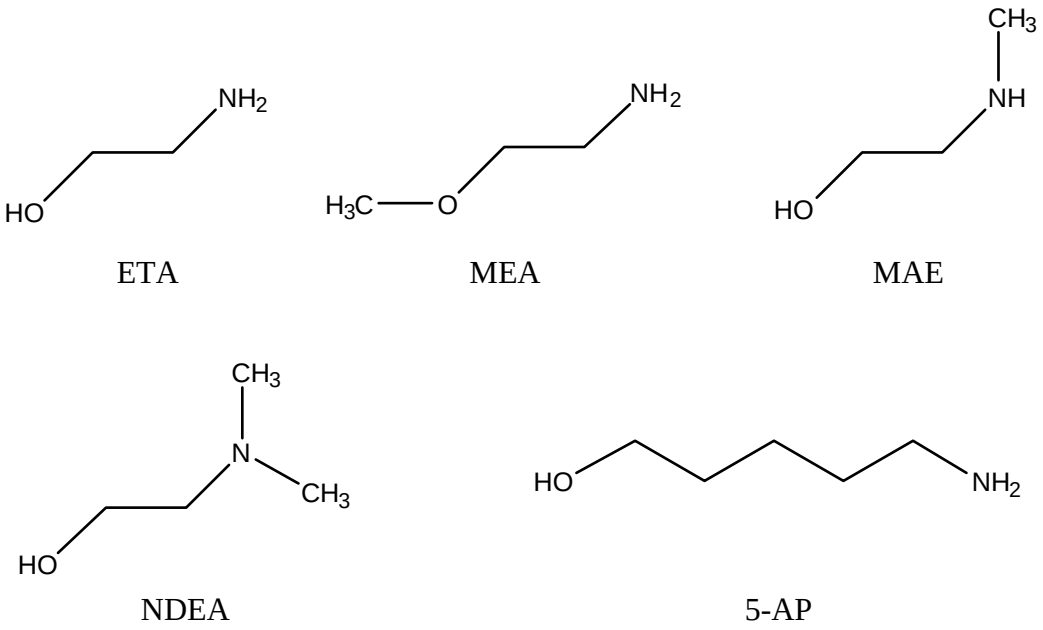

Figure 2-4: Chemical structures of pH control agents used in column experiments (ETA=ethanolamine, MEA=2-methoxtethylamine, MAE=2-methylaminoethanol, NDEA=2-dimethylaminoethanol, 5-AP=5-aminopentanol)

By modifying the –OH group to –OMe we got 2-methoxyethylamine, and by modifying the amine group in successive steps we got 2-methylaminoethanol and 2-dimethylaminoethanol. 5-aminopentanol was included since several plants have tested it. These pH control agents were purchased from Aldrich and were used as obtained.

Several sets of experiments were run on resins with varying pH conditions in batch as well column experiments in order to study the fouling process (Table 2-1). These experiments are described below.

Table 2-1. Column experiments

Experiment	pH control agent	Concentration (ppm)
1	ethanolamine (labeled with ^{15}N)	2
2	ethanolamine (labeled with ^{15}N)	10
3	2-methoxyethylamine	2
4	ammonia	2
5	2-methylaminoethanol	2
6	2-methylaminoethanol	10
7	ethanolamine + iron (2 ppm)	2
8	ammonia + iron (2 ppm)	2
9	ethanolamine	2
10	ethanolamine	10
11	2-dimethylaminoethanol	2
12	2-dimethylaminoethanol	10
13	2-methoxyethylamine	2
14	2-methoxyethylamine	10
15	5-aminopentanol	2
16	5-aminopentanol	10

Experiment 1:

Four test columns were operated with low concentrations of labeled and unlabelled ethanolamine at 60°C. A total of 3 sets of experiments were performed. The first set involved ^{15}N labeled ethanolamine (5% in unlabeled ethanolamine) and mixed bed resin columns containing Dowex and Amberjet resin brands. The second set contained the same labeled ethanolamine but columns contained individual resin type instead of mixed bed. In the third set, deuterated ethanolamine ($HOCD_2CD_2NH_2$) was used. The samples were withdrawn from the columns at 0, 14, and 28 days time intervals and chemical analysis was carried out as described above.

Experiment 2:

This set included different pH control agents with two different concentrations on the mixed bed resin column. In the first case, the concentration of the pH control agent was adjusted to 2 ppm, while in the other it was 10 ppm. The samples were withdrawn from the columns at 0, 14, and 28 days time intervals and chemical analyses were carried out as described. These experiments were performed in order to probe the correlation between the extent of fouling and the dosage of the pH control agent

Experiments 3-16:

These experiments were conducted in order to study the effect of different pH control agents using varying concentrations to determine the most appropriate pH control agent for replacement of ethanolamine. The catalytic effect of iron on the fouling process was also included in this study by running the column experiments in the presence of

2 ppm iron (Experiments 7 and 8). This was run in columns containing mixed bed resins with ethanolamine and ammonia as pH control agents. The experiment was conducted for a period of 28 days, at the end of which the samples were subjected to chemical analysis.[11]

Column results

The approach in the first set of experiments was to use ^{15}N and deuterium labeled ethanolamine in combination with solid state NMR, IR spectroscopy, and GC/MS analysis of organic compounds to elucidate resin-ethanolamine interactions. The ^{15}N and deuterium labeled ethanolamine were not detected in the resin extracts. However, detection of carbon-deuterium stretching vibrations in the infrared spectrum of the resins indicated that ethanolamine became chemically bound to the resin.

GC/MS analysis of the neutral extracts revealed a variety of compounds that are listed in Table 2-2. Neutral extraction was expected to remove only non-acidic compounds and would reveal fouling by non-polar hydrophobic compounds. The acidic extraction would neutralize any compounds that are basic, thereby releasing them from the resin and allowing their extraction into methylene chloride. Table 2-2 lists the concentrations of the compounds found when the methylene chloride extracts were analyzed by GC/MS.

Table 2-2: Compounds found in Experiment 1 by neutral extraction (ppb): Dowex resin ^{15}N labeled ethanolamine

Compound	Retention time (min)	Initial Cation Resin (ppb)	Final Cation Resin (ppb)	Initial Anion Resin (ppb)	Final Anion Resin (ppb)
1,2,4-trimethylbenzene	9.8	-	-	5	-
1,3,5-trimethylbenzene	10.6	-	-	7	-
Unknown amine	10.8	-	88	-	-
2-ethylhexanol	11.4	65	240	-	509
Acetophenone	12.9	-	214	-	221
Unknown (alcohol)	16.3	-	-	4	-
Unknown (alkane)	24.6	-	15	-	28
Unknown (aromatic)	24.8	-	-	-	82
2,4-di-t-butylphenol	25.1	-	-	-	74
Unknown	25.7	-	23	-	183
Unknown	27.1	-	9	4	66
Iso-octyl phenol	27.5	105	48	-	200
Unknown (alkane)	28.2	-	-	-	49
1-iso-octly-2-methyl phenol	28.5	16	29	-	269
Hexadecanol	28.9	-	-	-	66
Unknown (aromatic)	29.2	31	128	-	3113
Hexadecane	29.3	-	-	-	146
Unknown	29.5	-	11	-	133
Unknown	30.6	-	61	-	643

Hexacosane	32.2	-	-	-	100
Unknown (aromatic)	32.6	-	-	-	34
Eicosane	33.6	2	21	-	109
Unknown	34.4	2	18	-	95
Dibutyl phthalate	35.1	3	37	-	-
Unknown (aromatic)	35.5	-	-	-	69
Unknown	37.1	-	-	-	72
Octadecanol	37.3	51	288	-	2424
Unknown	38.3	-	16	-	-
Unknown (alkane)	39.3	-	18	-	-
Dioctadecylphosphate	41.0	-	401	-	1246
Tricosane	42.7	-	31	-	80
Heptacosane	44.4	-	39	-	98
Bis(2-ehtylhexyl)phthalate	45.6	68	220	4	275
Unknown (alkane)	46.3	3	40	-	136
Unknown (alkane)	48.8	-	51	-	164
Unknown (alkane)	51.8	-	59	-	166
Unknown (alkane)	53.2	-	282	-	146
Unknown(alkane)	55.5	-	60	-	740
Unknown (alkane)	60.1	-	44	-	173

The data clearly indicate that organic compounds build up on the anion resin during the column experiment. These compounds include 2-ethylhexanol, iso-octyl phenol, 1-iso-octyl-2-methyl phenol, hexadecanol, octadecanol, 2,4-di-tert-butylphenol, eicosane, bis-2-ethylhexylphthalate, and several unidentified compounds. Interestingly, several antioxidants, plasticizers, and alcohols observed in the initial cation resin but not in the unused anion resin were found to be present on the anion resin at the end of the experiment. This led to the conclusion that these compounds migrated from the cation resin to the anion resin with the caveat that some of these compounds may be from the recirculation system. Several new compounds were found in the used resins that were not initially present in the starting resins. These compounds included acetophenone, dioctadecylphosphate, and several unidentified compounds.

In order to identify acidic compounds present, the extracted resins were subjected to a second, acidic extraction followed by GC/MS analysis. The retention times, compounds identities, and concentrations are tabulated in Table 2-3.

Table 2-3: Compounds found in Experiment 1: Dowex resin ^{15}N labeled ethanolamine by acid extraction procedure

Compound	Retention time (min)	Final Cation Resin (ppb)	Initial Anion Resin (ppb)	Final Anion Resin (ppb)
Unknown	8.6	184	1070	-
Unknown	10.0	-	30	-
Unknown	10.5	-	16	-
Unknown (amine)	10.8	88	-	-
Unknown	11.2	-	14	-
2-ethylhexanol	11.4	240	-	509
Unknown	11.9	-	-	203
Unknown	12.1	-	-	155
Unknown	12.3	-	-	400
Acetophenone	12.9	214	70	143
Unknown	13.7	-	-	173
Unknown	14.2	-	-	735
Unknown	14.6	-	10	-
Unknown	14.8	-	-	179
Unknown	15.1	-	-	78
Benzoic acid	16.1	-	60	2963
Unknown	17.2	-	10	204
Phenylacetic acid	18.1	-	-	61
4-methylbenzoic acid	19.2	-	310	2587
Unknown	19.3	-	-	239

Unknown	19.5	-	-	96
Unknown	20.2	-	-	329
Decanoic acid	21.2	-	-	436
Unknown	21.7	-	70	-
Unknown	22.4	-	10	96
4-tert-butylbenzoic acid	22.6	-	-	78
Unknown	22.7	-	-	179
Unknown	23.7	-	-	173
Unknown	23.8	-	-	1087
Unknown	24.2	32	-	412
Unknown (alkane)	24.6	15	-	28
Unknown(aromatic)	24.8	-	10	142
Unknown	25.7	23	-	-
Dodecanoic acid	26.2	-	-	633
Unknown	26.5	-	-	460
Unknown	26.8	-	-	335
Unknown	27.1	9	5	-
Unknown	27.2	12	-	-
Iso-octyl phenol	27.5	-	48	1983
Unknown	27.8	-	3	155
Unknown	28.1	-	-	1876
Unknown	28.2	-	-	96
1-iso-octlyl-2-methyl phenol	28.5	29	-	288

Unknown	28.7	-	-	370
Unknown	28.9	-	-	281
Unknown	29.1	-	2	96
Unknown (aromatic)	29.2	128	-	2216
Unknown	29.5	11	-	1720
Unknown (aromatic)	30.0	-	-	137
Unknown	30.3	23	-	251
Unknown	30.6	61	-	4516
Unknown	30.9	-	-	72
2,4-Di-tert-butylphenol	31.3	17	-	460
N-butylbenzenesulfonamide	31.7	-	-	72
Unknown (alkane)	31.5	21	-	175
Hexacosane	32.1	-	-	460
Unknown	32.2	-	-	233
Unknown	32.3	-	-	466
Unknown (aromatic)	32.6	-	-	48
Pentadecanoic acid	32.8	-	-	60
Unknown	33.5	-	-	66
Eicosane	33.6	21	-	109
Unknown	34.2	22	-	42
Unknown	34.4	18	-	-
Unknown	34.5	-	-	382
Unknown	34.8	34	-	-

Hexadecanoic acid	34.9	-	-	717
Unknown (alkane)	35.0	26	-	-
Dibutyl phthalate	35.1	37	-	-
Unknown	35.7	-	-	573
Unknown	36.9	-	-	60
Unknown	37.0	-	-	60
Octadecanol	37.3	288	-	424
Unknown	37.6	-	-	42
Unknown	38.3	16	-	-
Unknown (aromatic)	38.4	-	-	8100
Octadecanoic acid	38.6	-	-	185
Unknown	39.0	21	-	-
Unknown (alkane)	39.3	18	-	-
Unknown	41.0	-	-	48
Dioctadecylphosphate	41.0	401	-	-
Tricosane	42.7	31	-	-
Heptacosane	44.4	39	-	98
Unknown(aromatic)	44.5	-	-	1846
Bis(2-ehtylhexyl)phthalate	45.6	220	4	-
Unknown(alkane)	46.3	40	-	-
Unknown	48.2	70	-	-
Unknown	48.8	51	-	-
Unknown (alkane)	51.8	59	-	-

Unknown (alkene)	53.2	282	-	-
Unknown	55.3	38	-	-
Unknown (alkane)	55.5	60	-	-
Unknown	56.2	47	-	-
Unknown	57.0	27	-	-
Unknown (alkane)	60.1	44	-	-

The initial and final anion resins were treated in this manner, as was the final cation resin, since it was no longer in the acid form due to neutralization with ethanolamine. The major acidic compounds present were benzoic acid and methylbenzoic acid that likely resulted from resin oxidation. There was a significant increase in these compounds during the course of the ethanolamine experiment. Also, decanoic acid, pentadecanoic acid, and octadecanoic acid were found on the used anion resin. Their origin is likely to be from hydrolysis or oxidation of some other material on the resin backbone or present as an additive to the resin (perhaps porogens used in resin manufacture). For example, the observed decanol and decanoic acid might share the same origins. Alternatively, the compounds may derive from a series of chemical reactions from simple precursor compounds, such as the ethanolamine, but this is unlikely. A remarkable increase in total organics on the resins was observed. This might have resulted from labilization of trapped species possibly due to resin swelling or chemical reactions. Several compounds that were present in the unused resin at low concentrations showed a large increase in concentration during the course of the experiment. For instance, octadecanol initially found at 2 ppb increased to 8773 and 15548 ppb after 14 days and 28 days, respectively.

At the same time, octadecanol began to appear in the anion resin although it was not detected in the unused resin. Assuming that octadecanol is trapped in pores within the cation resin, it was released under the experimental conditions and subsequently migrated to the anion resin. A build up of octadecyl aldehyde, a suspected strong anion resin poison, was also observed on the cation resin, which might have occurred due to the oxidation of octadecyl alcohol. The isotope labeled ^{15}N was not detected in any of the resin extracts. This suggests that the observed species have not incorporated the amino group of ethanolamine. Thus, the amine portion of ethanolamine does not appear to be incorporated to a major extent into the soluble reaction products and may instead be covalently bound to the resins.

The total amount of organic compounds was calculated by addition of all the compounds that were found in the methylene chloride extraction. Figure 2-5 shows the plot of total organics against the recirculation period. The plot shows that the total amount of organics found increases steadily as the exposure is increased.

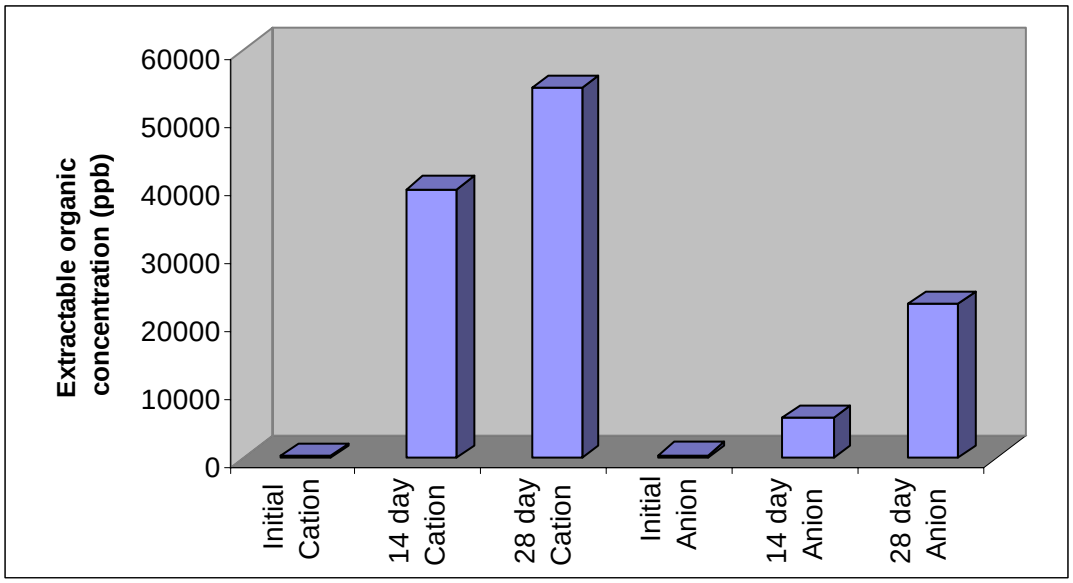

Figure 2-5: Total methylene chloride extractable organics from the column experiment in Dowex resins

The Rohm and Haas Amberjet resins showed a pattern similar to Dowex resins, i.e. fairly clean resins at the start that become increasingly contaminated with time (Figures 2-5 and 2-6). However, an increase in the contamination on the cation resin does not foreshadow the deposition of contaminants on the anion resin. Instead, the contamination of the anion resin grows exponentially with time. A number of the major contaminants are the same as those found in the Dowex resins: octadecanol, isooctyl phenol, 1-isooctyl-2-methylphenol, 2,6-di-tert-butyl-2,5-cyclohexanedione, tert-butylphenol, and several other unknown compounds in low concentrations that elute with the same retention time as those in the Dowex extracts. The identifiable minor compounds found in the Amberjet resins included 1,2,4-trimethylbenzene, 1,3,5-trimethylbenzene, 2-ethylhexanol, 5-aminotetrazole, decanal, 2,4-di-tert-butylphenol,

hexadecane, 2,4-di-tert-butylmethylphenol, 2-hexyl-1-decanol, and octadecyl acetate. Some of these are likely derived from oxidation of the resin backbone.

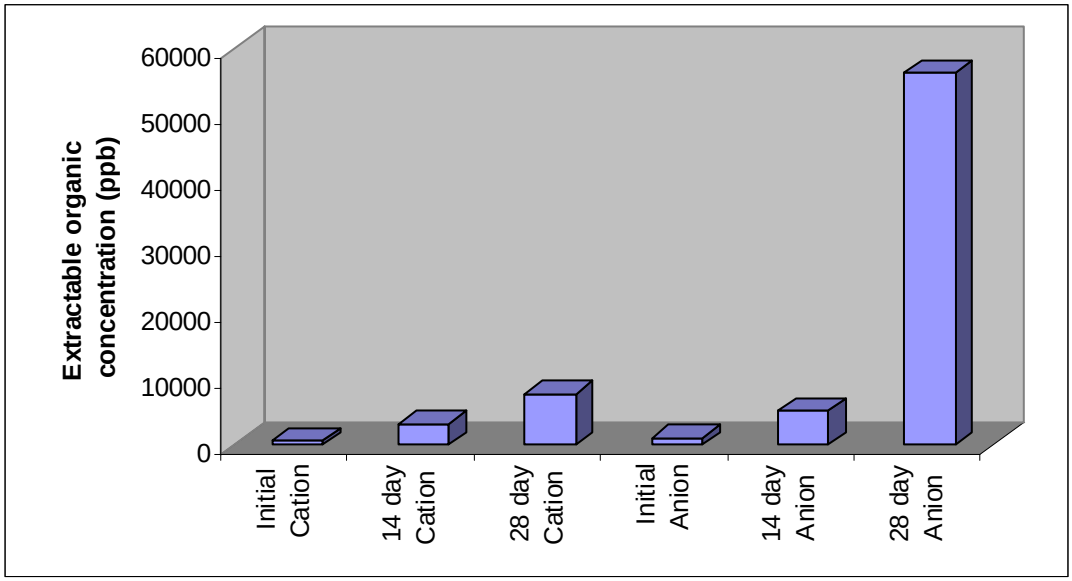

Figure 2-6: Total methylene chloride extractable organics from Amberjet Resins

In order to identify acidic compounds that might be present on the resins as anionic species resistant to extraction by methylene chloride, the previously extracted resin samples were acidified with hydrochloric acid and extracted again with methylene chloride. Surprisingly, this procedure not only led to the release of acids but also a burst of neutral and unidentified species. Presumably, the acid serves to open blocked pores and channels in the resin and allows a more complete extraction. The results of GC/MS analysis of the acidic extracts of the Dowex resins are given in Table 2-4 and Figure 2-7. It was expected that the acidic extraction would remove additional acidic phenols, which were bound in their deprotonated form in the anion resin. In addition to these acids, the Dowex anion resins also showed an increase in octadecanoic acid likely derived from

oxidation of the octadecanol found in the cation resin. Acids derived from oxidation of the resin, benzoic acid and methyl-benzoic acid, were observed in the unused and 14 day anion resins but disappeared by the end of the experiment. This suggests that resin oxidation was not extensive and these more water soluble acids were either flushed away by the recirculating water or they reacted away to other compounds. However, damage to the Dowex resins caused by radicals was demonstrated by the generation of numerous chlorinated aromatic compounds when the damaged portion of the resin reacted with hydrochloric acid. Unlike the Dowex resins, acid extraction of the Amberjet anion resins showed a profound increase in acids derived from oxidation of the resin including benzoic acid, methylbenzoic acid, dimethylbenzoic acid, ethylbenzoic acid, and benzeneacetic acid. Also, significant amounts of tridecanoic acid, tetradecanoic acid, pentadecanoic acid, hexadecanoic acid, and octadecanoic acid were found in the anion resins after they were used in the recirculation experiments. They are shown in Figure 2-8 and Table 2-5.

Table 2-4: Compounds found by acid extraction in treated with 10 ppm ^{15}N labeled ethanolamine on the column with Dowex resins (Experiment 2)

Compound	Retention time (min)	Initial Cation Resin	14 Day Cation Resin	Final Cation Resin	Initial Anion Resin	14 Day Anion Resin	Final Anion Resin
3-methyl-3-chlorobutene	4.6	-	-	-	185	-	-
Unknown	5.4	-	168	-	4428	-	-
Unknown	6.9	-	219	-	-	530	-
Unknown	7.3	-	-	-	80	-	611
Unknown	8.0	-	-	-	66	-	-
Unknown	8.1	-	-	-	115	-	-
Unknown	8.6	-	208	-	191	1265	-
2,3-dichloro-2-methylbutane	5.9	-	101	-	214	-	-
Benzaldehyde	9.7	-	-	-	32	-	-
Unknown	10.0	-	-	-	52	-	-
Unknown	10.4	-	-	-	15	-	-
Unknown	10.6	-	-	-	41	-	-
Unknown	11.2	-	26	-	44	-	-
Unknown	11.9	-	-	-	89	-	-
Unknown	12.1	-	-	-	83	-	-
Unknown	12.3	-	99	1145	15	1131	1920
Acetophenone	12.9	-	-	-	98	-	-
Unknown	13.7	-	-	390	-	106	247

Unknown	13.8	-	9	-	-	-	190
Unknown	14.0	-	20	1170	-	-	-
Unknown	14.1	-	-	-	-	-	3259
Unknown	14.4	-	-	-	12	808	-
Unknown	14.7	-	-	-	14	-	73
Unknown	15.1	-	23	-	-	529	480
Unknown	15.4	-	5	136	-	106	-
Benzoic acid	15.8	-	-	-	244	596	-
2,4-dichlorophenol	16.1	-	-	-	13	134	-
Unknown	16.4	-	12	-	-	-	-
Unknown (aromatic)	16.7	-	-	-	-	-	87
Unknown (aromatic)	17.0	-	-	136	-	-	349
Unknown	17.1	-	-	-	-	150	-
Unknown	17.3	-	-	-	34	-	-
Unknown	18.2	-	-	170	-	-	160
4-methylbenzoic acid	18.8	-	-	-	157	-	-
Unknown	19.1	-	-	-	9	-	-
2-chloro-1-phenyl ethanone	19.3	-	-	-	36	-	-
Unknown	19.4	-	15	-	10	-	-
Unknown	19.7	-	-	-	7	-	-
Unknown	19.8	-	8	127	-	-	-
Chloroxylenol	20.3	-	-	619	-	741	1571

Isobenzofuranone	21.3	-	-	-	34	-	-
Unknown	21.7	-	-	-	3	-	-
Tetradecane	21.9	-	-	-	3	-	-
Unknown	22.5	6	9	483	14	-	626
Unknown(aromatic)	22.7	-	-	3630	7	1092	4394
Unknown	23.0	-	-	382	-	-	-
Unknown	23.1	-	14	789	-	-	1353
Unknown	23.8	-	16	-	-	819	-
Unknown	24.0	-	-	161	-	162	189
Decene	24.1	-	31	-	-	-	-
2,6-di-t-butyl-2,5-cyclohexadiene-1,4-dione	24.2	-	-	-	-	-	21
Unknown	24.2	-	-	85	-	-	102
5-methyl-1-isobenzofuranone	24.4	-	-	102	-	-	-
Unknown	24.3	-	-	-	10	173	145
Unknown (alkane)	24.5	6	-	-	-	-	-
Unknown	24.6	-	-	68	-	-	102
Unknown	24.8	84	15	93	40	-	145
2,4-di-t-butylphenol	25.1	7	-	-	-	5	-
Unknown	25.1	-	6	229	-	128	480
Unknown (aromatic)	25.7	8	-	-	4	-	-
Unknown	25.9	-	-	1340	-	-	1964

Unknown	26.0	-	54	-	-	-	-
Tert-butyl phenol	26.1	-	78	2120	-	-	2081
Unknown	26.2	-	-	-	40	580	-
Unknown	26.3	-	4	373	-	-	451
Unknown	26.5	-	10	144	-	240	378
Hexadecane	27.0	-	-	-	4	106	-
Unknown	27.1	-	-	42	-	-	-
Unknown	27.2	-	-	110	15	-	-
Unknown	27.3	-	14	119	-	-	-
Unknown	27.4	-	-	-	-	145	-
Iso-octyl phenol	27.5	-	339	6581	-	3471	7653
Unknown(aromatic)	27.7	-	-	450	15	-	597
Unknown	27.8	-	22	178	-	-	-
Unknown	27.9	-	-	-	-	362	-
Unknown (aromatic)	28.0	-	124	4164	-	-	7187
Unknown	28.1	-	-	-	7	-	-
Unknown	28.2	-	11	161	-	11374	276
Unknown	28.4	-	-	-	8	-	-
1-iso-octyl-2-methyl phenol	28.5	-	54	1035	-	641	989
Octadecanol	37.3	-	34	1069	-	357	218
Tetradecene	28.9	-	28	-	-	-	-
Unknown	29.0	-	11	458	-	-	654

Unknown	29.1	-	-	3172	-	-	-
Unknown (aromatic)	29.2	-	120	1204	12	2842	5616
Unknown	29.3	-	-	-	-	2318	-
Unknown (aromatic)	29.4	-	-	3554	-	-	6154
Unknown	29.6	-	-	-	-	3108	-
Unknown	29.9	-	-	365	-	-	364
Unknown	30.0	-	14	-	-	373	-
Unknown	30.3	-	12	229	-	-	190
Unknown	30.6	-	178	7438	-	-	10752
Unknown	31.2	-	-	755	-	-	1178
Unknown	31.3	-	34	-	9	752	-
Unknown	32.2	5	18	1018	12	-	2008
Unknown (aromatic)	33.3	20	61	-	25	591	-
Unknown (aromatic)	33.6	-	17	-	-	206	-
Unknown	33.8	10	16	-	9	-	102
Unknown	33.9	-	-	-	-	697	160
Unknown	34.1	8	42	-	10	624	-
Unknown	34.4	-	40	424	-	-	-
Unknown	35.7	-	73	712	9	502	931
Unknown	36.4	-	-	-	-	189	-
Unknown	37.0	-	8	365	-	72	378
Octadecanol	37.3	-	34	1069	-	357	218
Unknown (aromatic)	37.7	-	-	-	-	123	-

Unknown	37.8	-	-	263	-	-	378
Diphenyl acetylene	38.3	-	-	263	-	-	378
Octadecanoic acid	38.6	-	-	332	-	170	531
Iso-octylphenoxy ethanol	38.8	-	76	-	-	-	87
Dioctadecyl phosphate	41.0	-	81	1077	-	-	-
Anthracene	42.9	-	59	-	-	-	-
2-hydroxyethyl octadecanoate	43.5	-	-	5971	-	-	-
Unknown	43.6	-	228	-	-	-	-
Unknown	44.4	-	527	-	-	-	5354
Unknown (aromatic)	44.6	-	-	-	-	5109	-
Unknown	46.4	-	-	3214	-	-	-
Unknown	47.4	-	352	-	-	-	144
Unknown	48.2	-	-	500	-	-	-
Unknown (alkane)	48.4	-	34	-	-	-	-

Table 2-5: Compounds found by acid extraction in treated with 10 ppm ^{15}N labeled ethanolamine on the column with Amberjet resins (Experiment 2)

Compound	Retention time(min)	Initial Cation Resin	14 Day Cation Resin	Final Cation Resin	Initial Anion Resin	14 Day Anion Resin	Final Anion Resin
2,2-dimethyl propanoic acid	4.9	-	-	-	11	81	384
Unknown	5.3	-	-	-	-	-	323
Unknown	5.8	-	-	-	17	-	91
Unknown	6.9	-	-	-	-	-	152
Unknown	7.3	-	122	102	101	-	-
Unknown	7.7	-	677	-	-	-	-
Unknown	8.6	-	-	-	-	-	81
Unknown	9.1	-	-	-	11	-	-
Benzaldehyde	9.8	-	-	-	28	-	-
Methylstyrene	10.2	-	-	-	7	-	-
Unknown	10.3	-	-	-	-	-	18
Unknown	11.1	-	-	-	-	-	165
Unknown	11.8	-	-	-	-	-	67
Unknown	12.3	-	-	-	-	-	67
Unknown	12.8	-	10	-	-	-	79
Acetophenone	12.9	-	-	-	26	-	-
Unknown	13.7	-	-	-	21	45	49
Unknown	13.8	8	15	48	-	-	73
Unknown	14.0	-	-	-	25	-	-

Unknown	14.1	5	-	31	-	90	158
Unknown	14.4	5	-	-	-	-	30
Unknown	15.3	-	-	-	-	-	81
Benzoic acid	15.6	-	-	-	7683	1667	14084
Unknown	16.4	6	11	-	-	-	-
Unknown	17.6	-	-	-	-	-	55
Unknown	17.8	-	-	-	-	-	37
Unknown	18.0	-	-	-	-	-	61
Benzeneacetic acid	18.3	-	-	-	-	-	158
Unknown	18.4	-	-	-	34	7	30
Unknown	18.6	-	-	-	-	-	49
Methylbenzoic acid	18.7	-	-	-	30	16	341
Unknown	19.1	-	-	-	28	-	165
m-tert-butyl phenol	19.3	-	-	-	4	7	37
Unknown	19.5	-	-	-	-	-	61
4-methylbenzoic acid	19.6	-	-	-	372	-	-
Unknown	19.8	-	-	-	-	-	67
Phthalic anhydride	20.3	-	-	-	-	-	91
Unknown	20.8	-	10	-	-	-	-
Unknown	20.9	-	-	-	4	-	73
Dimethylbenzoic acid	21.0	-	-	-	3	-	-
Unknown	21.1	-	-	-	-	15	43
Unknown	21.2	4	10	-	17	8	37

Isobenzofuranone	21.3	-	-	-	28	-	146
Unknown	21.7	-	-	-	-	-	73
Ethylbenzoic acid	21.5	-	-	-	9	-	-
Unknown	21.8	-	-	-	12	-	24
Unknown	22.5	7	10	60	25	31	201
Unknown	22.3	-	-	-	-	-	37
p-tert-butyl phenol	22.6	-	-	-	-	28	-
Unknown	22.7	18	54	252	-	168	433
Unknown	23.2	-	-	-	-	-	67
Phenol	23.5	-	-	-	-	-	116
Unknown	23.8	-	-	-	62	55	20
Unknown	24.0	-	-	-	-	6	189
Cyclodecane	24.1	-	48	87	-	-	-
2,6-di-tert-butyl-2,5-cyclohexadiene-1,4-dione	24.2	-	-	-	-	-	30
5-methylisobenzo furanone	24.4	-	-	-	-	-	61
Tetradecanol	24.1	14	-	-	-	-	-
Unknown	24.7	18	-	-	15	-	-
Unknown	25.1	1	-	-	-	7	104
Unknown	24.8	-	60	26	-	-	37
2,4-di-t-butylphenol	25.1	-	-	-	16	-	-
Unknown (aromatic)	25.2	-	-	15	-	27	951

Unknown	25.6	-	-	-	-	12	24
3,5-di-t-butylphenol	25.8	-	-	-	-	4	-
Unknown	26.1	9	-	193	-	83	-
Dodecanoic acid	26.2	-	-	-	19	-	-
Unknown	26.2	-	30	-	-	-	5175
Unknown	26.3	-	-	-	-	-	189
BHT	27.1	-	-	-	-	7	-
Iso-octyl phenol	27.6	20	24	315	-	1915	5351
Unknown	27.7	2	-	31	-	12	61
Unknown	28.1	2	-	23	-	-	67
Unknown	28.2	-	-	-	-	-	67
Tridecanoic acid	28.4	-	-	-	-	-	67
1-iso-octyl-2-methyl phenol	28.5	9	14	77	-	241	2145
Unknown (aromatic)	28.9	4	12	44	-	14	79
Unknown	29.2	10	-	102	-	377	3175
Unknown (aromatic)	29.5	11	26	102	-	58	2596
Unknown (aromatic)	29.9	7	15	29	-	12	152
Unknown	30.5	-	-	-	-	-	43
Unknown	30.6	9	-	175	-	206	5290
Nonyl phenol	30.2	-	-	-	-	-	37
Tetradecanoic acid	30.7	-	-	-	69	-	104
Unknown	30.8	1	-	-	-	26	67

Unknown	31.0	1	20	6	139	-	-
Unknown	31.2	3	11	44	-	17	301
Unknown	32.0	-	-	-	15	3	146
Unknown	32.3	-	13	34	48	3	122
Pentadecanoic acid	32.7	-	-	-	19	-	171
Unknown	32.9	-	-	14	-	-	116
Unknown	33.2	7	-	-	-	-	250
Unknown	33.7	1	-	-	-	5	152
Unknown	34.1	4	13	23	-	-	165
Unknown	34.5	-	-	-	-	2	165
Hexadecanoic acid	34.8	-	-	-	101	13	2273
Unknown	35.7	22	72	125	-	10	366
Unknown	36.5	4	19	-	-	10	43
Unknown	36.8	-	-	-	17	-	79
Unknown	37.3	7	22	93	18	-	104
Unknown	37.8	-	-	20	-	10	73
Unknown	38.3	16	31	1101	46	566	2060
Octadecanoic acid	38.7	-	-	-	54	-	360
Unknown	39.7	-	-	-	8	-	79
Unknown	41.8	-	-	-	-	-	67
Unknown	42.9	-	-	35	-	179	-
Unknown	44.4	-	269	1012	12	273	3279

Figures 2-7 and 2-8 show plots of total organics that were extracted from acidified ion exchange resins versus their exposure time during the column experiments.

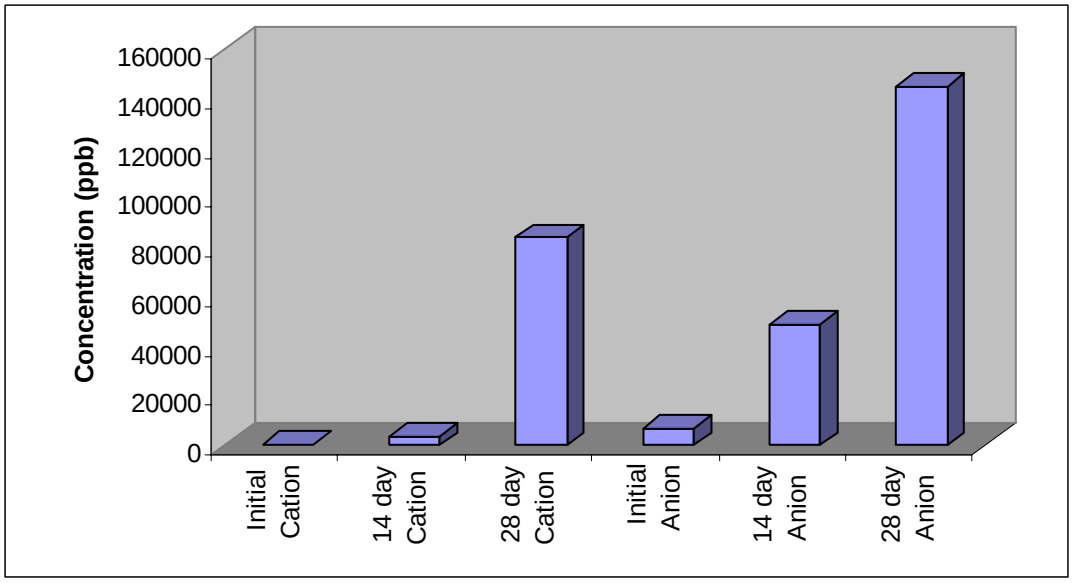

Figure 2-7: Total methylene chloride extractable organics from acidified Dowex resins exposed to 10 ppm ^{15}N labeled ethanolamine (Experiment 2)

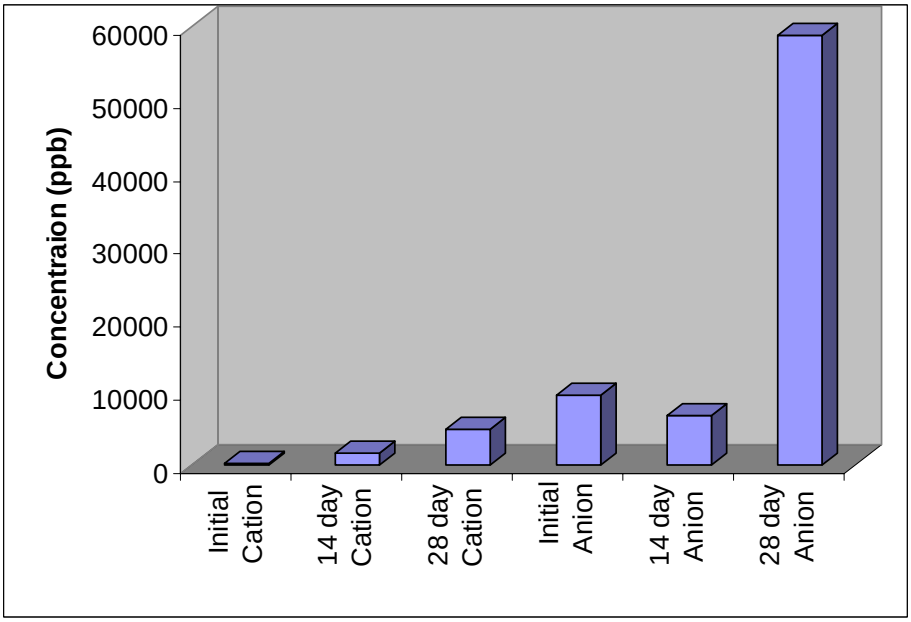

Figure 2-8: Total methylene chloride extractable organics from acidified Amberjet resins exposed to 10 ppm ^{15}N labeled ethanolamine (Experiment 2)

Table 2-6: Compounds found in Dowex resins exposed to 2 ppm ammonia and 2 ppm iron by neutral extraction (ppb) (Experiment. 8)

Compound	**Retention time (min)**	**14 day cation resin**	**28 day cation resin**	**14 day anion resin**	**28 day anion resin**
Ethylbenzene	6.9	-	-	12	38
Styrene	7.7	-	-	40	75
Triethylbenzene	10.7	-	-	-	9
2-ethylhexanol	11.5	-	4	9	44
Acetophenone	13.1	-	-	30	136
(4-methylphenyl) ethanone	17.1	-	-	-	44
Dodecanol	24.2	-	2	120	697
Octadecanol	37.6	-	-	7	119

Table 2-7: Compounds found in Dowex resins exposed to 2 ppm ethanolamine and 2 ppm iron by neutral extraction (ppb) (Experiment 7)

Compound	**Retention time (min)**	**14 day cation resin**	**28 day cation resin**	**14 day anion resin**	**28 day anion resin**
Styrene	7.7	-	-	19	116
2-ethylhexanol	11.5	-	-	-	29
Acetophenone	13.5	-	-	-	78
Dodecanol	24.2	-	-	-	765
Unknown (aromatic)	34.7	-	-	-	25
Unknown	35.4	-	-	-	224
Unknown (aromatic)	36.1	-	-	-	13
Octadecanol	37.6	-	-	-	390

Table 2-8: Compounds found in Dowex resins exposed to 2 ppm ethanolamine by neutral extraction (ppb) (Experiment 9)

Compound	Retention time (min)	14 day cation resin	28 day cation resin	14 day anion resin	28 day anion resin
Styrene	7.7	-	289	3.4	6.9
2-cyclohexene-1-one	8.8	-	68	-	-
2-ethylhexanol	11.5	-	248	5.7	-
Acetophenone	13.5	-	-	3.7	-
Dodecanol	24.2	-	288	47	205
Unknown (alcohol)	25.0	30	-	-	-
Octadecanol	37.4	-	-	-	11

Table 2-9: Compounds found in Dowex resins exposed to 10 ppm ethanolamine by neutral extraction (ppb) (Experiment 10)

Compound	Retention time (min)	14 day cation resin	28 day cation resin	14 day anion resin	28 day anion resin
Styrene	7.7	-	-	60	6.0
Unknown	0.2	-	-	-	5.0
2-ethylhexanol	11.5	-	2.0	8.3	-
Acetophenone	13.5	-	-	3.7	-
Unknown	14.5	-	-	36	-
Dodecanol	24.2	-	-	530	-
Unknown (alcohol)	25.0	36	-	-	-
Octadecanol	37.4	-	-	24	-

Table 2-10: Compounds found in Dowex resins exposed to 2 ppm 2-methylaminoethanol by neutral extraction (ppb) (Experiment 5)

Compound	Retention time (min)	14 day cation resin	28 day cation resin	14 day anion resin	28 day anion resin
Ethylbenzene	6.9	-	-	24	-
Styrene	7.7	-	-	83	15
Acetophenone	13.1	-	-	-	52
Dodecanol	24.2	-	-	129	230
Unknown	34.8	-	-	49	7
Unknown	36.1	-	-	-	5
Octadecanol	37.6	-	-	33	117

Table 2-11: Compounds found in Dowex resins exposed to 10 ppm 2-methylaminoethanol by neutral extraction (ppb) (Experiment 6)

Compound	Retention time (min)	14 Day Cation Resin	28 Day Cation Resin	14 Day Anion Resin	28 Day Anion Resin
Styrene	7.7	-	-	246	26
Unknown	11.7	-	18	-	-
2-ethyl-6-methylbenzeneamine	15.5	-	16	-	-
Unknown amine	22.6	-	58	-	-
Unknown amine	23.7	-	658	-	-
Dodecanol	24.2	-	-	853	468
Unknown	34.7	-	-	24	16
Unknown	35.1	-	-	-	6
Unknown	35.4	-	-	-	4
Unknown	36.1	-	-	9	-
Octadecanol	37.6	-	-	336	253

Table 2-12: Compounds found in Dowex resins exposed to 2 ppm

2-dimethylaminoethanol by neutral extraction (ppb) (Experiment 11)

Compound	Retention time (min)	14 day cation resin	28 day cation resin	14 day anion resin	28 day anion resin
Styrene	7.7	-	10	48	3.4
Unknown	8.9	-	2.3	-	-
2-ethylhexanol	11.7	-	7.0	-	-
Unknown	24.6	-	-	122	7.0

Table 2-13: Compounds found in Dowex resins exposed to 10 ppm

2-dimethylaminoethanol by neutral extraction (ppb) (Experiment 12)

Compound	Retention Time (min)	14 Day Cation Resin	28 Day Cation Resin	14 Day Anion Resin	28 Day Anion Resin
Styrene	7.7	143	5.9	34	-
2-cyclohexene-1-one	8.8	35	-	-	-
2-chlorocyclohexanol	11.6	170	-	-	-
2-ethylhexanol	11.7	-	3.7	-	-
Unknown	24.6	-	-	126	-
Octadecanol	37.9	-	-	8.0	-

Table 2-14: Compounds found in Dowex resins exposed to 2 ppm 2-methoxyethylamine by neutral extraction (ppb) (Experiment 13)

Compound	Retention Time (min)	14 Day Cation Resin	28 Day Cation Resin	14 Day Anion Resin	28 Day Anion Resin
Styrene	7.7	2.0	11	-	-
2-cyclohexene-1-one	8.8	-	2.3	-	-
2-ethylhexanol	11.7	0.7	8.7	-	-
Dodecanol	24.0	-	-	-	9.0

Table 2-15: Compounds found in Dowex resins exposed to 10 ppm 2-methoxyethylamine by neutral extraction (ppb) (Experiment 14)

Compound	Retention time (min)	14 day cation resin	28 day cation resin	14 day anion resin	28 day anion resin
Styrene	7.7	8.4	-	3.0	2.7
2-cyclohexene-1-one	8.8	1.4	6.3	-	-
2-ethylhexanol	11.7	7.2	4.7	0.7	-
Dodecanol	24.0	-	-	16	6.2

Table 2-16: Compounds found in Dowex resins exposed to 2 ppm 5-aminopentanol by neutral extraction (ppb) (Experiment 15)

Compound	Retention time (min)	14 day cation resin	28 day cation resin	14 day anion resin	28 day anion resin
Styrene	7.7	-	10	6.0	6.6
2-cyclohexene-1-one	8.8	-	2.4	-	-
Unknown	10.2	-	-	30	-
2-ethylhexanol	11.7	-	6.2	-	-
Unknown	15.0	-	-	6.1	-
Dodecanol	24.0	-	-	-	26

Table 2-17: Compounds found in Dowex resins exposed to 10 ppm 5-aminopentanol by neutral extraction (ppb) (Experiment 16)

Compound	Retention time (min)	14 day cation resin	28 day cation resin	14 day anion resin	28 day anion resin
Styrene	7.7	5.3	4.8	7.7	-
Unknown	10.2	-	-	-	-
2-ethylhexanol	11.7	4.4	3.0	-	-
Dodecanol	24.0	-	-	-	12

Table 2-18: Compounds found in Dowex resins exposed to 2 ppm ammonia and 2 ppm iron by acidic extraction (ppb) (Experiment 8)

Compound	Retention time (min)	14 day cation resin	28 day cation resin	14 day anion resin	28 day anion resin
Unknown	5.4	23	-	609	197
Unknown	5.9	0.9	-	535	360
Unknown	6.9	-	-	106	335
Unknown	7.3	-	-	50	-
Unknown	8.0	-	-	100	-
Unknown	8.6	-	-	2,380	2,480
Benzaldehyde	9.8	-	-	141	193
Alpha-methylstyrene	10.2	0.2	-	82	163
2-ethylhexanol	11.5	1.0	18	-	-
Unknown	11.9	-	-	81	123
Unknown	12.1	-	-	371	-
Acetophenone	12.9	-	-	98	261
Unknown	13.4	-	-	84	-
Unknown	13.8	-	-	34	-
2-ethylhexanoic acid	14.0	-	-	90	-
Benzoic acid	15.8	-	-	1,530	2,310
Methyl Phenylacetate	16.1	-	-	-	-
3-ethylheptanoic acid	17.0	-	-	-	90

Unknown	17.3	-	-	-	210
4-methylbenzoic acid	18.8	-	-	500	755
Mandelic acid	19.4	-	-	241	241
Unknown aldehyde	19.7	-	-	-	-
Decanoic acid	21.2	-	-	117	157
Unknown aromatic	21.4	-	-	115	-
Unknown	21.9	-	-	49	245
Unknown	23.3	-	5.0	-	-
Dodecanol	24.2	-	-	276	623
Unknown	26.2	-	-	212	112
Tetradecanoic acid	30.7	-	-	164	-
Unknown	31.3	-	-	47	81
Octadecanol	37.3	-	-	-	342

Table 2-19: Compounds found in Dowex resins exposed to 2 ppm ethanolamine and 2 ppm iron by acidic extraction (ppb) (Experiment 7)

Compound	Retention time (min)	14 day cation resin	28 day cation resin	14 day anion resin	28 day anion resin
Unknown	5.4	8.0	21	479	682
Unknown	5.9	-	-	494	506
Unknown	6.9	-	-	145	-
Unknown	7.3	-	-	64	-
Unknown	8.6	-	-	3042	4548
Benzaldehyde	9.8	-	-	87	117
Alpha-methyl styrene	10.2	-	-	91	98
2-chlorophenol	10.7	-	-	-	-
2-ethylhexanol	11.5	20	19	-	44
Unknown	11.9	-	-	71	152
Unknown	12.1	-	-	46	-
4-methylstyrene	12.3	14	-	-	-
Acetophenone	12.9	-	-	30	179
Unknown	13.4	-	-	49	-
Unknown	13.8	-	-	34	-
Unknown	14.2	4.0	-	-	-
Unknown	15.0	3.0	-	-	-
Benzoic acid	15.8	-	-	705	2013

Methyl Phenylacetate	16.1	-	-	77	-
Unknown	17.3	-	-	-	235
4-methylbenzoic acid	18.8	-	-	156	-
Mandelic acid	19.4	-	-	181	190
Unknown aldehyde	19.7	-	-	-	36
Decanoic acid	21.2	-	-	-	87
Unknown	21.9	-	-	-	140
Unknown	23.3	9.0	5.0	-	-
Dodecanol	24.2	-	2	162	539
Unknown	25.4	-	-	-	59
Unknown	26.2	-	-	-	132
Unknown	31.3	-	-	-	43
Octadecanol	37.3	-	-	-	97

Table 2-20: Compounds found in Dowex resins exposed to 2 ppm ethanolamine by acidic extraction (ppb) (Experiment 9)

Compound	Retention time (min)	14 day cation resin	28 day cation resin	14 day anion resin	28 day anion resin
Unknown	5.4	-	-	77	11
Unknown	5.8	-	-	22	-
Unknown	7.3	-	-	4.7	-
Unknown	7.9	-	-	10	-
Unknown	8.5	-	-	6.0	3.2
2-ethylhexanol	11.6	-	-	-	2.3
Unknown	12.9	-	-	-	3.2
Benzoic acid	15.8	-	4.0	30	-
Unknown	16.9	-	-	-	-
Unknown	17.3	-	-	9.5	2.6
4-methylbenzaldehyde	19.0	-	-	-	5.7
Mandelic acid	19.5	-	-	9.3	3.2
Dodecanol	24.0	-	-	85	54
Unknown	24.7	-	-	-	1.8
Unknown	26.2	-	-	4.5	2.5

Table 2-21: Compounds found in Dowex resins exposed to 10 ppm ethanolamine by acidic extraction (ppb) (Experiment 10)

Compound	Retention time (min)	14 day cation resin	28 day cation resin	14 day anion resin	28 day anion resin
Unknown	5.4	-	-	100	84
Unknown	5.8	-	-	-	-
Unknown	7.3	-	-	-	-
Unknown	8.2	-	-	-	13
Unknown	8.5	-	-	60	39
2-ethylhexanol	11.6	-	-	26	21
Unknown	11.9	-	-	14	6.1
Unknown	12.3	-	-	11	20
Acetophenone	12.9	-	-	73	62
Unknown	14.1	-	-	15	-
Unknown	15.4	-	-	41	27
Benzoic acid	15.8	-	-	173	200
Unknown	17.3	-	-	26	34
4-methylbenzaldehyde	19.0	-	-	62	-
Mandelic acid	19.4	-	-	24	98
Unknown	21.3	-	-	12	22
Unknown	22.4	-	-	5.5	-
Dodecanol	24.0	-	-	40	232

Unknown	24.7	-	-	15	1.8
Unknown	26.2	-	-	11	30
Unknown	26.4	-	-	-	13
Octadecanol	37.2	-	-	15	45

Table 2-22: Compounds found in Dowex resins exposed to 2 ppm 2-methylaminoethanol by acidic extraction (ppb) (Experiment 5)

Compound	Retention time (min)	14 day cation resin	28 day cation resin	14 day anion resin	28 day anion resin
Unknown	5.4	8.0	-	1563	1587
Unknown	5.9	-	-	1002	1036
Unknown	7.3	-	-	-	60
Unknown	8.0	-	-	-	97
Unknown	8.6	-	-	-	93
Benzaldehyde	9.8	-	-	-	115
Alpha-methylstyrene	10.2	-	-	-	65
2-ethylhexanol	11.5	15	23	21	-
Unknown	11.9	-	-	100	125
Acetophenone	12.9	-	-	105	-
2-ethylhexanoic acid	14.0	-	-	37	-
Benzoic acid	15.8	-	-	850	1,363
Unknown	17.3	-	-	203	431
Unknown acid	18.4	-	-	215	-
4-methylbenzoic acid	18.8	-	-	219	425
Mandelic acid	19.4	-	-	-	146
Decanoic acid	21.2	-	-	37	88
Unknown	21.9	-	-	44	88

Unknown	22.6	18	120	-	-
Unknown	23.7	174	942	-	-
Dodecanol	24.2	-	-	86	660
Unknown aromatic	24.8	-	-	55	126
Unknown	25.4	-	-	-	18
Unknown	26.2	-	-	76	102
Unknown	30.7	-	-	-	71
Unknown	31.3	-	-	18	59
Octadecanol	37.3	-	-	-	605

Table 2-23: Compounds found in Dowex resins exposed to 10 ppm 2-methylaminoethanol by acidic extraction (ppb) (Experiment 6)

Compound	Retention time (min)	14 day cation resin	28 day cation resin	14 day anion resin	28 day anion resin
Unknown	5.4	43	-	963	272
Unknown	5.9	14	-	678	263
Unknown	7.3	-	-	-	60
Unknown	8.6	-	-	1172	247
Benzaldehyde	9.8	-	-	-	115
Alpha-methylstyrene	10.2	-	-	82	94
2-ethylhexanol	11.5	15	21	-	-
4-methylstyrene	12.3	25	-	19	-
Acetophenone	12.9	-	-	91	115
Phenylmethyl formate	13.2	-	-	33	-
4-methyl benzaldehyde	13.5	-	-	39	-
2-ethylhexanoic acod	14.0	-	-	-	50
Benzoic acid	15.8	-	-	477	742
Methyl Phenylacetate	16.1	-	-	45	-
Unknown aromatic	16.3	-	-	35	-
Unknown	17.3	-	-	218	57
4-methylbenzoic acid	18.8	-	-	131	185
Mandelic acid	19.4	-	-	-	109

Unknown aldehyde	19.7	-	-	-	32
Unknown	21.9	-	-	187	219
Unknown	22.6	53	137	30	-
Unknown	22.7	-	-	32	-
Unknown	23.7	500	268	-	-
Dodecanol	24.2	-	-	119	269
Unknown aromatic	24.8	-	-	26	53
Unknown	26.2	-	-	40	-
Unknown	31.3	-	-	22	42
Octadecanol	37.3	-	-	-	121

Table 2-24: Compounds found in Dowex resins exposed to 2 ppm 2-dimethylaminoethanol by acidic extraction (ppb) (Experiment 11)

Compound	Retention time (min)	14 day cation resin	28 day cation resin	14 day anion resin	28 day anion resin
Unknown	5.4	-	-	81	100
Unknown	5.8	-	-	39	-
Unknown	7.3	-	-	4.7	-
Unknown	7.9	-	-	11	-
Unknown	8.5	-	-	18	38
2-ethylhexanol	11.6	-	-	-	19
Unknown	11.9	-	-	6.1	11
Acetophenone	12.9	-	-	3.7	37
Unknown	14.1	-	-	-	5.5
Unknown	15.4	-	-	-	14
Benzoic acid	15.8	-	4.4	8.1	103
Unknown	16.1	-	-	1.3	-
Unknown	17.0	-	-	1.5	-
Unknown	17.3	-	-	7.3	13
4-methylbenzaldehyde	19.0	-	-	-	30
Mandelic acid	19.5	-	-	9.2	15
Dodecanol	24.0	-	-	1.5	51
Unknown	24.8	-	-	3.2	13
Octadecanol	37.3	-	-	-	13

Table 2-25: Compounds found in Dowex resins exposed to 10 ppm 2-dimethylaminoethanol by acidic extraction (ppb) (Experiment 12)

Compound	Retention time (min)	14 day cation resin	28 day cation resin	14 day anion resin	28 day anion resin
Unknown	5.4	-	-	11	684
Unknown	5.8	-	-	63	258
Unknown	7.3	-	-	6.5	-
Unknown	7.9	-	-	14	-
Unknown	8.5	-	-	55	-
Unknown	10.0	-	-	5.1	-
Unknown	10.3	-	-	4.2	-
Unknown	11.9	-	-	14	94
Acetophenone	12.9	-	-	11	56
Unknown	13.6	-	-	4.1	-
Unknown	15.4	-	-	-	20
Benzoic acid	15.8	-	-	5.0	120
Unknown	16.1	-	-	-	-
Unknown	17.0	-	-	1.5	-
Unknown	17.3	-	-	13	24
Unknown	18.4	-	-	12	-
4-methylbenzaldehyde	19.0	-	-	-	33
Mandelic acid	19.5	-	-	18	6.2

Unknown	22.5	-	-	3.6	-
Dodecanol	24.0	-	-	31	67
Unknown	24.8	-	-	6.6	6.7
Unknown	26.2	-	-	7.0	5.2
Octadecanol	37.2	-	-	16	5.2

Table 2-26: Compounds found in Dowex resins exposed to 2 ppm 2-methoxyethylamine by acidic extraction (ppb) (Experiment 13)

Compound	**Retention time (min)**	**14 day cation resin**	**28 day cation resin**	**14 day anion resin**	**28 day anion resin**
Unknown	5.4	-	-	39	192
2-ethylhexanol	11.6	-	-	22	31
Unknown	11.9	-	-	-	8.9
Acetophenone	12.9	-	-	40	52
Unknown	14.1	-	-	8.3	10
Unknown	15.4	-	-	18	-
Benzoic acid	15.8	-	-	52	185
Unknown	17.3	-	-	9.4	28
4-methylbenzaldehyde	19.2	-	-	-	70
Mandelic acid	19.4	-	-	-	17
Dodecanol	24.0	-	-	130	538
Unknown	24.7	-	-	-	15
Unknown	26.2	-	-	-	18

Table 2-27: Compounds found in Dowex resins exposed to 10 ppm 2-methoxyethylamine by acidic extraction (ppb) (Experiment 14)

Compound	Retention time (min)	14 day cation resin	28 day cation resin	14 day anion resin	28 day anion resin
Unknown	5.4	-	-	9.7	175
Unknown	5.8	-	-	51	-
Unknown	8.6	-	-	46	20
2-ethylhexanol	11.6	-	-	29	20
Unknown	11.9	-	-	5.2	11
Acetophenone	12.9	-	-	58	-
Unknown	14.1	-	-	11	-
Unknown	15.4	-	-	27	17
Benzoic acid	15.8	3.2	3.4	75	147
Unknown	17.3	-	-	16	22
Unknown	18.9	-	-	23	-
4-methylbenzaldehyde	19.2	-	-	-	50
Mandelic acid	19.4	-	-	14	16
Unknown	22.4	-	-	3.3	-
Dodecanol	24.0	-	-	31	345
Unknown	24.7	-	-	8.0	15
Unknown	26.2	-	-	7.5	18
Unknown	35.7	-	-	1.3	-
Octadecanol	37.2	-	-	-	14

Table 2-28: Compounds found in Dowex resins exposed to 2 ppm 5-aminopentanol by acidic extraction (ppb) (Experiment 15)

Compound	Retention time (min)	14 day cation resin	28 day cation resin	14 day anion resin	28 day anion resin
Unknown	5.1	-	-	75	100
Unknown	5.3	-	-	-	161
Unknown	6.9	-	-	116	-
Unknown	7.6	42	-	-	-
Unknown	8.6	-	-	1010	26
Benzaldehyde	9.8	-	-	-	16
2-ethylhexanol	11.6	1.6	-	197	35
Unknown	11.9	-	-	194	105
Acetophenone	12.9	-	-	-	37
Unknown	14.1	-	-	-	21
Unknown	15.4	-	-	107	34
Benzoic acid	15.8	5.8	-	-	343
Unknown	16.1	-	-	485	-
Unknown	17.0	-	-	221	-
Unknown	17.3	-	-	-	36
4-methylbenzaldehyde	19.2	-	-	374	150
Mandelic acid	19.4	-	-	-	27
Unknown	20.7	-	-	130	-

Unknown	21.3	-	-	-	26
Unknown	21.6	-	-	356	-
Unknown	22.4	-	-	-	9.4
Unknown	22.6	-	-	-	5.0
Dodecanol	24.0	-	-	82	41
Unknown	24.7	-	-	-	38
Unknown	26.2	-	-	-	31
Unknown	26.4	-	-	-	8.4
Unknown	30.6	-	-	-	2.5

Table 2-29: Compounds found in Dowex resins exposed to 10 ppm 5-aminopentanol by acidic extraction (ppb) (Experiment 16)

Compound	Retention time (min)	14 day cation resin	28 day cation resin	14 day anion resin	28 day anion resin
Unknown	5.1	-	-	75	100
Unknown	5.3	-	-	-	161
Unknown	6.9	-	-	116	-
Unknown	7.6	42	-	-	-
Unknown	8.6	-	-	18010	26
Benzaldehyde	9.8	-	-	-	16
2-ethylhexanol	11.6	1.6	-	197	35
Unknown	11.9	-	-	194	105
Acetophenone	12.9	-	-	-	37
Unknown	14.1	-	-	-	21
Unknown	15.4	-	-	107	34
Benzoic acid	15.8	5.8	-	-	343
Unknown	16.1	-	-	485	-
Unknown	17.0	-	-	221	-
Unknown	17.3	-	-	-	36
4-methylbenzaldehyde	19.2	-	-	374	150
Mandelic acid	19.4	-	-	-	27
Unknown	20.7	-	-	130	-

Unknown	21.3	-	-	-	26
Unknown	21.6	-	-	356	-
Unknown	22.4	-	-	-	9.4
Unknown	22.6	-	-	-	5.0
Dodecanol	24.0	-	-	82	41
Unknown	24.7	-	-	-	38
Unknown	26.2	-	-	-	31
Unknown	26.4	-	-	-	8.4
Unknown	30.6	-	-	-	2.5

Samples of the recirculating water in the column experiments were also analyzed. These were collected along with the resin samples and were also subjected to neutral and acidic extraction with methylene chloride followed by GC/MS analysis. None of the solutions had detectable organic species present. Therefore, it can be concluded that the concentration of any extractable compound must be below the 0.01 ppb detection limit.

Batch results

Batch reactions between different resins and aqueous ethanolamine were run in sealed bottles at 60°C for 4 weeks. The ethanolamine concentration used was set high at 1000 ppm in order to accelerate chemical reactions between the pH control agent and the resins. Dowex 650C/550OH and Rohm & Haas Amberjet resins (1600H/900OH) were tested individually and in mixed beds as outlined in Table 2-30. Before use, the Dowex 650 cation resin was converted to the ethanolamine form by reaction with excess

ethanolamine at room temperature. For each resin type, experiments were performed with 5.0 g total of resin. Experiments used either 5.0 g of anionic resin, 5.0 g of cationic resin, or 5.0 g of mixed resin 1:1 by volume. An ethanolamine blank consisted of the 1000 ppm ethanolamine solution without any added resin. In each case, the amount of aqueous ethanolamine used was 50 g. In order to make a comparison of the influence of free ethanolamine in solution, an experiment was also performed with Amberjet 1600H in the protic form. In this case, when the resin and ethanolamine solution are mixed, the majority of ethanolamine would be absorbed by the resin. Initially, ethanolamine would exchange for H ions in the Amberjet 1600H (protic) experiment; however, in all other experiments, the resin begins in the amine form so no additional ion exchange is expected. After 4 weeks at 60°C, the aqueous solution above the resins was tested for pH (pH electrode), oxygen concentration (dissolved oxygen probe), and conductivity. The ultraviolet/visible spectra of the solutions were also obtained in order to see if aromatic compounds were released by the cation resins. The results are listed in Table 2-30.

One of the objectives of using sealed containers for batch reactions was ability to assess the extent of oxidation reactions by monitoring the oxygen concentration. It was found that the oxygen consumption was markedly high in mixed beds showing a significant synergism between the two forms of resin. Interestingly, individually the Dowex 550OH anion resin and the Amberjet 1600C cation resin did not consume oxygen, correlating with the analysis of total organics released discussed previously. In the absence of cation resin, the anion resin reactions all displayed marked increases in conductivity and pH that is most likely due to release of trimethylamine groups due to

hydrolysis. The anion resins were also visibly damaged since the solutions contained fuzzy white suspensions and/or colorless crystalline shards. It appears that in the presence of the cation resin, either such damage does not occur or, more likely, the released materials are absorbed on the cation resin. The release of organic species (from both cation and anion resins) was also demonstrated by ultraviolet absorptions found in the spectra of the supernatant solutions. Essentially, all samples tested from these batch experiments (Table 2-30) displayed bands at approximately 227 or 250 nm or both. The absorptions are broad and poorly resolved and therefore difficult to quantify. For this reason, the fluorescence spectra of some of the solutions were measured. It was found that the anion resin solutions have emission at 308 and 370 nm while the cation resin has emission at 373 nm. Model compounds such as para-toluene sulfonic acid and benzyltrimethylammonium chloride were found not to contain fluorescent peaks at these positions. Thus, these peaks appear to be either due to exogenous compounds present in the resins or, they may represent a signature of the compounds produced by resin/ethanolamine interactions. The last case was proved incorrect by performing experiments with ammonia as the pH control agent. The same peaks were observed but at much lower intensity suggesting that the compounds are derived from the resins and are not products resulting from degradation of the pH control agent or its covalent linking to resin-derived organic species.

Table 2-30: Experimental results for batch reactions (125ml bottles)

Sample	pH	O_2 (mg/L)	Redox pot. (mv)	Cond. (µS)	Observations	UV abs (nm)
Dowex-650C-ethanolamine form	10.25	5.1	318	536	Clear	248s
Dowex-550OH	11.8	7.0	71	2190	Suspension & crystals	226, 245
Dowex mixed bed	10.71	2.5	52	289	Very few crystals	227w
Ethanolamine blank	10.49	6.7	174	375	Clear	None
Amberjet 1600-ethanolamine	7.2	5.7	566	284	Clear	226, 246s
Amberjet 1600H	3.29	6.7	660	162	Clear	227, 253
Amberjet 900OH	11.84	4.7	84	2310	Suspension & crystals	225, 252
Amberjet mixed bed	10.14	3.2	227	76	Clear	223s, 253w
Ethanolamine 1000ppm blank	10.51	6.8	176	330	Clear	none

The batch reactions between different resins and aqueous ethanolamine were repeated on a larger scale in sealed 2 liter bottles at 60°C for 4 weeks. In each case, the

amount of aqueous solution used was 1000 ml and the amount of resin was 100 g (mixed beds had 100 g of each resin). After 4 weeks at 60°C, the aqueous solution above the resins was tested as described above and tests for sulfate and surfactants (aromatic sulfonates), and quaternary amines were also performed. The results are listed in Table 2-31.

Table 2-31: Experimental results for batch reactions (2L bottles)

Sample	**pH**	**O_2 (mg/L)**	**Cond. (µS)**	**[SO_4^{2-}] (ppm)**	**[Surf.] (ppb)**	**[QA] (ppm)**
Dowex-650C-ethanolamine form	10.0	4.7	290	61	28	N.D.
Dowex-550-OH	10.6	4.0	240	N.D.	N.D.	45
Dowex mixed bed	10.5	3.5	170	N.D.	N.D.	N.D.
Amberjet 1600-ethanolamine form	9.9	4.3	323	19	16	N.D.
Amberjet 900-OH	10.5	3.8	249	N.D.	N.D.	53
Amberjet mixed bed	10.3	2.9	167	N.D.	N.D.	33
Ethanolamine blank	10.4	6.8	159	N.D.	N.D.	N.D.

Cond. = conductivity, Surf. = surfactants, QA = quaternary amine, N.D. = none detected

In the absence of the opposite charge ion exchange resin, the cation and anion resin reactions all displayed marked increases in conductivity. The aqueous solution in contact with the cation resins also had measurable decreases in pH. These changes are likely mainly due to release of sulfate and trimethylamine groups due to hydrolysis. In the mixed beds, the increase in conductivity was low, reflecting the ability of each ion exchanger resin to absorb ions from its opposite counterpart.

Scanning electron microscopy (SEM) was used to determine whether physical damage or adsorbed particles could be seen on the resin beads in the Dowex 650C and Dowex 500A/ 1000 ppm ethanolamine batch reactions. At the end of the reactions, the resins were separated from the aqueous solution, and then were air dried and prepared for scanning electron microscopy by coating with a thin film of sputtered gold. Samples of unused, as-received resin beads were also prepared in the same fashion. The scanning electron microscopy images of individual anion resin beads are displayed in Figure 2-9. The initial beads have very smooth, homogeneous surfaces but after one month in ethanolamine there is slight deterioration to give a few small pits as well as a few small particles on the surface. Physical deterioration was most pronounced in the anion resin used in the mixed bed. The surface had numerous pits and large patchy white areas that on higher magnification (Figure 2-10) can be seen to consist of shallow trenches and numerous raised nodules of a material that shows bright white in the scanning electron microscopy image. The latter particles show brightly since they appear to be absorbed on the resin bead's surface and are not efficiently electrically-grounded leading to charging effects in the electron beam. Elemental mapping by Energy-Dispersive Analysis of

X-rays (EDAX) in the scanning electron microscope showed that the nodules contained sulfur and can therefore be identified as particulates of cation resin. Surprisingly, the cation resin shows no physical degradation in 1000 ppm ethanolamine either by itself or in mixed bed. The magnification of a scanning electron microscopy cannot reveal loss of molecular species or small fragments from the cation resin. Instead, it can only reveal gross damage due to extensive damage to the polymer backbone as well as the adsorption of larger particles. Thus, the release of polymer fragments from the cation resin cannot be ruled out. The scanning electron microscopy images definitely demonstrate that physical deterioration of anion resins occurs when the resin is exposed to ethanolamine at elevated temperature. It can also be concluded from the results that here is a synergism in the degradation of anion resins by ethanolamine that involves the cation resin.

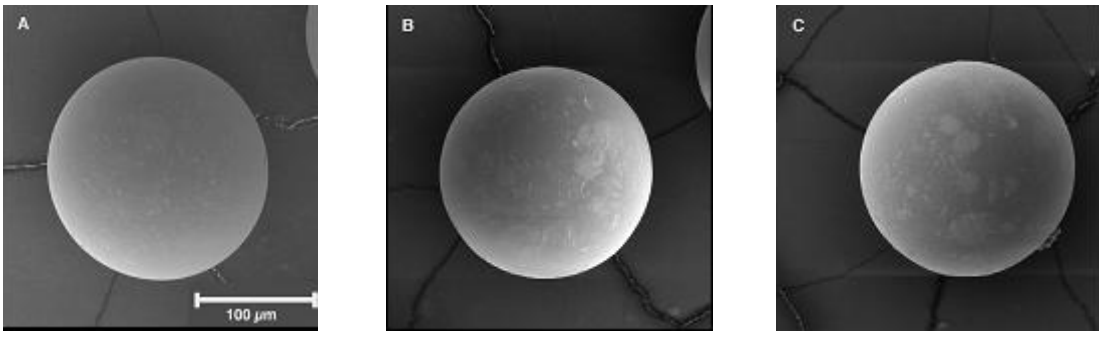

Figure 2-9. Scanning electron microscopy images of Dowex 550 anion resin beads. (A) unused, (B) 1 month in 1000 ppm ethanolamine @ 60ºC (C) 1 month in a mixed bed in 1000 ppm

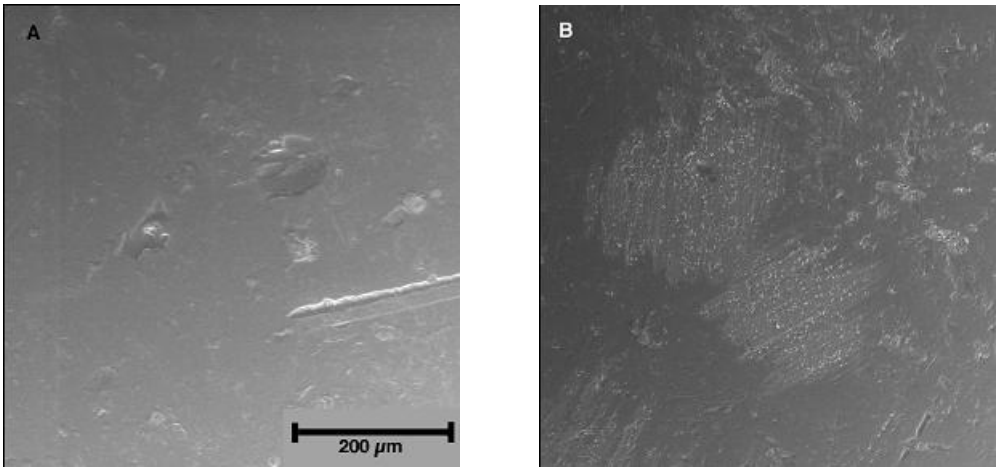

Figure 2-10: Scanning electron microscopy images of Dowex 550 anion resin beads. (A) unused (B) 28 days in a mixed bed in 1000 ppm ethanolamine at 60ºC

Discussion

In this investigation, several different pH control agents were tested at two different concentrations, 2 and 10 ppm. In all cases, it was found that the amount of degradation of resin kinetics was the greatest for the higher concentration as would be expected for a chemical reaction. However, this is not a first-order correlation indicating either multiple fouling mechanisms (some of which are independent of pH control agent concentration) or a complex chemistry with complicated kinetic parameters. The amount of organics present on the resins was also strongly dependent on the quantity and identity of the pH control agent as reflected in Figure 2-11. However, there is no direct correlation between the amount of organics and degradation of resin kinetics. This reflects the likelihood that only some of the organic species are deleterious while the others are benign. Also, in some cases (2-methylaminoethanol, 2-methoxyethylamine, and 5-aminopentanol), the total organics detected were lower for the higher concentrations of pH control agent. This might reflect a difference in pH between the

solutions of different concentrations. The degradation of anion resin kinetics versus pH control agents is presented in Figure 2-12 below. The results indicate that the degree of loss of Mass Transfer Coefficient behavior of the anion resin is dependent on the identity of the pH control agent. The specifics of this dependency are discussed below. The dependence of Mass Transfer Coefficient loss on both, the concentration and identity of the pH control agent are definite indicators of deleterious reactions involving the pH control reagents.

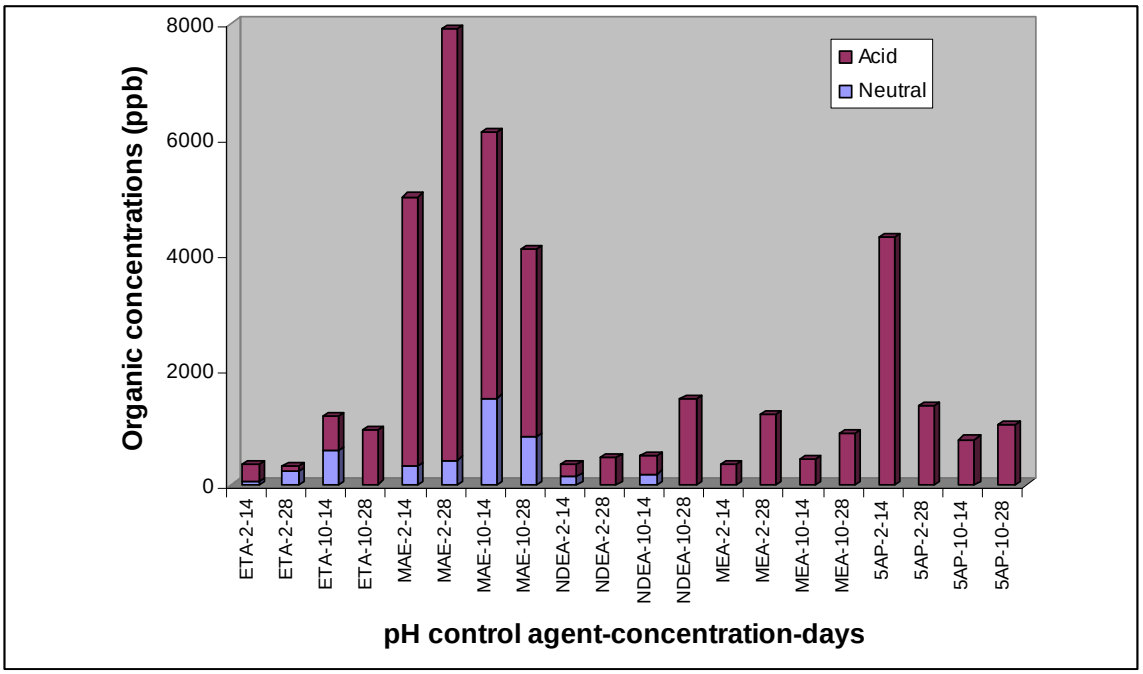

Figure 2-11: Total organics (ppb) found in anion resins

The GC/MS analysis of the anion resins showed organic content that roughly correlated with the degradation of the resin's kinetics. Most of the organic species identified were dodecanol and oxidized resin fragments, such as benzoic acid, mandelic acid, and methylbenzoic acid. The source of dodecanol is uncertain but one possibility is

that it was used as a porogen during resin manufacture. Batch experiments with resin beds in sealed bottles also demonstrated the existence of oxidation reactions since dissolved oxygen was consumed during the course of the experiments. As expected, inclusion of iron into the column experiments enhanced the resin oxidation and led to more serious degradation of anion resin kinetics.

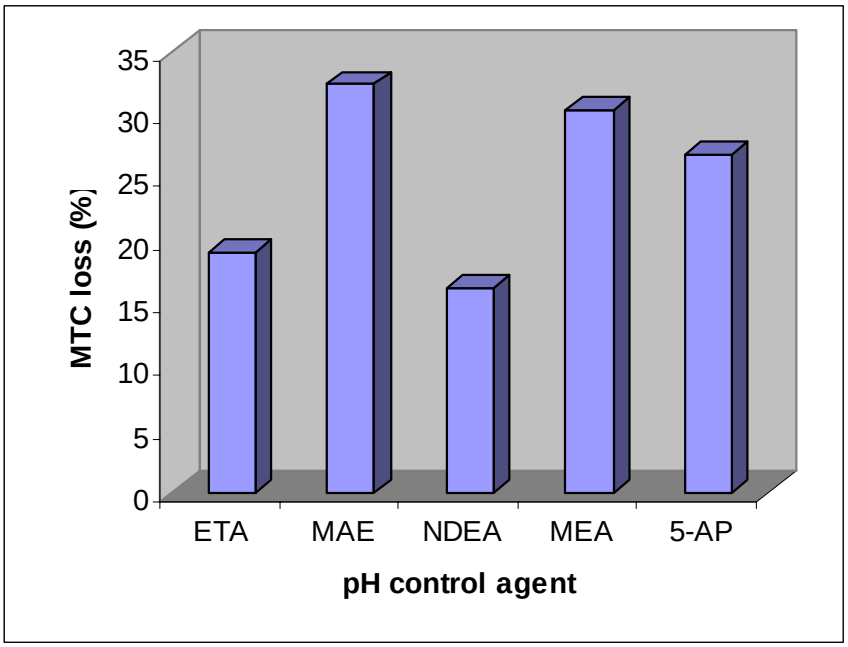

Figure 2-12: Percent anion resin Mass Transfer Coefficient loss versus pH control agent (ETA=ethanolamine, MAE=2-methylaminoethanol, NDEA=2-dimethylaminoethanol, MEA=2-methoxyethylamine, 5-AP=5-aminopentanol)

Mechanisms of resin degradation

There are numerous mechanisms, by which ethanolamine and other pH control agents can have a negative effect on ion exchange resins and these can be divided into physical

effects and chemical effects. Each mechanism is discussed below and any evidence for or against is provided.

Physical effects

Enhanced transport of non-polar organics:

The organic pH control agents can act as surfactants, since they have a combination of polar and non-polar substituents. Thus, they could enhance the solubility and transport of extraneous weakly polar or non-polar compounds present in the resin. It was found that the two monomethylated ethanolamines (2-methylaminoethanol, 2-methoxyethylamine) were associated with more organics present on the resin and lower Mass Transfer Coefficients than 2-dimethylaminoethanol, which would be expected to be the better (more alkylated) surfactant. Thus, enhanced transport due to the pH control agent can be ruled out as a major contributor to degradation of resin kinetics. This is supported by the plot of percent Mass Transfer Coefficient loss by the anion resin versus the total concentration of long chain alcohols in the resin calculated by adding the concentrations of all such alcohols from the acidic and neutral extractions of the column experiments (Figure 2-13). No correlation between resin fouling and the presence of these alcohols was observed. In this investigation, the cation resins were found to be mostly devoid of methylene chloride extractable organics. Even cation resins in the batch tests were found to contain no extractable organics. Thus, it does not appear that the release of non-polar organics by the cation resins a plausible source of foulants for the anion resin.

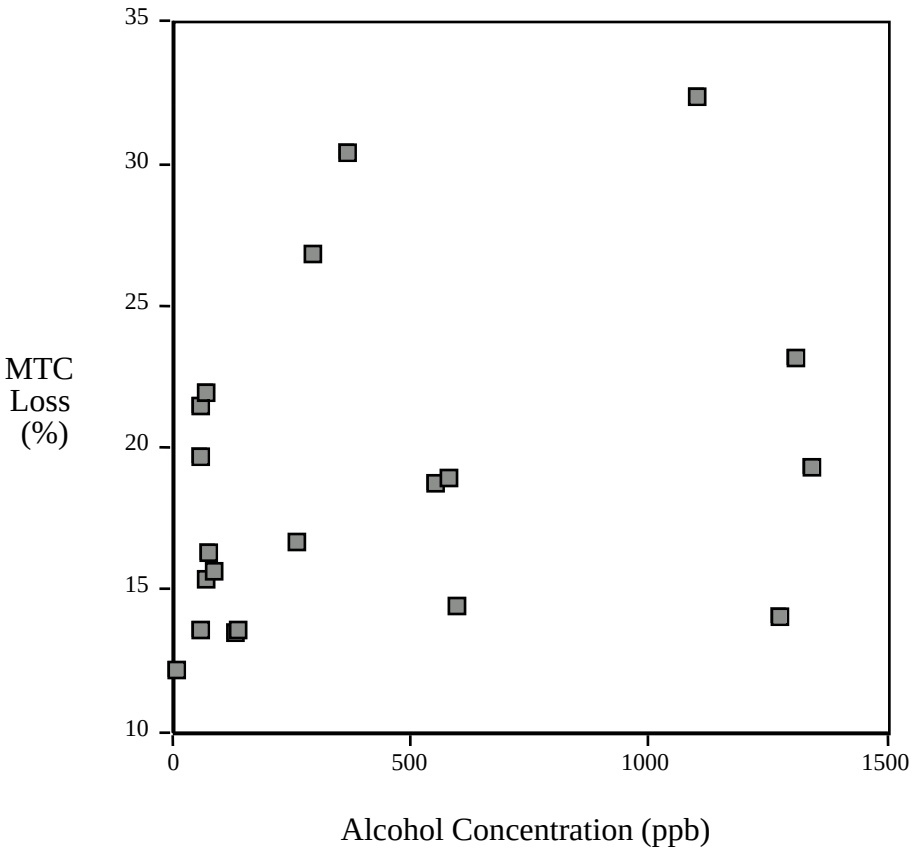

Figure 2-13: Anion resin Mass Transfer Coefficient loss versus alcohol concentration

Enhanced transport of acidic organics:

Since the pH control agents are basic, they would be expected to also tremendously enhance the transport of weakly acidic compounds, such as phenols or carboxylic acids by deprotonating these compounds and making them more water-soluble. Phenols are often detected in unused resins (probably added as antioxidants by the manufacturer). As a result, this deprotonation mechanism could be partially responsible for degradation of anion resin kinetics. A similar mechanism might also cause migration of polyacrylic acid declumping agents that are employed by resin manufacturers. Very little phenols were observed by GC/MS in the resin extracts and

tests for aqueous phenols in the batch tests were negative so phenols can be eliminated as candidates for resin poisoning. However, resin oxidation products, especially benzoic acid, mandelic acid, and 4-methylbenzoic acid are seen to collect on the anion resins and not the cation resins. Presumably, oxidation produces these acids in both resins but they are transported to the anion resin where they are bound to the ion exchange groups. Figure 2-14 shows a strong correlation between the concentrations of these species and Mass Transfer Coefficient loss in the anion resin. The slope of the linear fit corresponds to a decrease of 19% per ppm of aromatic acids. This is a rather dramatic response to a small concentration and probably reflects that the oxidation products simply serve as a measure of resin backbone damage. The non-zero intercept of 14.1 is also indicative of other mechanisms playing a role in the degradation of resin kinetics. This might also be attributed to the necessity for a specific limit to be exceeded before Mass Transfer Coefficient is affected. Nevertheless, a small contribution to anion resin fouling due to facilitated transport of acidic compounds to the anion resin is supported by the data.

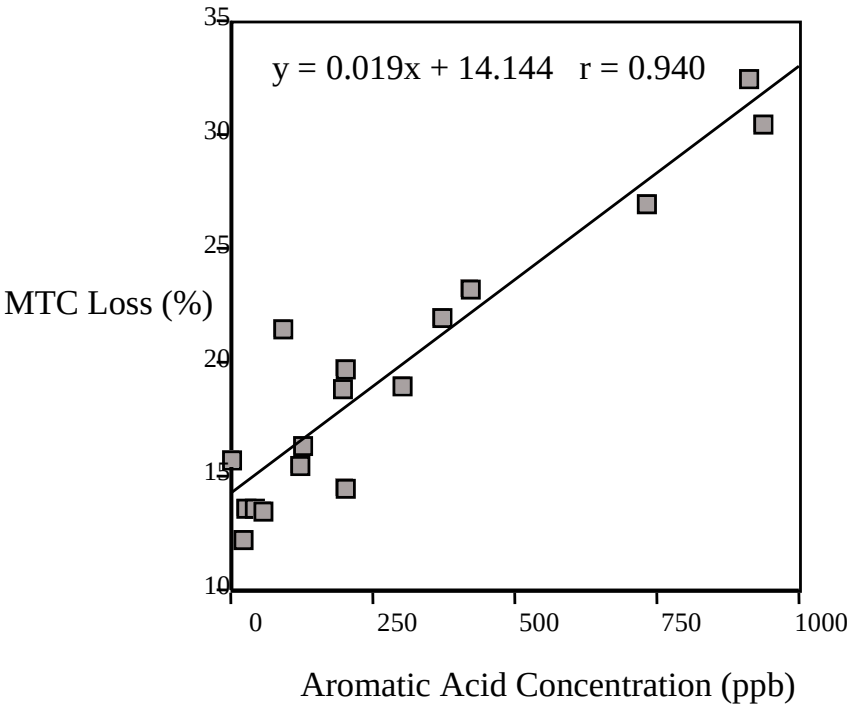

Figure 2-14: Mass Transfer Coefficient loss versus aromatic acid concentration for anion resins

Chemical effects:

Nucleophilic Attack:

In terms of chemical effects, the pH control agents can attack the resins in several ways. They can act as nucleophiles and attack either the resin backbone or the aromatic rings of the resin. Nucleophilic attack on aromatic rings is rare and cannot take place without a readily-displaced leaving group. Therefore, such reactions may be discounted. However, it is possible for amines or alcohols to displace trimethylammonium groups from the anion resin (Figure 2-15). In fact, reactions of this type involving hydroxide as the nucleophile are the reason for production of trimethylamine by the hydroxide form of anion resins and their typical fishy smell. It has been shown that thermal decomposition

of the hydroxide form of a strong base anion exchanger at 100°C gives poly(vinylbenzylalcohol) and poly(vinylbenzyldimethylamine) [11] (the formation of the latter is discussed below). The attack of hydroxide ions on the quaternary amines probably plays some role in gradual deterioration of anion resins since it replaces the ion-exchange site with a non-exchangeable alcohol group (Figure 2-16). No matter whether the trimethylamine group is displaced by a hydroxide or by a pH control agents, the final product – a benzyl alcohol or amine – is quite susceptible to oxidative attack. Indeed, the study cited above found that the initially-formed de-trimethylaminated polymers underwent oxidation to form aldehyde and acid groups and eventually oxidation of the polymer backbone occurred. Thus, nucleophilic attack of the pH control agents on the benzyl carbon of the benzyltrimethylammonium groups could precede a general oxidative degradation of the resin.

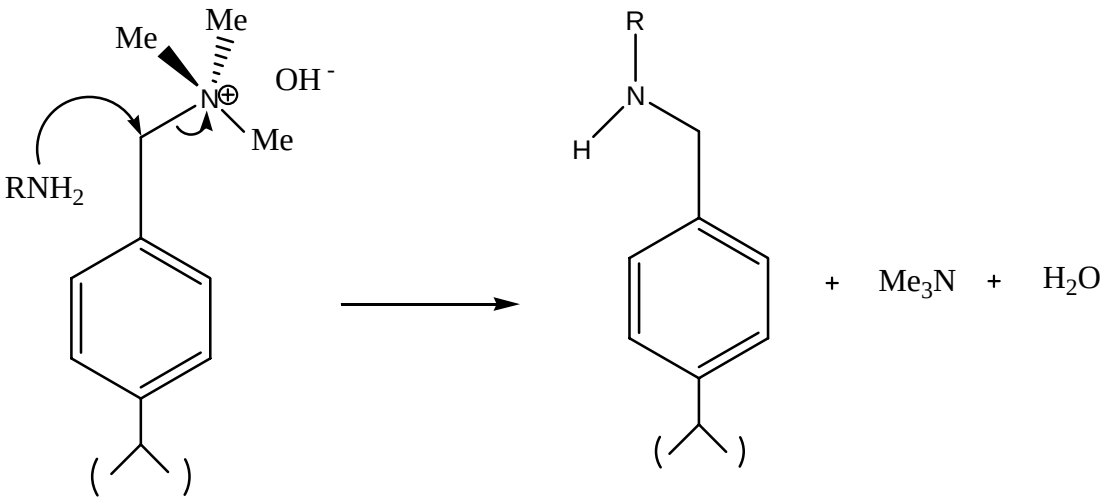

Figure 2-15: Nucleophilic attack of an amine on the benzylic carbon of a benzyltrimethylammonium group

The displacement of trimethylamine from the anion exchange resin by a primary or secondary amine would lead to kinetic degradation since strongly basic sites would be converted to weakly basic sites. However, the overall ion-exchange capacity would remain unchanged. An important point here is that displacement of trimethylamine by 2-dimethylaminoethanol would preserve a strong base ion-exchange group (Figure 2-17). This could explain, in part, the low degree of Mass Transfer Coefficient loss when using this amine as the pH control agent.

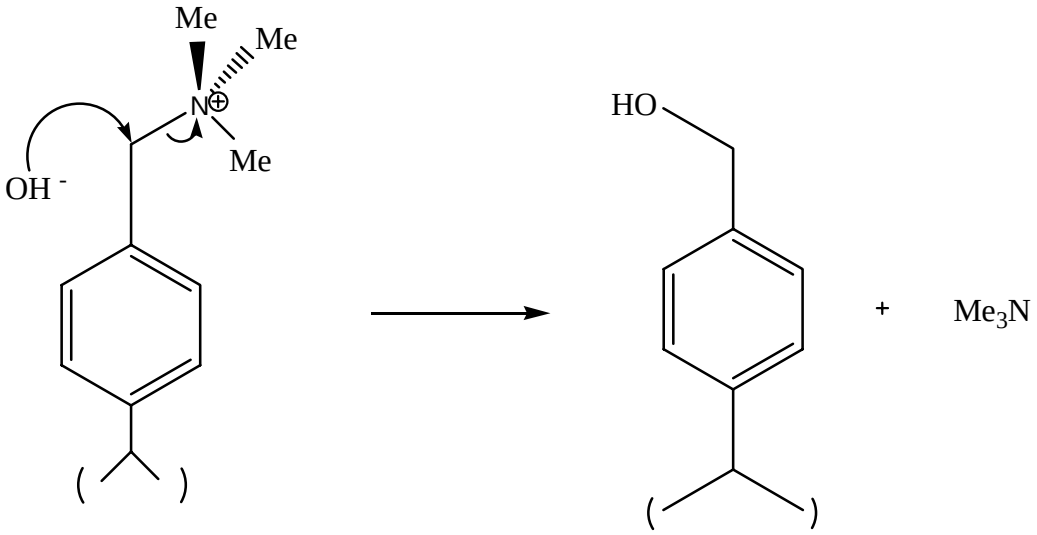

Figure 2-16: Nucleophilic attack of hydroxide on the benzylic carbon of a benzyltrimethylammonium group

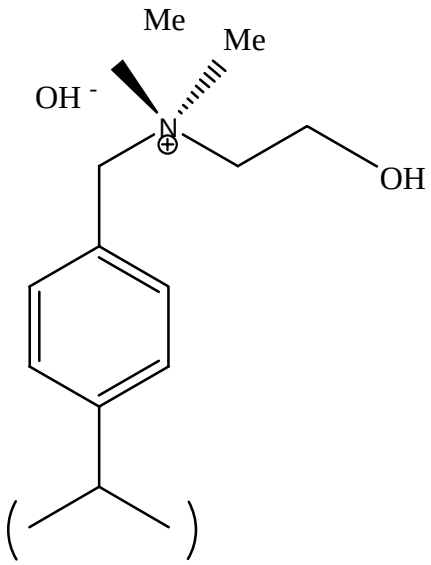

Figure 2-17: Product from attack of 2-dimethylaminoethanol on benzylic carbon of benzyltrimethylammonium group

Nucleophilic attack on the anion exchanger can also occur at one of the methyl groups of the quaternary amines. In such reaction, the nucleophile is methylated and the resin is left with a weakly basic dimethylamine group (Figure 2-18). A similar reaction involving hydroxide ion is responsible for formation of poly(vinylbenzyldimethylamine) and methanol in the thermal degradation of strong base anion exchange resins [11]. One method for prevention of alkylation is to use a base that is already fully alkylated. Again, 2-dimethylaminoethanol fits these criteria and provides second possibility for better performance of this pH control agent. Again, it is possible that either the alcohol or the amine end of the pH control agent could be alkylated. However, the comparison of the effects of a variety of pH control agents (see below) suggests that the amine group is most injurious to anion resins.

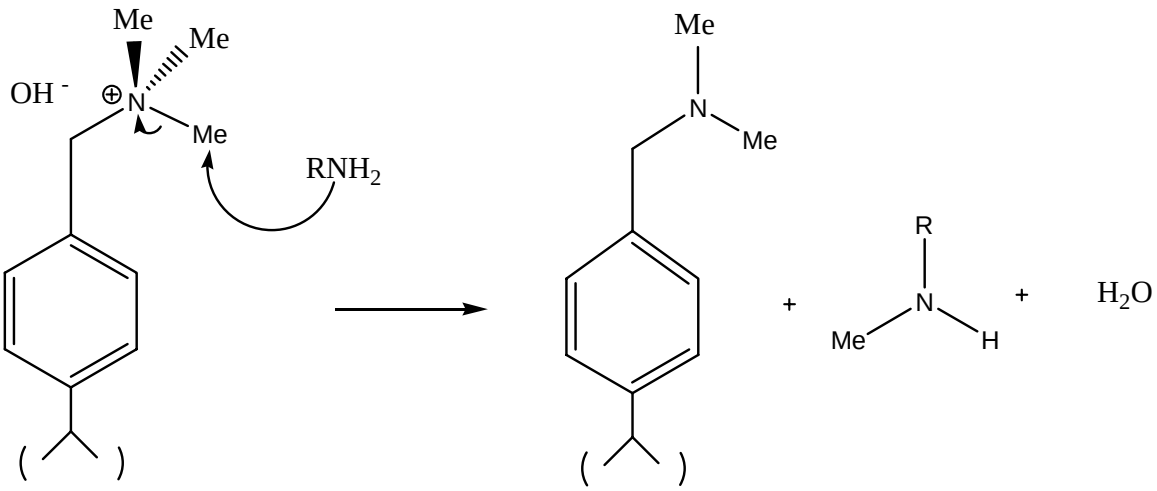

Figure 2-18: Alkylation of an amine by the benzyltrimethylammonium group

Nucleophilic attack on the resin backbone is possible because of the susceptibility of benzylic carbons. Such reactions would lead to polymer degradation, collapse of the pore structure, and generation of resin fines. It was determined using a colorimetric method in the batch reactions that aromatic sulfonates are released by cation resins when they are exposed to ethanolamine at 60°C. Furthermore, in a mixed bed, these become adsorbed on the anion resin. In fact, they build up to an extent that they can be seen by scanning electron microscopy as small nodules on the surface of anion resin beads. Elemental maping using Energy Dispersive Analysis of X-rays in the electron microscope showed that these nodules contained sulfur and were indeed cation resin. X-ray photoelectron spectroscopy also confirmed that the surface of regenerated anion resin beads still contained sulfur compounds that were not removed during the regeneration process. The strong evidence for contamination of the anion resin with cation resin fragments spurred the development of a simple method for detection of such fouling of anion resins. This involved the use of a dye, ortho-phenylenediamine, that

fluoresces under ultraviolet light when it is protonated but is non-fluorescent in the unprotonated state. When exposed to this dye, anion resin shows no fluorescence but when cation resin is present, it protonates the dye and a yellow fluorescence is observed. This provides a simple qualitative test for fouling of anion resin with cation resin fragments. Using this method with anion resin from the 28 day 5-aminopentanol experiment (a resin with low Mass Transfer Coefficient) showed definite contamination with cation resin. It definitely can be concluded that deposition of cation resin fragments does occur. The question is what role, if any, do the pH control agents play in the breaking of the resin backbone. As mentioned above, nucleophilic reactions may play a role but oxidation reactions (see below) play a definite role.

For ethanolamine (and several other pH control agents) the question arises as to whether the alcohol or amine groups are the nucleophilic substituents. Amines tend to be better nucleophiles than alcohols but this does not eliminate the possibility that the alcohol may be involved. Therefore, in this investigation, several different pH control agents were studied and the effects on the anion resin Mass Transfer Coefficients were determined. In particular, to prevent nucleophilic reactions, compounds that were completely alkylated at the alcohol group, 2-methoxyethylamine and 2-dimethylaminoethanol, were used. In the first case, the conversion of the alcohol produces an ether group that is a poor nucleophile. This is because any nucleophilic reaction would produce a highly unstable oxonium cation. In the second case, the presence of two additional methyl groups on the amine provides steric bulk that tremendously retards nucleophilic reactions. As mentioned above, column experiments were performed with both 2-methoxyethylamine and 2-dimethylaminoethanol as

well as 2-methylaminoethanol, ethanolamine, and 5-aminopetrol. The structures are shown below again for the sake of convenience (Figure 2-19).

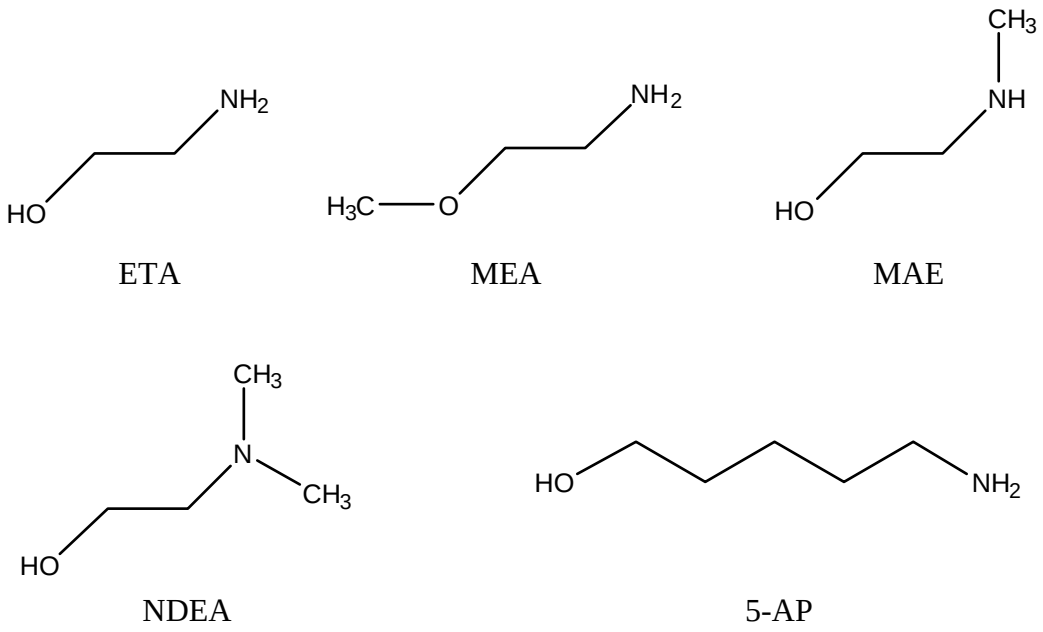

Figure 2-19: Structure of pH control agents
(ETA=ethanolamine, MEA=2-methoxtethylamine, MAE=2-methylaminoethanol, NDEA=2-dimethylaminoethanol, 5-AP=5-aminopentanol)

The degradation of anion resin kinetics versus pH control agents is presented in Figure 2-12 above. The results indicate that the alcohol terminus of ethanolamine is not the culprit in resin degradation since 2-methoxyethanolamine caused a significant decrease in anion resin kinetics. On the other hand, 2-dimethylaminoethanol gave low Mass Transfer Coefficient loss and low organic extractables. Thus, it appears that the amine terminus is responsible for resin degradation. Notably, the amine must be completely alkylated to make it relatively inert since the monomethyl derivative,

2-methylaminoethanol, is also quite destructive. Partial alkylation augments the nucleophilicity of the nitrogen atom due to electron donation from the methyl group but complete alkylation hinders nucleophilic reactions due to steric factors. Figures 2-11 and 2-12 indicate that ethanolamine is a preferred amine to 2-methylaminoethanol and 2-dimethylaminoethanol. However, even though the column experiments show a comparatively low loss of Mass Transfer Coefficient for ethanolamine, it has been our and the power industry's experience that ethanolamine appears to be quite destructive to anion resins. One cause for better ethanolamine performance in this study might be the elimination of oxygen in the column experiments. In the next section, oxidation reactions will be discussed along with the possible augmentation of them by ethanolamine.

Oxidation reactions:

Finally, the pH control agents could aggravate oxidation or other radical processes occurring within the resins by becoming involved in the propagation of radical species. The net result of such processes would be degradation of the resin, collapse of pores, and generation of resin fines.

Poor resistance to oxidation has plagued synthetic ion exchange resins since their first inception. Strong oxidizing agents can rapidly attack ion-exchange resins, but these are not generally present in condensate polishing plants. Here, the culprit for oxidation is usually oxygen gas. The oxygen levels in the experiments are likely to be higher than those in power plants, since experimentation did not use hydrazine as an oxygen scavenger. Fortunately, dioxygen generally exhibits high activation barriers for reaction with saturated organic molecules and aromatic species in the absence of catalysts.

However, in the presence of ultraviolet light, radiation, transition metal catalysts (especially iron) or elevated temperatures, resin oxidation by dissolved oxygen can proceed. In this investigation, the detection of benzoic acid, methylbenzoic acid, phenyl acetic acid, and mandelic acid is indicative of reactions releasing organic fragments from the resin. Beyond these simple compounds that are readily extracted and identified by GC/MS, oxidation of the resin backbone can also release fragments of resin. The fragments from cation resins are negatively charged and those from anion resins are positively charged. As a result, they stick quite strongly to resin beads of the opposite type of exchange resin. This can lead to blocking of ion exchange sites and occlusion of pores leading to poor resin performance. In a set of batch reactions, analyses were performed using a method for detection of surfactants, materials that are quite similar to fragments from a sulfated polystyrene cation exchange resin. It was found that these could be detected in water from a cation resin bed but not in a mixed bed. Presumably, in the latter case, the organic sulfonates were adsorbed on the anion resins. Both, cation and anion resins are susceptible to loss of their effectiveness in this manner. The damage caused by oxidation can also lead to undesirable consequences within the resin itself. This is especially true when one considers that the cross-linking dialkylbenzene groups are the most prone to oxidative attack.

Perhaps the simplest method to determine the extent of oxidation is to monitor the loss of oxygen in the system. This is most easily done with batch reactions, since sealed jars do not allow ingress of oxygen. The experiments that were run in 2L bottles with 1000 ppm ethanolamine were most notable for the consideration of oxygen uptake since they had 1L of free air space above the resin bed and solution, providing a sizeable reservoir

of oxygen. Oxygen consumption was noticeable for all resin beds whether cation, anion, or mixed (Figure 2-20). The Amberjet resins were somewhat more prone to oxidation than the Dowex resins. The mixed beds reacted with slightly less oxygen than the sum of the oxygen absorbed by the separate anion and cation resin beds. This is an unexpected result that might suggest that significant fouling might be occurring, reducing the surface area available for reaction with oxygen.

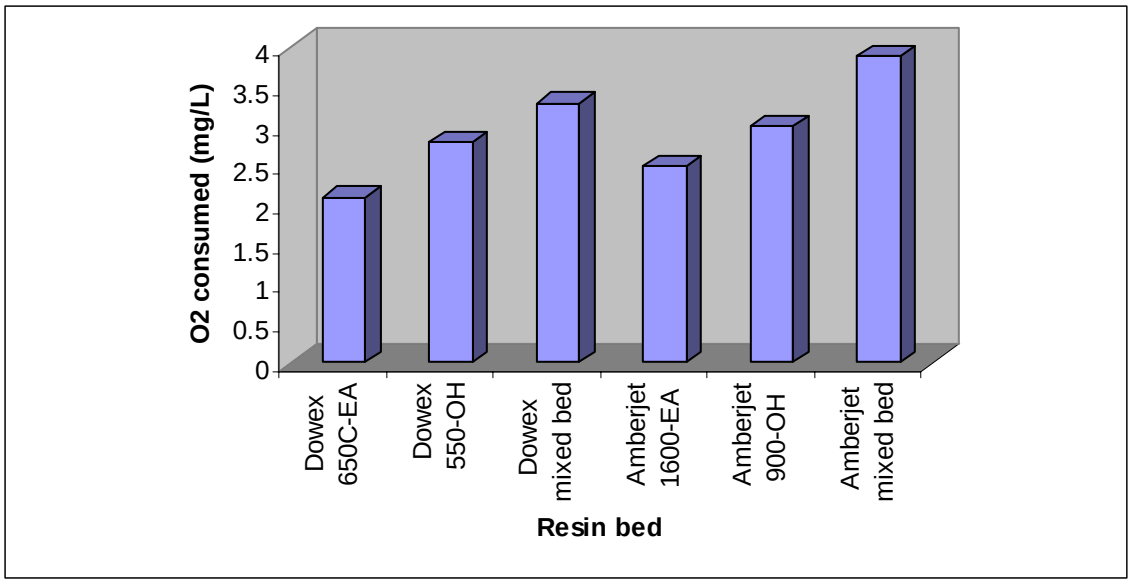

Figure 2-20: Oxygen consumption by resin beds exposed to 1000 ppm ethanolamine at 60º C for 28 days

Another parameter that provides insight into the status of redox reactions is the redox potential (Figure 2-21). In the case of reactions of various resin beds with aqueous 1000 ppm ethanolamine at 60°C, the redox potential proved quite informative. First of all, reaction of the ethanolamine blank at 60°C for 28 days resulted in slight increase in the redox potential from 127 to 165 mv. This implies a reaction of ethanolamine with

oxygen to produce a more strongly oxidizing species. In the presence of Dowex 650C cation resin in the ethanolamine form, the increase was much more dramatic to 454 mv. A smaller increase was seen for the Amberjet 1600 cation resin in the ethanolamine form to 317 mv. When oxygen is consumed, the redox potential should become smaller. Therefore, the large increase indicates the release of strongly oxidizing species from the cation resin. It would not be surprising that oxidative degradation of the cation resin would generate radical species that would be strongly oxidizing. It is also possible that the sulfonates released by the cation resin can also act as oxidizing agents. Since the rate of oxidation reactions can increase exponentially with an increase in redox potential, enhanced oxidation of anion resins in mixed beds would be expected. This is borne out by the data. In the mixed beds, only a moderate increase or a decrease in redox potential is observed suggesting that oxidizing species produced by the cation resin have reacted with the anion resin. On their own, anion resins show only a small increase in redox potential similar to that seen for the ethanolamine control solution.

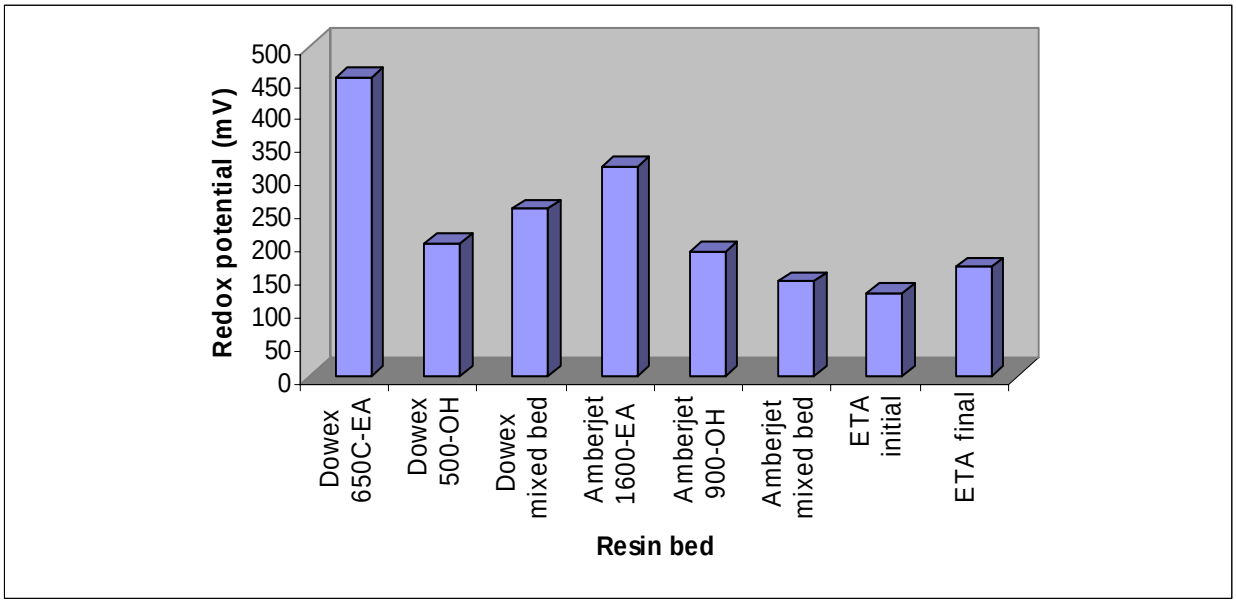

Figure 2-21: Redox potential for resin beds exposed to 1000 ppm ethanolamine at 60º C for 28 days

The involvement of ethanolamine in redox processes, as demonstrated by an increase in redox potential in the absence of ion exchange resins, raised questions concerning the behavior of the other pH control agents. The data for the reagents are presented in Figure 2-22. These are for 150 ml of 0.0164 M pH control agent (equivalent to 1000 ppm ethanolamine) heated to 60°C for 28 days in 500 ml bottles. Only ethanolamine produced a higher redox potential upon heating – all others produced lower values presumably due to oxygen consumption. This test was duplicated to confirm this effect since the result was inconsistent with the other amines. The latter reactions are in themselves alarming since they could generate carboxylic acids or other foulants. The data also suggest that ethanolamine is unique when it comes to redox reactions.

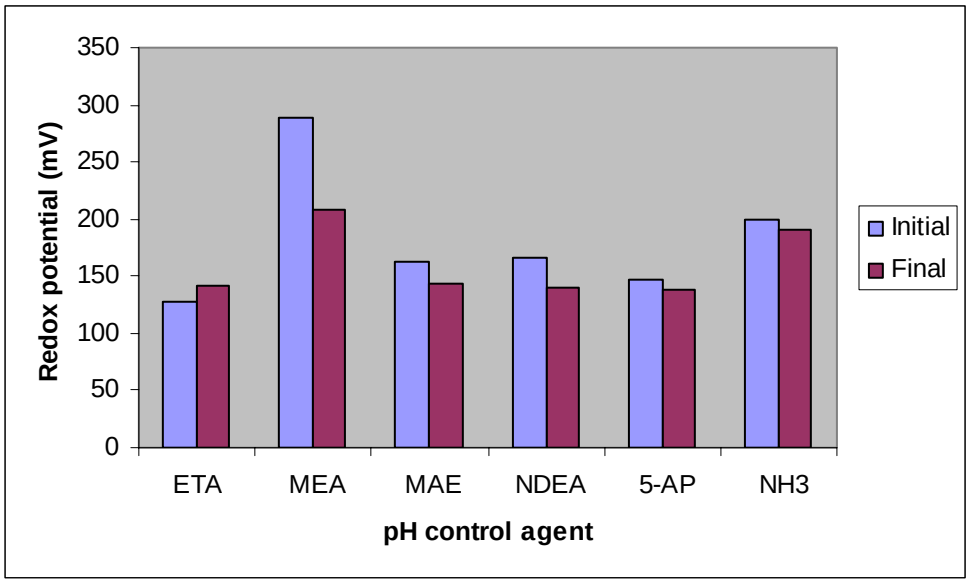

Figure 2-22: Redox potential for solutions of 0.016 M solutions of pH control agents before and after heating at 60º C for 28 days

Reactions of 100 g of Dowex cation and anion resins (each separately) with 150 ml of 0.0164 M pH control agent heated to 60°C for 28 days in 500 ml bottles gave the results presented in Figures 2-23 and 2-24. The oxygen consumed by the resin relative to that of the pH control agent blank showed very high consumption of oxygen by anion exchange resins for all pH control agents with 2-dimethylaminoethanol having the lowest oxygen consumption. Methylaminoethanol was also slightly better than the rest. On the other hand, the cation resins displayed higher oxygen consumption in the presence of 2-dimethylaminoethanol and ethanolamine with the latter being the highest. Thus, there is a complex interaction between the pH control agent and the reaction of the ion exchange resin with oxygen. The redox potentials of the solutions above the ion-exchange resins versus those of the pH control agents without resins present (Figure 2-24) also show this

complex behavior. All of the cation resins released species that made the solutions more oxidizing. This effect was quite small for ammonia but was very large for 5-aminopentanol (in this case the pH of the solution dropped to 5.2 indicating a large release of acid on consumption of 5-aminopentanol). The redox potential increase for 2-dimethylaminoethanol was also quite modest suggesting that, like ammonia, it prevents harmful release of oxidizing species from cation resins. This correlates well with the column experiments performed in this study and the results from the use of ammonia in the field. The anion resins displayed a pH control agent-dependent decrease in redox potential as would be expected for oxygen consumption.

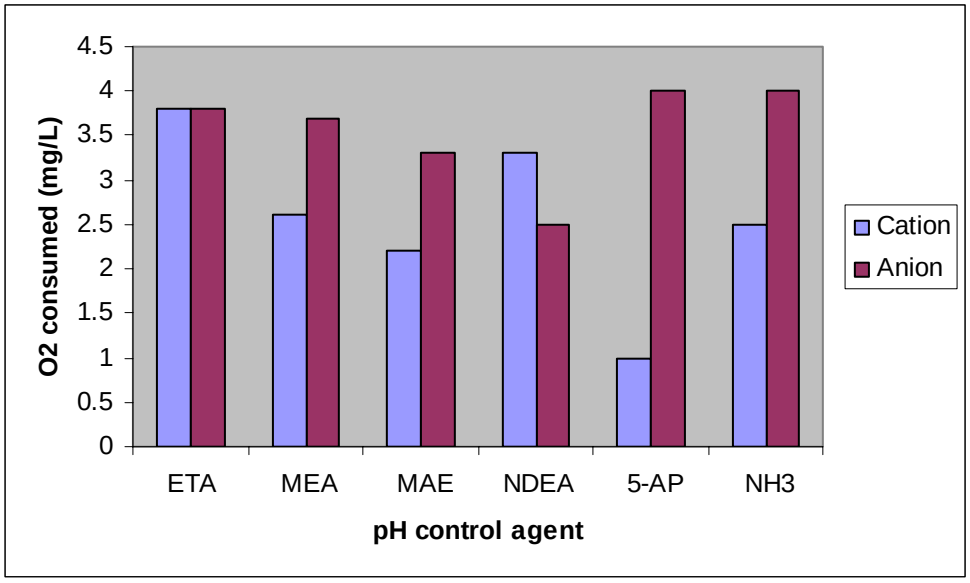

Figure 2-23: Oxygen consumed by resin in the presence of various pH control agents at 60º C for 28 days

The results of the batch experiments clearly indicate that the pH control agents are not innocent by-standers in redox processes but play a role in direct reaction with oxygen and

in release of oxidizing species from the cation resin. They could influence radical reactions by forming reactive N-oxides or N-hydroxides that could help sustain the oxidation process and/or provide the means to propagate radical reactions from one site in the resin to another. It is clear that oxidation of cation resins damages anion resins by additional mechanisms other than release of resin fragments that contaminate the anion resins.

As mentioned previously, it can be expected that iron would participate in or catalyze redox reactions. In the presence of iron, significant amounts of anion resin oxidation products were detected in acidic methylene chloride extracts (Figure 2-25). At the same time, the anion resin kinetics deteriorates to a far greater extent in the ethanolamine/iron experiments than in the ammonia/iron or ethanolamine (without iron) experiment demonstrating that ethanolamine is more injurious to resin performance than ammonia. Interestingly, iron played a protective role with respect to cation resin degradation. This might simply be due to complexation between iron and ethanolamine or reaction of iron with intermediates in the oxidation of cation resin, preventing a radical chain reaction.

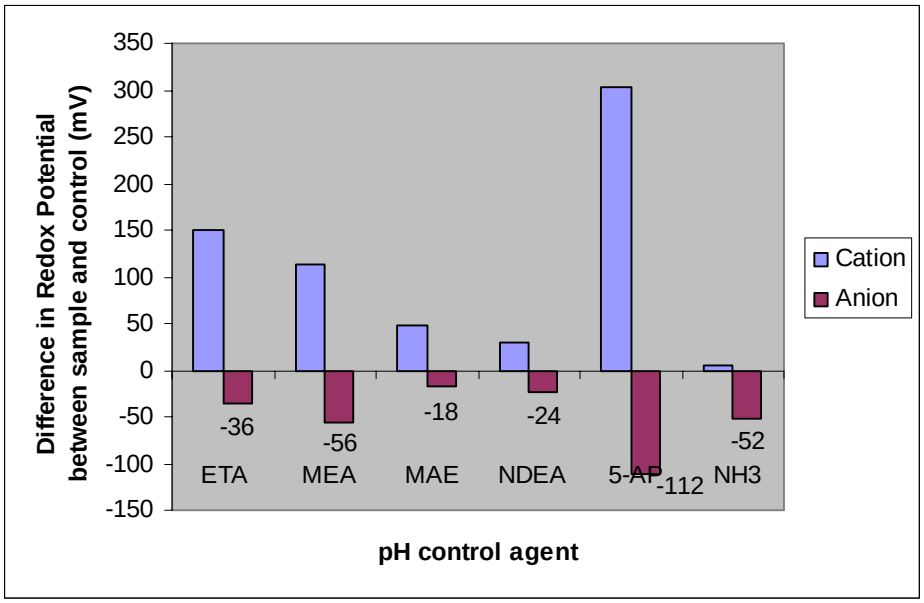

Figure 2-24: Difference in redox potential between resin/pH control agent reactions and reagent blanks after 28 days at 60 ºC

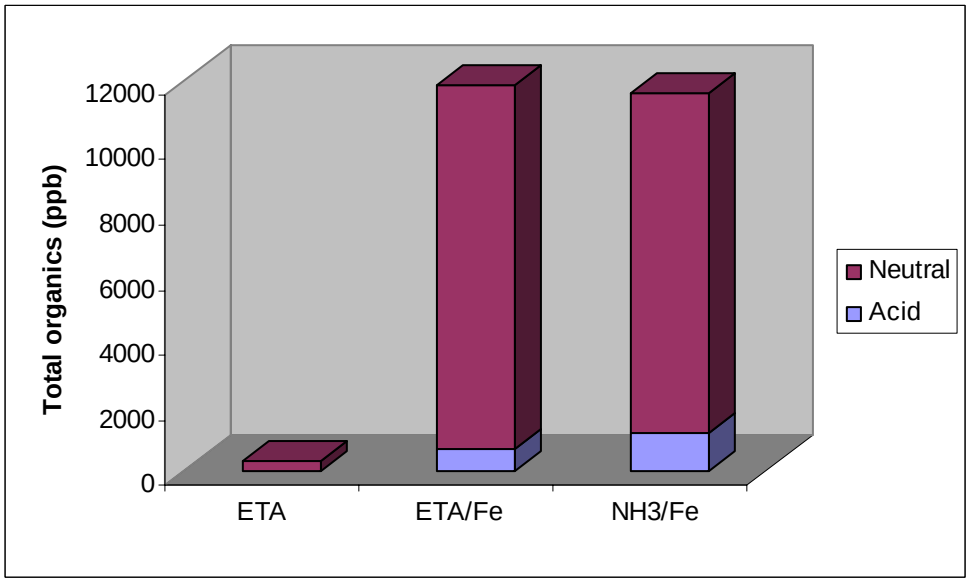

Figure 2-25: Total organics detected in iron experiments

Conclusions

This investigation has shown that there are several significant mechanisms that lead to resin fouling. It has been shown by electron microscopy that anion resin beads are eroded when heated to 60°C in aqueous ethanolamine; and in mixed beds, sulfur-containing deposits can be observed on the surface of the anion resin beads. The surmise that the latter materials are cation resin fragments was confirmed by a fluorescent labeling technique. It is most likely that these fragments are released from the cation resin by oxidation processes, confirmed through the determination of oxygen consumption and the detection of oxidation products from the resins via GC/MS analysis. However, it was discovered that the cation resins were also a source of strongly oxidizing species that likely contribute to the deterioration of the anion resin. There was also a strong correlation between degradation of anion resin kinetics with the presence of aromatic acids derived from resin oxidation. Direct reaction of the pH control agents with the resin backbones through direct nucleophilic attack is probably less important to generation of resin fragments but could influence the number and nature of ion-exchange sites. Further work is necessary to fully determine the extent of these changes. Ethanolamine was observed to react directly with oxygen and so is likely intimately involved in redox reactions. This would be in keeping with the results of experiments with deuterated ethanolamine in which the deuterium label was incorporated into the resin backbone. The change in impact on anion resin Mass Transfer Coefficient s with variation of structure of the pH control agents suggested that the amine terminus of the pH control agents are involved in detrimental attack on the resins. This would be consistent with nucleophilic attack of the pH control agent on the backbone or iron-exchange sites of the resins.

Future work can focus on the relative importance of the oxidation and nucleophilic reactions in resin degradation remains to be determined.

2-dimethylaminoethanol emerged as an excellent choice for a pH control agent that had minimal impact on the resin kinetics. This may be due to steric effects that prevent nucleophilic attack, the fact that displacement of trimethylamine by 2-dimethylaminoethanol does not result in a weak acid ion exchanger, or the failure of 2-dimethylaminoethanol to participate in and exacerbate oxidation reactions. A combination of all three properties might be responsible for the superior performance of 2-dimethylaminoethanol. Although 2-dimethylaminoethanol had improved stability compared with ethanolamine, it has yet to be evaluated for application to steam cycle water chemistry. Complete volatility data, thermal stability pH as a function of temperature and selectivity coefficients would need to be studied in detail before 2-dimethylaminoethanol could be recommended as an alternative amine. Some data are available. For example the boiling point of 2-dimethylaminoethanol is 133°C compared to 170°C for ethanolamine. 2-dimethylaminoethanol's vapor pressure at 20°C is 4 mm Hg while that of ethanolamine is 0.2 mm Hg. These results indicate that 2-dimethylaminoethanol is likely to be more volatile than ethanolamine and prefer the vapor phase to the liquid phase. This might limit 2-dimethylaminoethanol as a pH control agent in crevices. On the other hand 2-dimethylaminoethanol is significantly less volatile than ammonia as indicated by Yuzwa [12].

Key conclusions

1. Ethanolamine does interact with ion exchange resin and has been confirmed to interact with the cationic backbone.
2. The actual chemical mechanism for ethanolamine requires additional illumination.
3. Cationic fragments migrate and deposit onto the surface and within the pores of anionic resins.
4. If ethanolamine is used in condensate polishing, reactions with the ion exchange resins will occur and should be expected. However, efforts to minimize the impact of ethanolamine – such as the use of macroporous anion resins – can delay the effects of ethanolamine.
5. 2-dimethylaminoehtanol appears to be a possible alternative amine because it is likely to interact with resin to a much lesser degree than ethanolamine.

References

1. Passell, T.O.; Welty, C.S.; Hobrart, S.A. *Progress in Nuclear Energy* **1987**, *20*, 235-54.
2. Nordmann, F. Proceedings of 14th International Conference on the Properties of Water and Steam, Kyoto, Japan, August 29 - September 3, 2004.
3. Klimas, S.J.; Petralik, J.H.; Fruzzetti, K.; Tapping, R.L. Proceedings of 2003 ECI Conference on Heat Exchanger Fouling and Cleaning: Fundamentals and Applications, Santa Fe, NM, May 18-22, 2003.
4. Millett, J.P., Fruzzetti, K. *PowerPlant Chemistry* **2005**, *7*, 599-603.
5. Miller, A.D. *Final Report TR-103042;* Electric Power Research Institute: Palo Alto, CA, 1993.
6. Alther, G.R. Preventing resin and membrane fouling with clay prepolish. www.biomininc.com/the_analyst_article.htm.
7. Gonder, B.Z.; Kaya, Y.; Vergili, I.; Barlas, H. *Desalination* **2006**, *189*, 303-307.
8. *Condensate polishing guidelines for PWR and BWPR's;* Electric Power Research Institute: Palo Alto, CA, 2004.
9. Raught, D.P.; Foutch, G.L.; Apblett, A.W. *Power Plant Chemistry* **2005**, *7*, 741-747.
10. *Investigation of ETA Interactions in Mixed Bed Ion Exchange Systems: Phase I*; Electric Power Research Institute: Palo Alto, CA, 1003599, 2002.
11. *Investigation of ETA Interactions in Mixed Bed Ion Exchange Systems: Phase II;* Electric Power Research Institute: Palo Alto, CA, 1003613, 2003.

12. Yuzwa, G.F. *Corrosion protection of condensate systems.* Presented at Alberta Public Works, Water Treatment Coordinators' meeting #27, Alberta Reynolds Museum, Wetaskiwin, Alberta, April 15, 1998.

CHAPTER III

SYNTHESIS OF NANOMETRIC AGGREGATES OF IRON, ZINC, NICKEL AND ALUMINUM OXIDE FROM ION EXCHANGE RESINS

Introduction

Transition metal oxide nanoparticles have applications in numerous areas. In the field of medicine, nanometric metal oxides are used for enhancing of magnetic resonance imaging (MRI), tissue repair, bioanalysis, biosensing, detoxification of biological fluids, controlled drug delivery, cell separation [1,2], and cancer diagnosis [3.] Nanoscale metal oxides can also be used to help identify Bacillus anthracis – an agent that may be used in bioterrorism.[4] Other uses of nanoparticulate metal oxides include metal coating [5], dye degradation [6], optoelectronics, antimicrobial agents, tailored UV absorption [7], cosmetics additive, and catalytic materials [8.]

Nanostructured materials are increasingly being used in novel applications in various areas of science, one such area being pollution remediation and water treatment.[9] The higher chemical reactivity of nanoparticles, as compared to their bulk counterparts, arises from their smaller sizes, higher surface areas, unusual crystal shapes, and lattice orders that lead to greater adsorption of the contaminant species on their surfaces.[10] In spite of these apparent advantages, their practical application in water purification is hampered by their facile suspension issues in water leading to clogging of filters, and high pressure

requirements. In this investigation, a breakthrough in water treatment technology was achieved by the utilization of agglomerated nanoparticles.[11] Suitably porous agglomerated nanoparticles overcome the above mentioned setbacks quite conveniently without losing too much of their chemical reactivity. They also have other advantages, such as ease of packing in a column and maximum interaction with the flowing media due to their spherical shape. This would also enhance their activity and application in the field of catalysis. These benefits and necessity of taking advantage of nanometric materials for practical applications have fuelled this investigation in order to develop synthetic routes to prepare nanometric metal oxides with relative ease and convenience. The synthesis of nanometric aggregates of iron, zinc, nickel, and aluminum oxides will be discussed in this chapter. A detailed account of the utilization of agglomerated nanoparticles for water treatment and catalysis will be given in Chapter IV.

Synthesis of Spherical Aggregates of Iron Oxide

Experimental:

The resin used was Dowex 650C (H) form resin, a cross-linked sulfonated polystyrene-divinylbenzene polymer that was purchased directly from Aldrich in the form of monodisperse spherical beads. These resin beads were used to exchange Fe^{+3} with exchangeable H^{+} in order to get iron loaded resin beads. Iron loaded resins were obtained by using Dowex 650 cation exchange resin (20.0 g, 58.0 mmol of ion-exchange sites), which was stirred for 12 hours with a solution of iron(III) chloride hexahydrate (32.44 g, 120 mmol) in water (100 ml). Since ferric ions are trivalent, the determined iron concentration would be three times lower as compared to that of Dowex Cation exchange

resins (i.e. exchange of 3 H^+ for each Fe^{+3} in order to maintain charge neutrality). The supernatant solution was poured off and the iron chloride treatment was repeated with fresh solution. After stirring for 12 hours, the resin was isolated by filtration, washed extensively with distilled water, and air-dried. This general scheme was used in order to prepare other nanometric transition metal oxide agglomerates. This is shown below in Scheme 3-1.

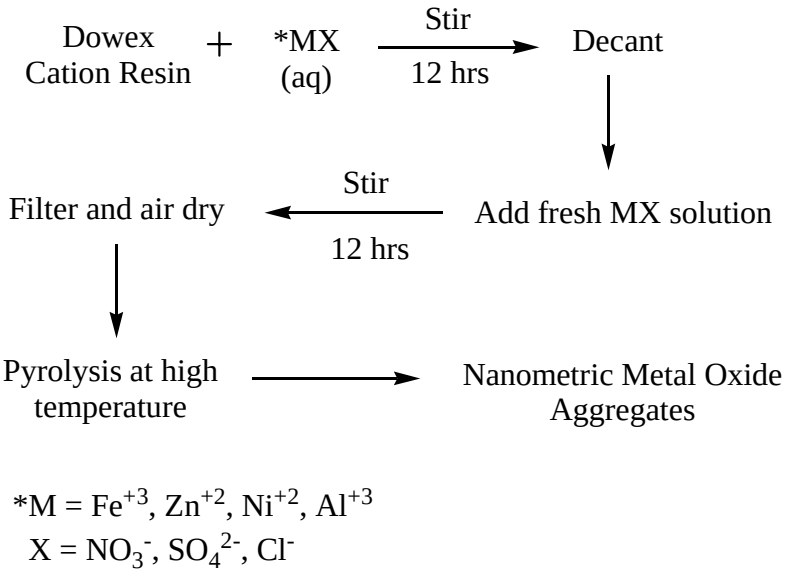

Scheme 3-1: General scheme for the synthesis of nanometric metal oxide aggregates

Characterization:

The iron loaded material was characterized using following techniques:

Thermogravimetric Analysis (TGA):

Bulk pyrolysis at various temperatures was performed in ambient air in a muffle furnace using a ramp of 5 °C/min and a hold time of 12 hr. Nanocrystalline iron oxide was obtained by firing the resulting resin (15.0 g) at 550^{o}C under the foresaid conditions.

The iron oxide (2.3 g) was obtained in a 14.9 % ceramic yield as dark red spherical aggregates of an average diameter around 170 µm.

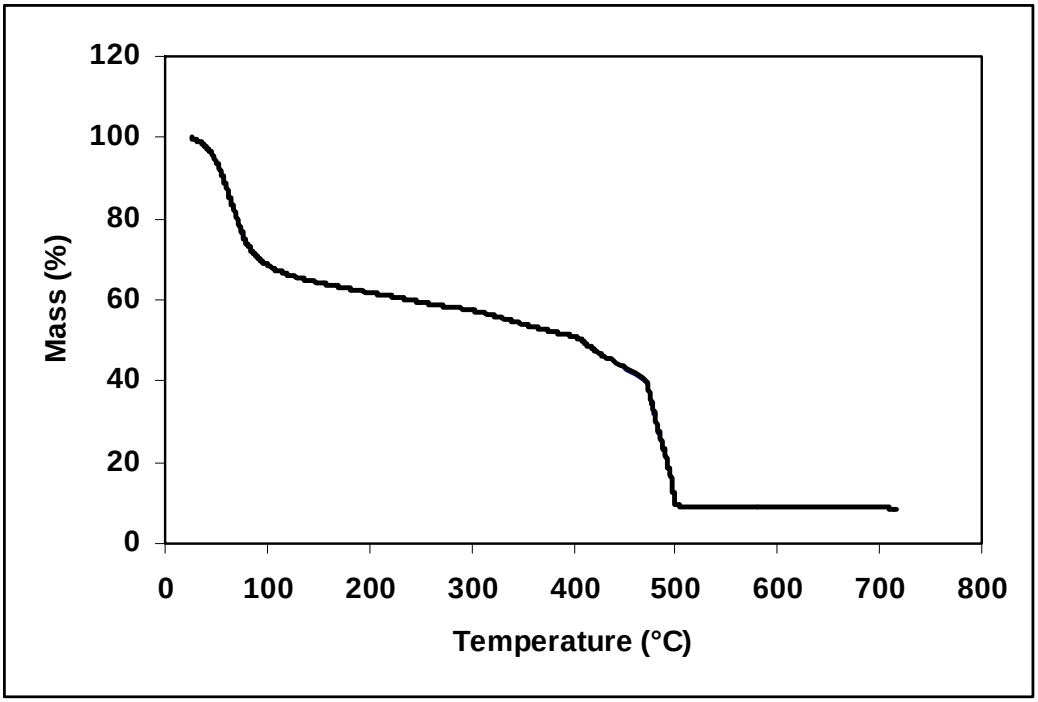

Figure 3-1: Thermogravimetric analysis trace for iron loaded cation exchange resin

The thermal gravimetric analysis (TGA) trace for the iron-exchanged resin is shown in Figure 3-1. Thermogravimetric studies were performed using 10-20 mg samples on a Seiko ExStar 6500 TGA/DTA instrument under a 50 ml/min flow of dry air. The temperature was ramped from 25°C to 600°C at a rate of 2°C/min. The material loses approximately 35.8% by weight of the water between room temperature and 152 ºC. Above this temperature, gradual decomposition of the ion-exchange resin occurs up to 391 ºC and a sharp decrease in mass starts to occur that eventually becomes quite rapid and culminates in the formation of iron oxide at 510 ºC. During the latter step, extensive evolution of sulfur dioxide occurs, so care must be taken to vent the fumes to a hood. A

sample prepared by pyrolysis at a temperature just lower than that of the final weight loss step of 385 ºC was found to be a hygroscopic while solid, which was obtained in a ceramic yield of 35.6 %. This weight indicates that much of the carbon remains in the sample and the material is not ferric sulfate. Diffuse reflectance infrared spectroscopy confirms this because the spectrum contains three strong bands at 1230, 1134, and 1034 cm^{-1} that are typical of aromatic sulfonates[12] and are unlike the absorptions due to sulfate observed for anhydrous ferric sulfate (1138 and 1073 $cm^{-1)}$. Absorptions that can be attributed to organic carbon are also observed at 2899, 2836, and 1420 cm^{-1} in the spectrum of the sample.

X-Ray Diffraction:

X-ray powder diffraction (XRD) patterns were recorded on a Bruker AXS D-8 Advance X-ray powder diffractometer using copper K_α radiation. The X-ray diffraction pattern (Figure 3-2) was matched to hematite pattern in the International Center for Diffraction Database (ICDD).

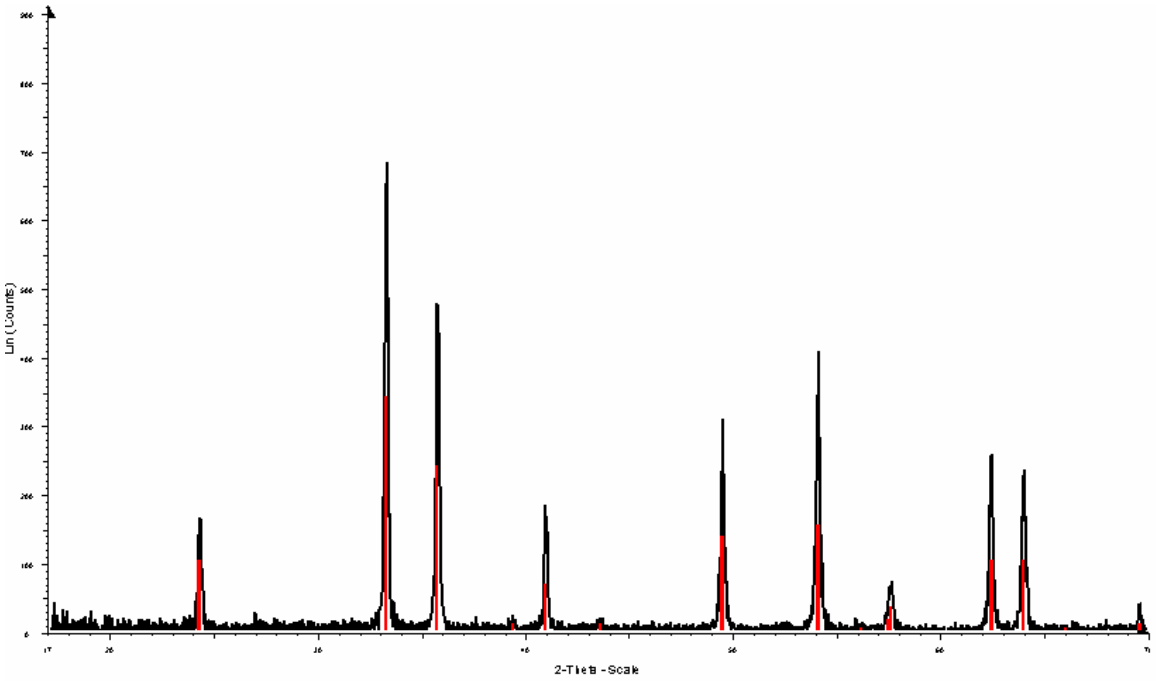

Figure 3-2: X-ray diffraction pattern of iron loaded cation exchange resin heated to 550ºC

Crystallite Size Analysis:

The observed X-ray reflections were broadened as compared to a highly crystalline sample of hematite, so the crystalite size of the particles was analyzed. This was done by profiling the broadened peaks with a Pearson 7 model using Topas P version 1.01 software (Bruker Analytical X-ray systems, Madison, WI, USA, 1997). Bruker's CrySize program uses the Warren-Averbach evaluation method to determine crystallite size. The result of this analysis, shown in Figure 3-3, revealed an average crystallite size of 12.0 nm, with a somewhat broad distribution (16.9 nm full width at half-height). The maximum in relative frequency of crystallite size occurs at 6.9 nm.

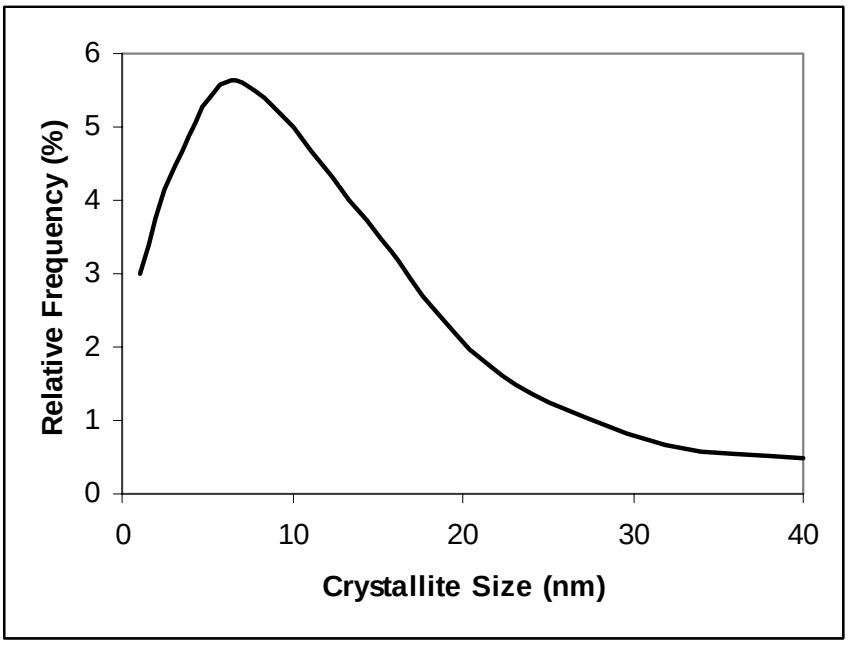

Figure 3-3: Crystallite size analysis of spherical nanometric hematite aggregates[13]

Scanning Electron Microscopy:

Scanning electron microscope images were taken using a JEOL JXM 6400 Scanning Electron Microscope at Oklahoma State University Microscopy Lab.

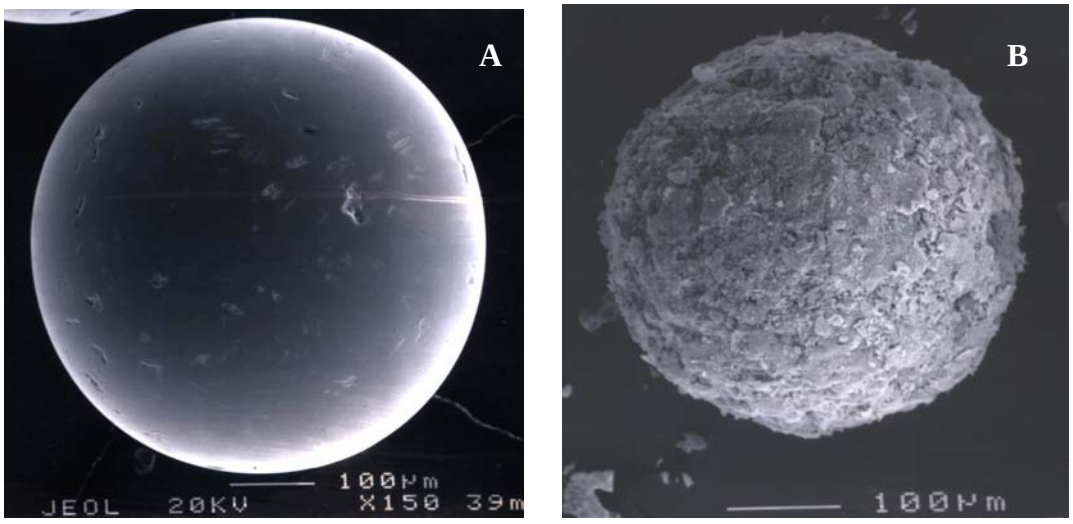

Figure 3-4: Scanning electron microscopy images of iron loaded resin A) after B) before pyrolysis at 550 ºC[5]

The images show that the particles are spherical with an average diameter of 170 μm and are porous aggregates of smaller particles. The spheres consist of condensed Fe_2O_3 throughout and are composed of aggregates of nanoparticles that are further fused together to yield the larger spherical particles as shown in Figure 3-4. The spheres are fairly mechanically robust and do not break into smaller particles when shaken vigorously within a glass vial. However, they can be easily crushed into fine powder with an agate mortar and a pestle. The final product (after the pyrolysis) has a low density of 2.4 g/cm^3 as determined by Archimedes method.

The spherical hematite agglomerates were casted into a polymer block and cut horizontally in order to see the cross sectional view of the agglomerates. This revealed highly porous interior part of the spherical agglomerates. There were many channels and pores, which were created when the resin backbone was pyrolysed. The remaining iron oxide crystallites fused in order to form the porous structure as shown in Figure 3.5 A), which shows scanning electron microscope image of the hematite sphere cut open.

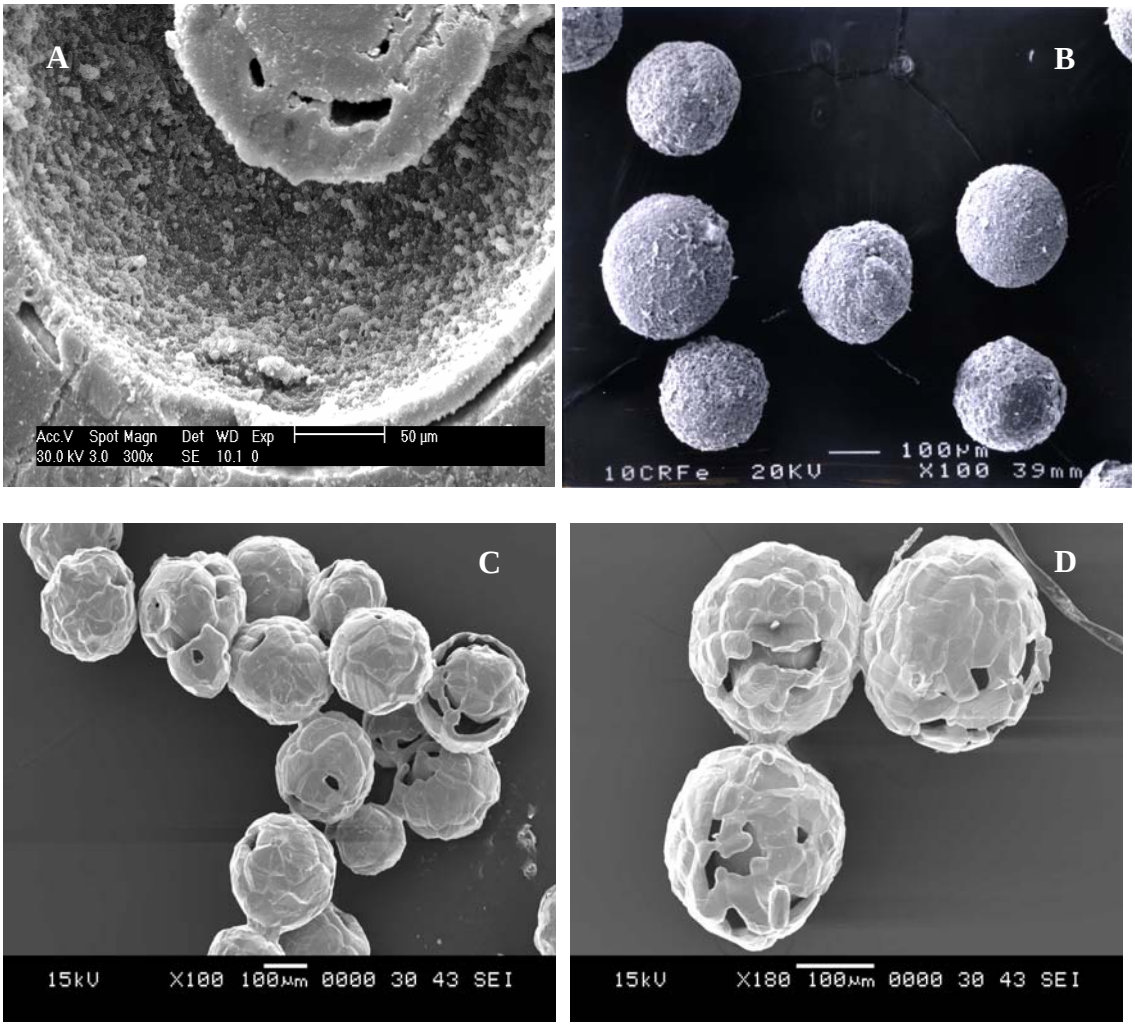

Figure 3-5: Scanning electron microscope images of hematite agglomerates

A) cross- section at 550ºC, B) 1000ºC, C) 1300 ºC, and D) 1500 ºC

Shrinkage of Hematite Spheres on Sintering:

The agglomerates of iron oxide were heated at various temperatures and their reduction in size as well as the surface area was analyzed (Table 3-1). Also, the reduction in their surface area at higher sintering temperatures was measured. Surface areas were measured by nitrogen adsorption isotherms on a Quantachrome Nova 10 instrument using the

Brunauer, Emmett, and Teller analysis method and six points in the range 0.05 to 0.3 P/P_0.

Table 3-1: Effect of sintering on the diameter and surface area of hematite agglomerates

TEMPERATURE (ºC)	**SHRINKAGE (%)**	**SURFACE AREA (m^2/g)**
550	71.42	30.0
700	57.41	4.8
800	46.60	2.8
900	42.23	0.8
1000	41.45	0.4

On sintering, the hematite agglomerates showed a shrinking in their size. The original resin was heated at different temperatures from 550ºC up to 1500ºC and their diameter was measured. Their diameters were compared against diameter of dry untreated Dowex 650H cation resin bead. It can be seen from Table 3-1 that there is a steady increase in the percentage shrinkage of the agglomerates with increasing temperatures. Scanning electron microscopy images revealed that the particles are getting fused together and are forming a group of spheres adhering together through fused ends. Above 1200 °C, the formation of large Fe_2O_3 crystalites is obvious. Their growth depletes material in some areas of the aggregates leading to open holes and channels. Unfortunately, the particles do not sinter to dense spherical Fe_2O_3 spheres. The spheres got harder with increasing temperature but still could be crushed to powder form using an

agate pestle and mortar. The analysis of their shrinkage as a function of sintering temperature has been plotted in Figure 3-6 shown below.

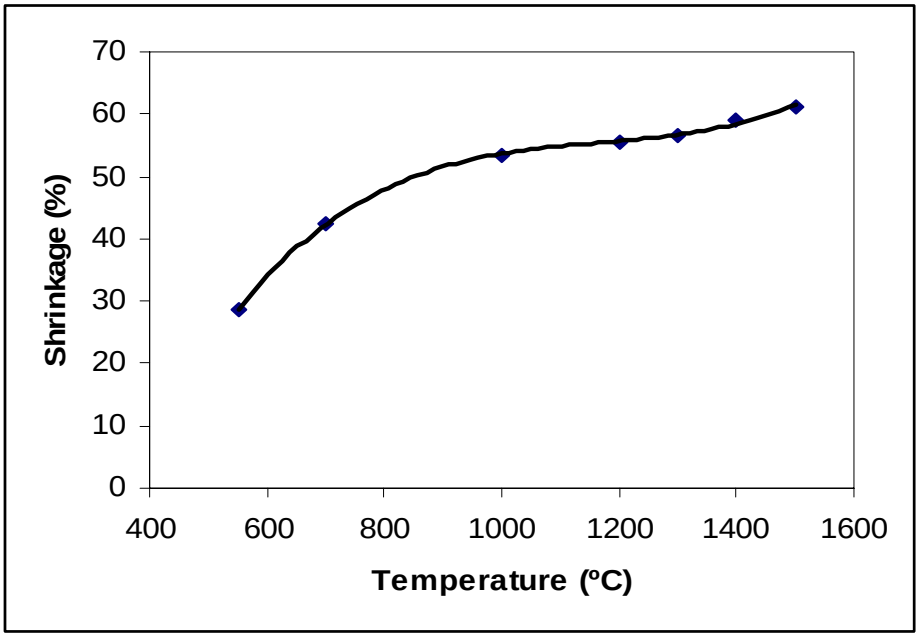

Figure 3-6: Effect of sintering temperature on the size of the hematite agglomerates

The surface area of agglomerates was analyzed by Brunauer, Emmett, and Teller method as mentioned previously. Samples from different temperatures were used in order to see the sintering effect on their surface area. Surface area values showed an exponential decrease with the sintering temperature. This behavior is shown in Figure 3-7 below.

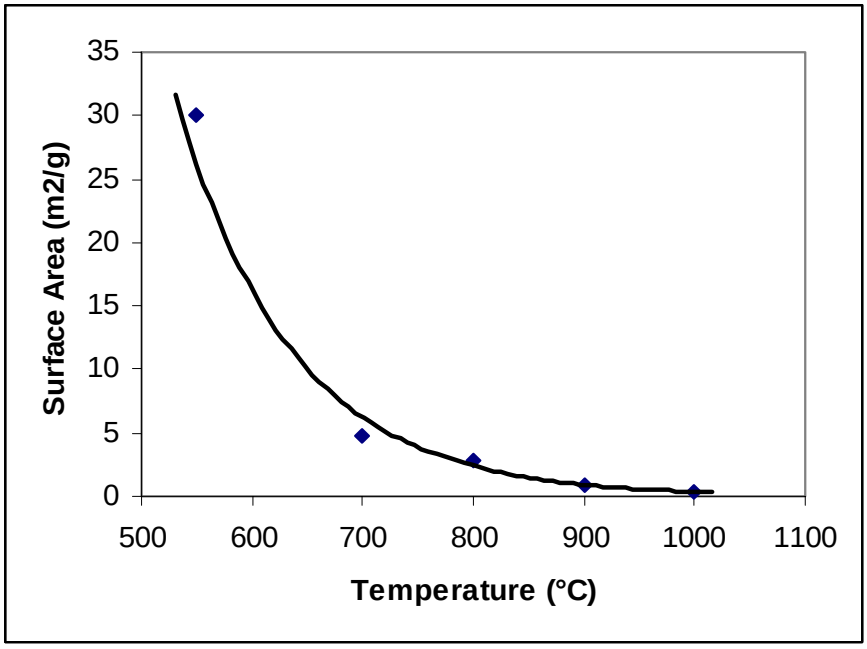

Figure 3-7: Effect of sintering temperature on surface area of hematite agglomerates

Synthesis of spherical aggregates of zinc oxide nanoparticles

Experimental:

The synthesis of nanometric agglomerates of zinc oxide was carried out similarly to that of hematite aggregates. Dowex 650C (H) form resin (20.0 g, 58.0 mmol of ion-exchange sites) was stirred for 12 hours with a solution of zinc sulfate (34.5 g, 120 mmol) in water (100 ml). The supernatant solution was poured off and the zinc sulfate treatment was repeated with fresh solution. After stirring for 12 hours, the resin was isolated by filtration, washed extensively with distilled water, and air-dried as shown in general Scheme 3-1 previously. Nanocrystalline zinc oxide was obtained by firing the resulting resin (15.0 g) at 560^{o}C for 8 hours using a ramp rate of 4^{o}C per minute to raise the temperature from room temperature to 560^{o}C. The zinc oxide (2.41g) was obtained in

a 16.0 % ceramic yield as pale yellow spherical aggregates. The material obtained was characterized using various techniques.

Characterization:

Thermogravimetric studies were performed as previously mentioned. The plot of temperature versus percent mass showed a similar profile to that of iron loaded cation resin. Thermal gravimetric analysis demonstrated that this material loses approximately 25% by weight of water between room temperature and 300^{o}C. At 360^{o}C gradual decomposition of the ion exchange resin occurs until 490˚C when a sharp decrease in mass starts to occur that eventually culminates in formation of zinc oxide at 560˚C. Thermogravimetric analysis of the zinc loaded cation resin is shown in Figure 3-8 below.

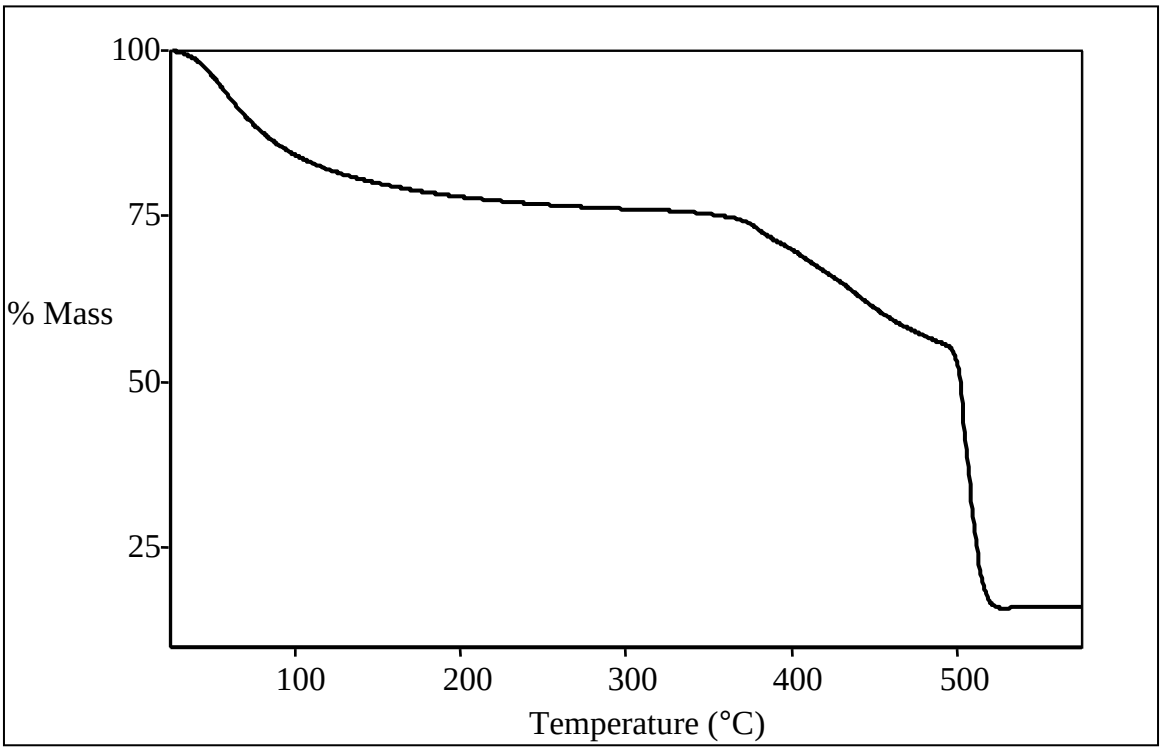

Figure 3-8: Thermogravimetric analysis of zinc loaded Dowex cation resin

X-ray powder diffraction (XRD) patterns were recorded as mentioned previously. The X-ray diffraction pattern (Figure 3-9) was obtained and was compared to the International Center for Diffraction Database (ICDD), which confirmed the identity of the material to be zincite (ZnO).

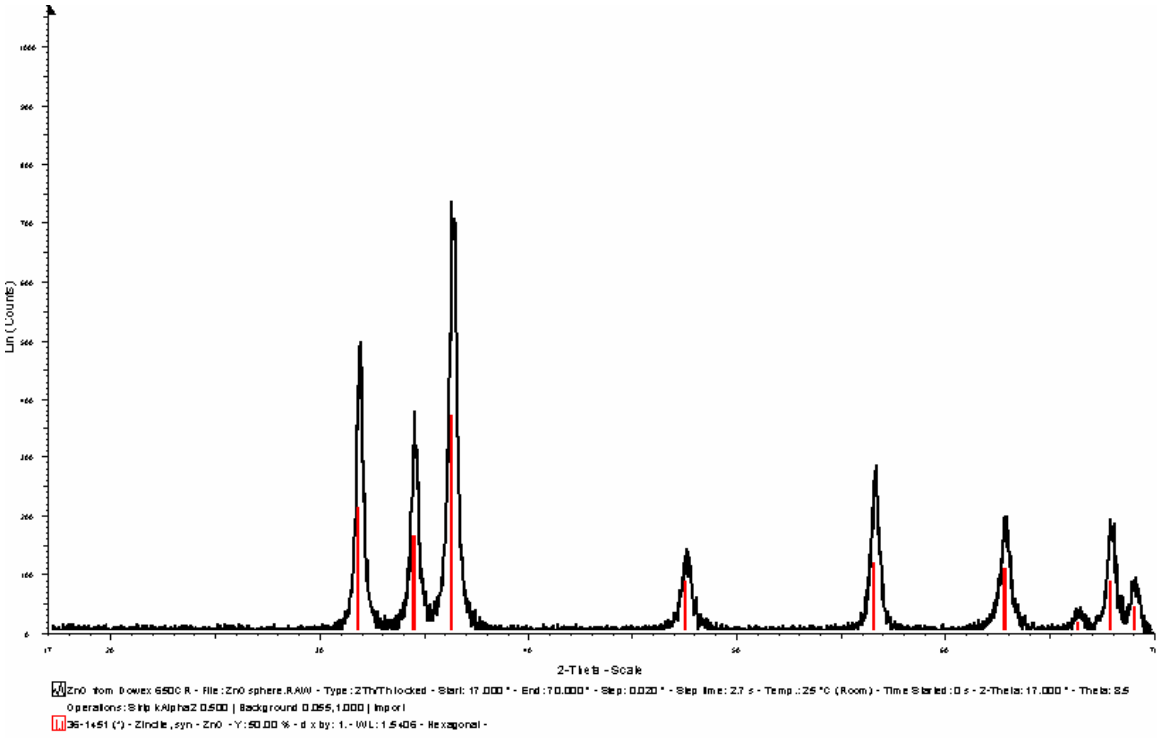

Figure 3-9: X-ray diffraction pattern of nanometric spherical zincite aggregates

The observed X-ray reflections were broadened as compared to a highly crystalline sample of zincite so the crystallite size of the particles was analyzed as shown in Figure 3-10. The result of this analysis was an average crystallite size of 12.3 nm with a somewhat broad distribution (12.9 nm full width at half-height). The maximum in relative frequency of crystallite size was 7.6 nm. Interestingly, hematite (Fe_2O_3) prepared in a similar manner had an almost identical distribution of crystallite sizes (an average

crystallite size of 12.0 nm, 16.9 nm full width at half-height and maximum at 6.9 nm).

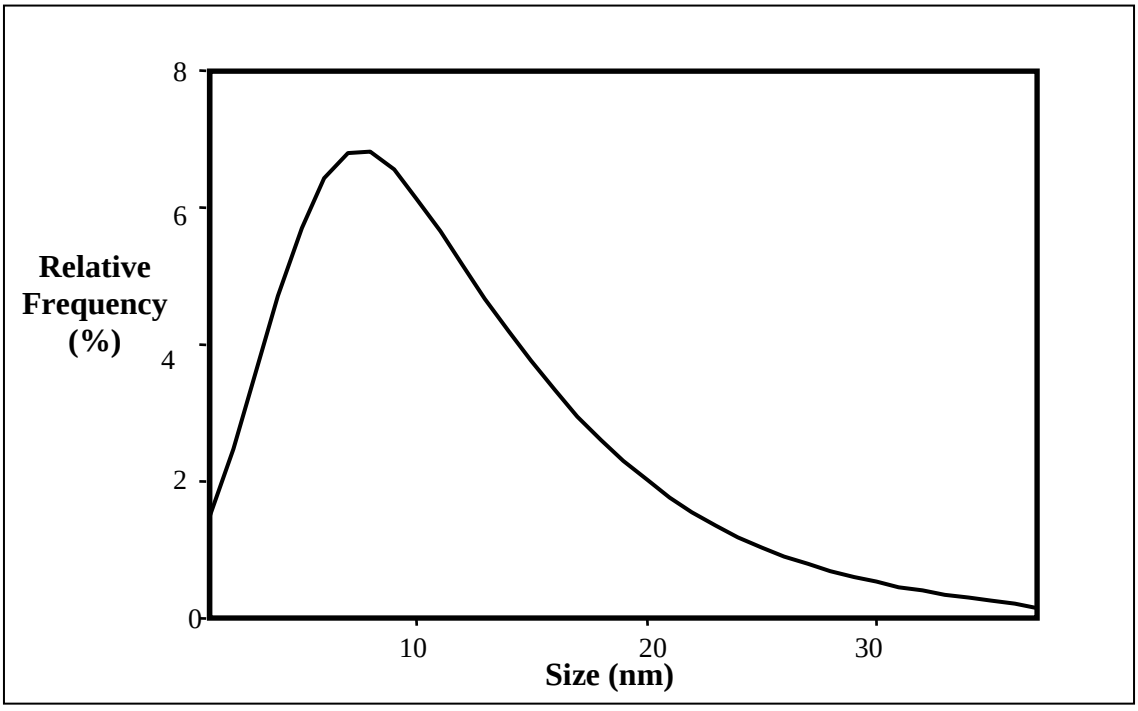

Figure 3-10: Crystallite size analysis for zincite aggregates

Scanning electron microscopy demonstrated that the particles are spherical with an average diameter of 170 μm and are porous aggregates of smaller particles as shown in Figure 3-11. The spheres consist of condensed ZnO throughout and are composed of aggregates of nanoparticles that are further fused together to yield the larger spherical particles. The spheres clearly show openings and pockets indicating the presence of interconnecting channels within thereby increasing the contact area.

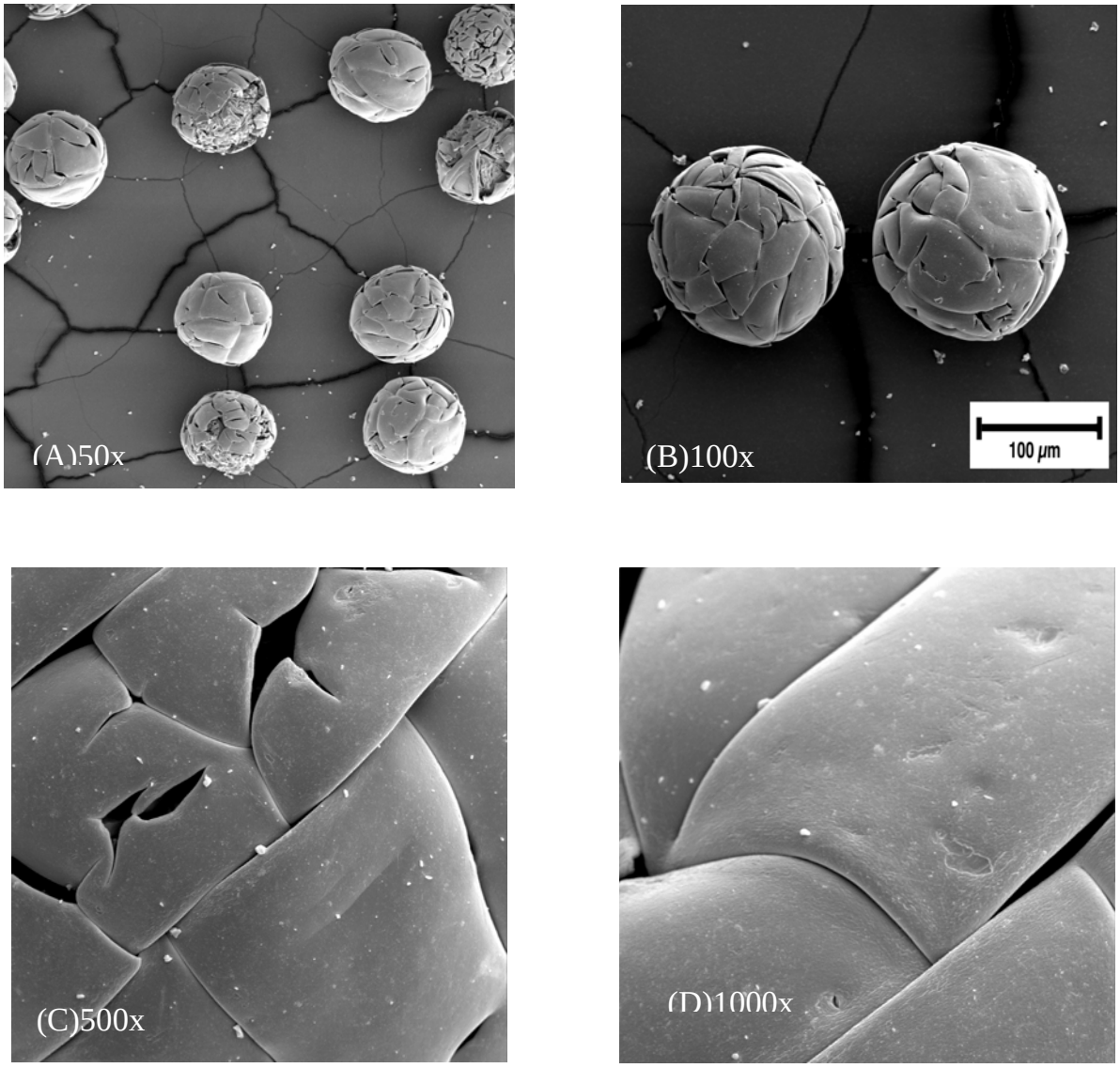

Figure 3.11: Scanning electron microscope images of zincite spheres with magnifications A) 50, B) 100, C) 500, and D) 1000

The spheres are fairly mechanically robust and do not break into smaller particles when shaken vigorously within a glass vial in a simulation of a fluidized bed. However, they can be easily crushed with an agate mortar and pestle to a fine powder. The zincite formed had a relatively high surface area of 30.7 m^2/g as determined by nitrogen absorption isotherms (Brunauer, Emmett, and Teller analysis) measured in the same way

as mentioned earlier. In order to investigate the internal porous structure of the zincite spheres they were embedded in a polymer matrix and then sectioned using a diamond blade.

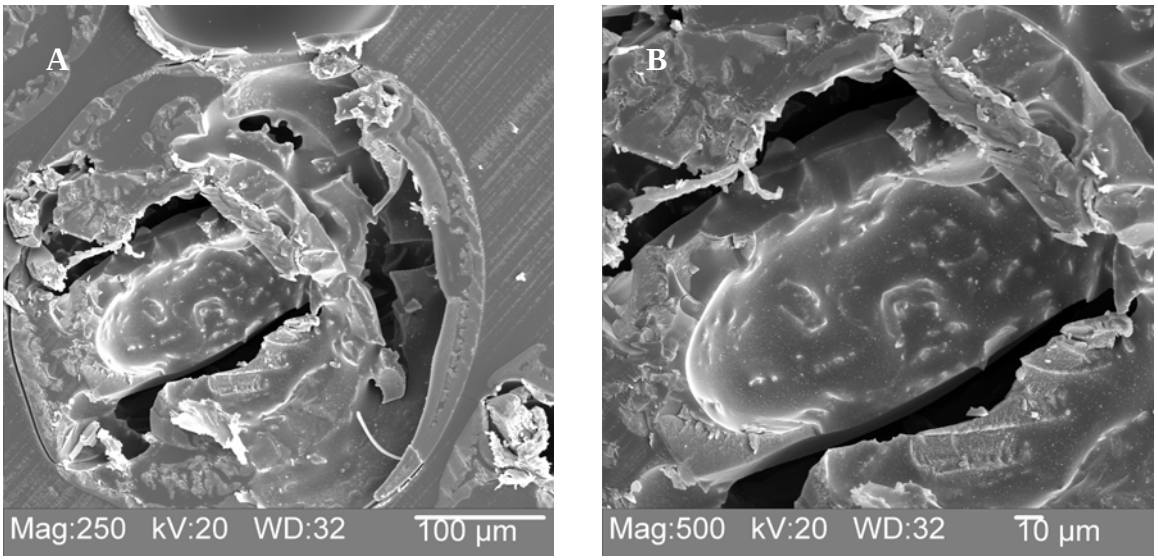

Figure 3-12: Scanning electron microscope images of cross sectional view of zincite spheres embedded in a polymer matrix at magnifications A) 250 and B) 500

The sections were cut in such a way that it would split open the spheres at the center. Scanning electron microscope images were taken in order to see the characteristics of the porous nature of the material. The cross sectional image shows highly porous spheres made up of cross linked channel like structures shown in Figure 3-12. This resulted from pyrolysis of resin when the organic matter was incinerated leaving behind zinc oxide, which then fused to make these porous agglomerates.

Synthesis of nanometric nickel oxide aggregates

Experimental:

Dowex 650C (H) form resin (20.0 g, 58.0 mmol of ion-exchange sites) was stirred for 12 hours with a solution containing two times excess of $Ni(NO_3)_2.6H_2O$ (Formula Weight 290.8, used as obtained from Aldrich) (34.9 g, 120 mmol) in water (100 ml). The supernatant solution was poured off and the nickel nitrate treatment was repeated with fresh solution. After stirring for 12 hours, the resin was isolated by filtration, washed extensively with distilled water, and air-dried. Nanocrystalline nickel oxide was obtained by firing the resulting resin (15.0 g) in the presence of air at 560^{o}C for 8 hours using a ramp rate of 4^{o}C per minute to raise the temperature from room temperature first to 590^{o}C and then to 800^{o}C . Nickel oxide was obtained with a ceramic yield of 14.1% (2.1g) at 560 °C, which upon heating to 800 °C yielded 6.9 % (1.0g) of the material. The material obtained was fine greenish black powder along with few light and black colored spherical aggregates. The spherical aggregates were very soft and turned into a fine powder very easily when they were violently shaken in a vial. The material obtained was fine powder which was greenish color. Most of the spheres were destroyed during the heating process. The synthesis scheme is shown in general Scheme 3-1. This material was characterized using different techniques.

Characterization:

Thermogravimetric analysis of the nickel loaded resin showed similar characteristics to that of iron loaded cation exchange resins as shown in Figure 3-13. The material loses approximately 32.5% by weight of the water between room temperature

and 152 ºC. Above this temperature, gradual decomposition of the ion-exchange resin occurs up to 391 ºC and a sharp decrease in mass starts to occur that eventually becomes quite rapid and culminates in the formation of iron oxide at 490 ºC. During the later step, extensive evolution of sulfur dioxide occurs, so care must be taken to vent the fumes to a hood. The material obtained at 490 ºC had light color on black spheres. Therefore, the material was heated to 800 ºC at which point it was mostly black powder with some spheres.

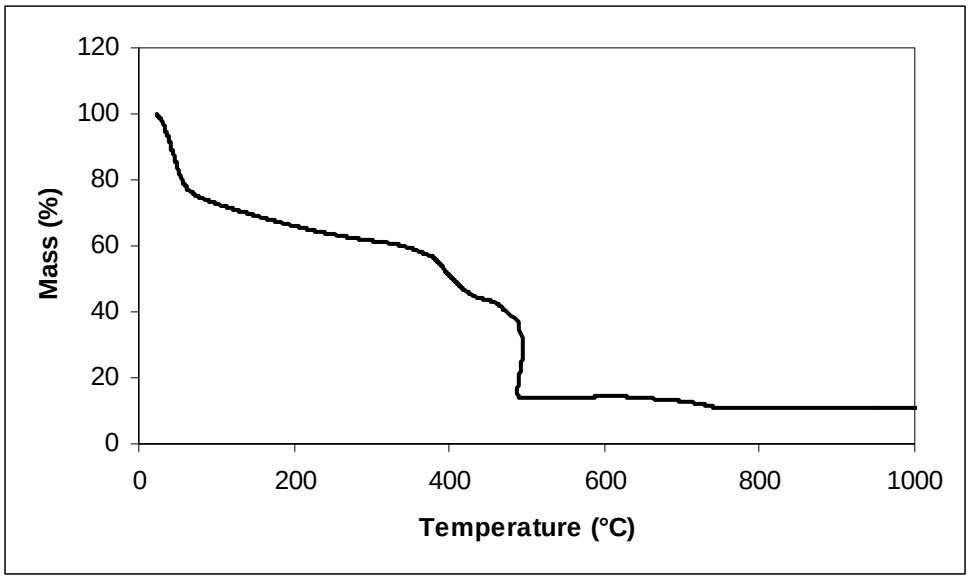

Figure 3-13: Thermogravimetric analysis of nickel loaded cation exchange resins

X-ray diffraction pattern of nanometric nickel oxide powder was recorded as previously mentioned. The X-ray diffraction pattern confirmed the identity of the material to be nickel oxide (NiO). The X-ray diffraction pattern of nickel oxide is shown in Figure 3-14 below. The sample, which was heated to 590ºC as well as the one at 800ºC showed the same pattern, which was matched to rhombohedral nickel oxide (NiO) structure.

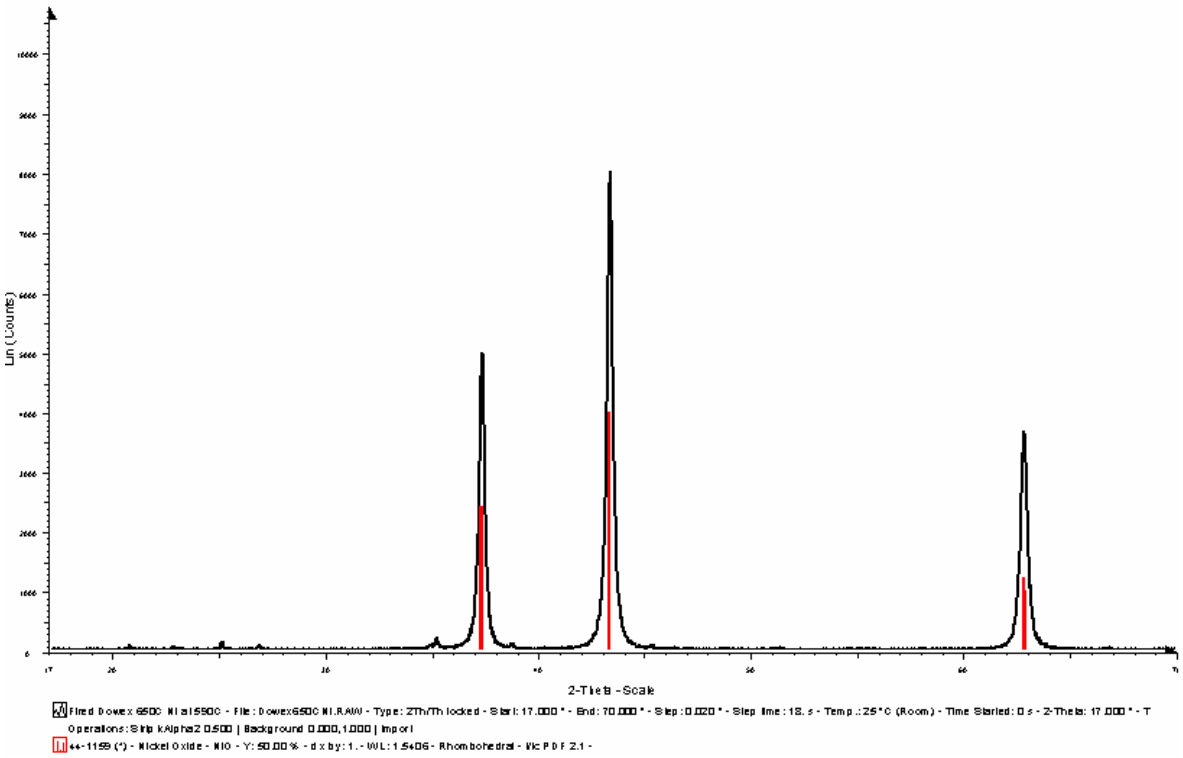

Figure 3-14: X-ray diffraction pattern of nanometric nickel oxide aggregates

The observed X-ray reflections were broadened as compared to a highly crystalline sample of sintered nickel oxide, so the crystalite size of the particles was analyzed. The result of this analysis, shown in Figure 3-15, is an average crystallite size of 15.3 nm, with a somewhat broad distribution (16.9 nm full width at half-height). The maximum in relative frequency of crystallite size occurs at 7.8 nm.

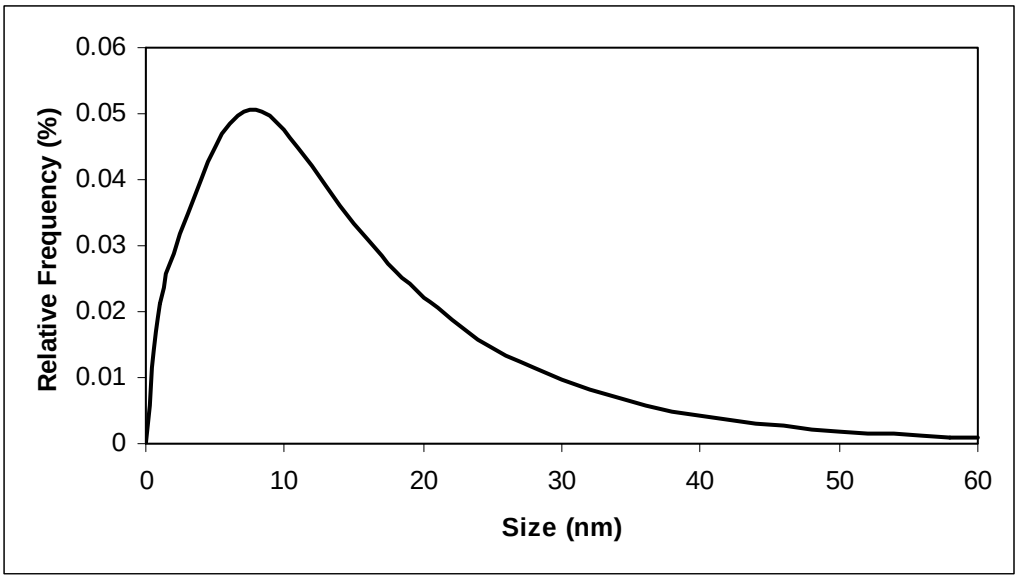

Figure 3-15: Crystallite size analysis of nanometric nickel oxide aggregates

Scanning electron microscope images of nickel oxide spheres heated to different temperatures were taken at different magnifications are shown in Figure 3-16. Nickel oxide spheres were almost spherical with minor irregularity in shape. Nickel oxide spheres at 590 ºC still showed little breaking of spheres and many of them fell apart easily once they were heated to 800 ºC. However, for the purpose of taking these images some of the intact spheres were selected and used. The images of the sample heated at 800 ºC clearly show some deterioration of the spheres, which eventually fell apart and formed fine powdered nickel oxide containing some spheres. Also, the surface of the 800 ºC sample showed rough surface and some reduction in the size of the spheres.

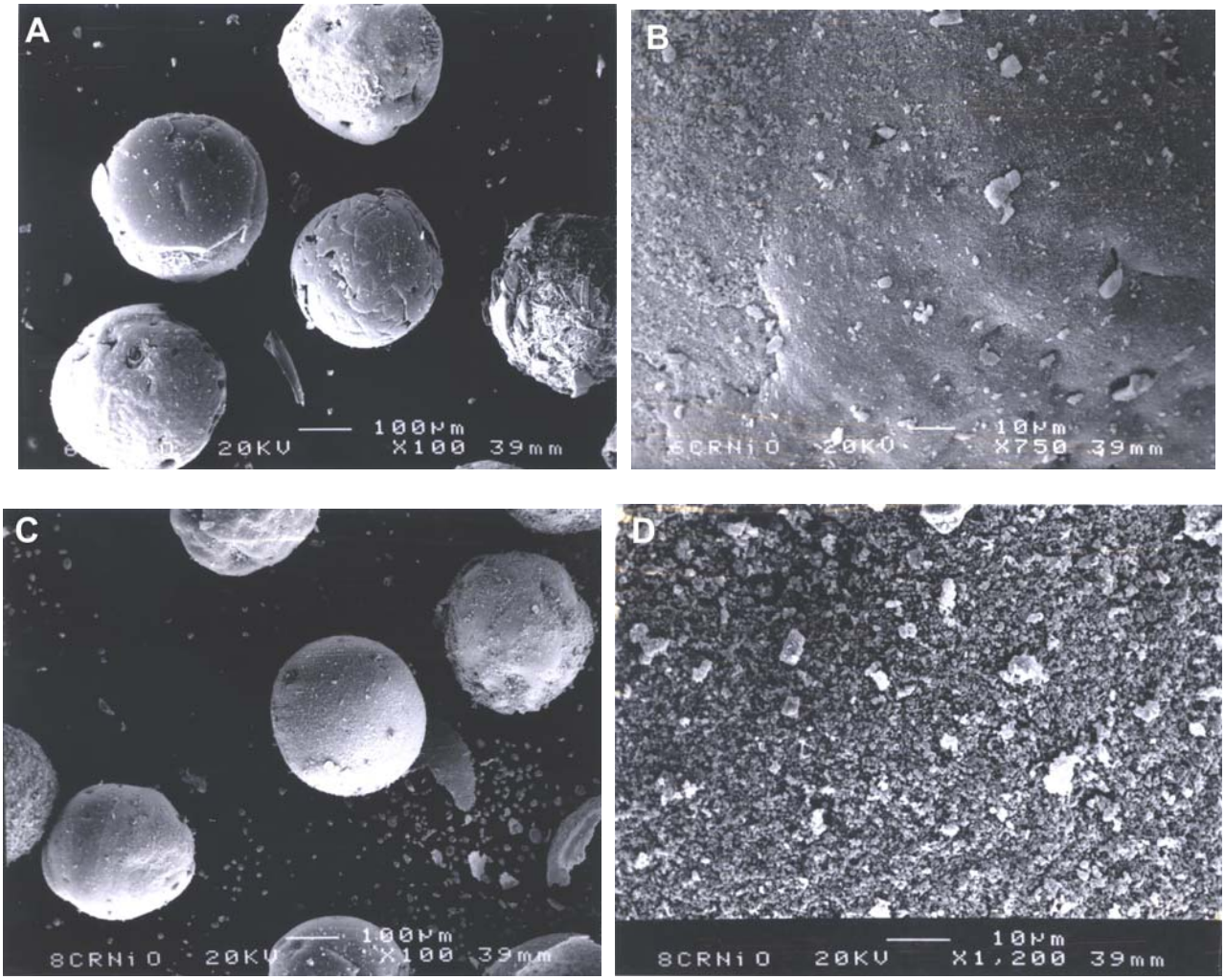

Figure 3-16: Scanning electron images of nickel oxide spheres at 590 ºC with magnifications A) 100, B) 750; and at 800 ºC with magnifications C) 100, D) 1200

Surface area analysis was carried out by Brunauer, Emmett, and Teller analysis method. Surface area for nickel oxide spheres heated at 590 ºC and 800 ºC was found to be 27.5 and 3.2 m^2/g, respectively. This reduction in surface area was due to sintering at higher temperature.

Synthesis of nanometric alumina aggregates from cation exchange resins

Experimental:

Dowex 650C (H) form resin (20.0 g, 58.0 mmol of ion-exchange sites) was stirred for 12 hours with a solution containing two times excess of $Al(NO_3)_2.9H_2O$ (Formula Weight 375.2, used as obtained from Aldrich) (45.02 g, 120 mmol) in water (250 ml). The supernatant solution was poured off and the aluminium nitrate treatment was repeated with fresh solution. After stirring for 12 hours, the resin was isolated by filtration, washed extensively with distilled water, and air-dried. Nanocrystalline alumina was obtained by firing the resulting resin (15.0 g) in the presence of air at 550^{o}C for 8 hours using a ramp rate of 4^{o}C per minute to raise the temperature from room temperature to 560^{o}C. Alumina (1.17 g) was obtained with a ceramic yield of 7.8 %. The resultant material was a white fine powdered aggregates with few spheres. The spherical aggregates were very soft and turned into a fine powder very easily when they were shaken in a vial. The synthesis scheme is shown in general Scheme 3-1. The material obtained after pyrolysis was characterized using different techniques.

Thermogravimetric analysis of the aluminum loaded cation exchange resin follows the same pattern as that of iron and zinc loaded cation exchange resins as seen in Figure 3-17. The pattern shows a rapid loss of water in the first step, which contributes to a weight loss of 20% by the end of 150ºC. The resin material starts to decompose rapidly around 385ºC, which ends around 528 ºC. The material is completely converted to aluminum oxide at 530 ºC.

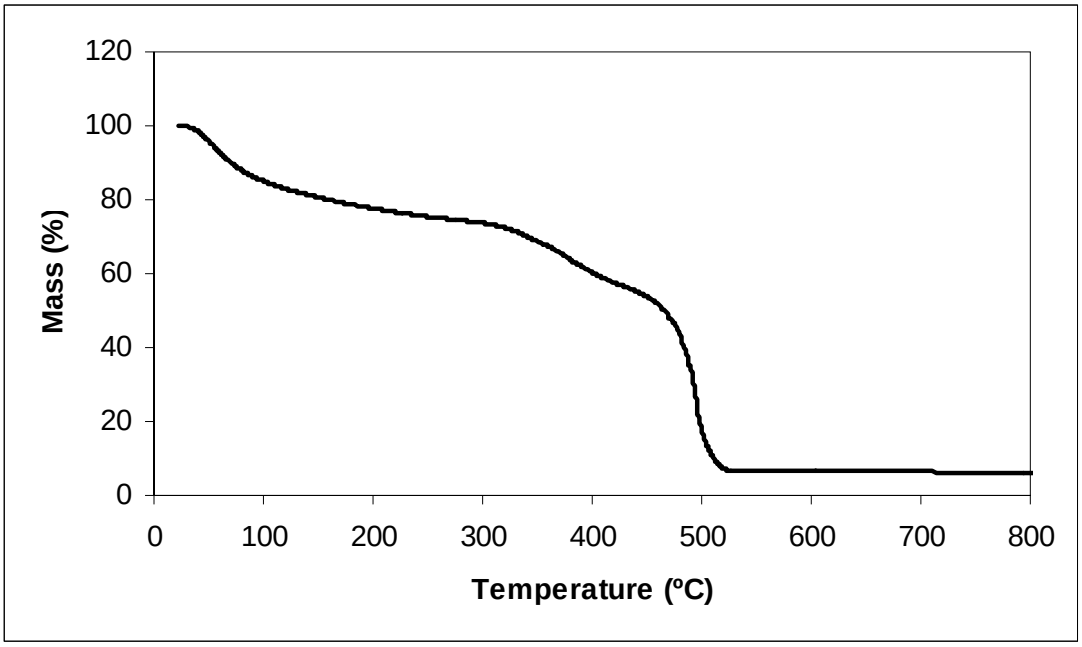

Figure 3-17: Thermogravimetric analysis of aluminum loaded cation exchange resin

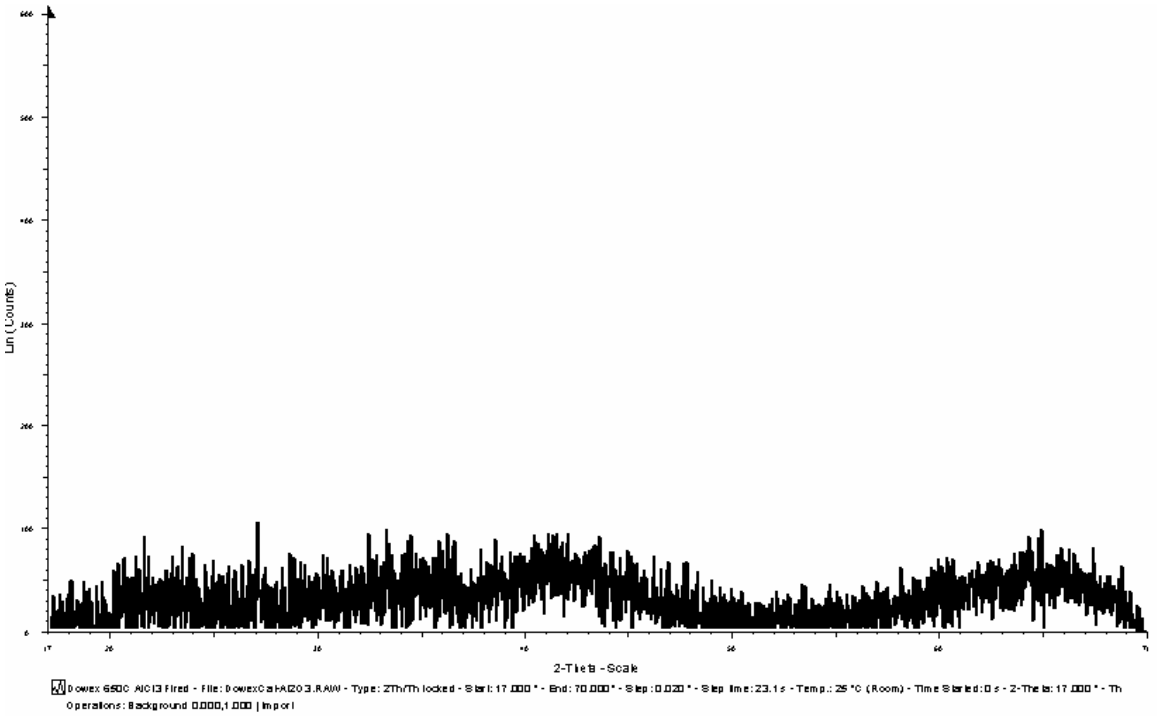

Figure 3-18: X-ray diffraction pattern of alumina obtained by pyrolysis of aluminum loaded cation exchange resin

The X-ray diffraction pattern (Figure 3-18) for the alumina showed that the material was amorphous. Surface area analysis was carried out by Brunauer, Emmett, and Teller analysis method and the surface area after heating to 560 ºC was found to be $110 m^2/g$.

A different approach was explored in order to prepare alumina using anion exchange resins. The idea was to use Dowex 550 OH anion exchange resin (used as obtained from Aldrich Chemicals) instead of cation exchange resin and synthesize high surface area materials.

Synthesis of nanometric alumina agglomerates from anion exchange resin

The resin used was Dowex 550A (OH^-) form resin, a cross-linked polystyrene-trimethylbenzyl ammonium polymer that was purchased directly from Aldrich in the form of monodisperse spherical beads. Dowex 550 OH-form resin (20.0 g, 70.0 mmol of ion-exchange sites) was stirred for 12 hours with a solution containing two times excess of sodium aluminum oxide ($Al_2O_3.Na_2O$, formula weight 163.94, used as obtained from Aldrich Chemicals) (22.95 g, 140 mmol) in deionized water (1000ml) and NaOH pellets (upto15g) in order to dissolve sodium aluminum oxide were used. Also, the same procedure was repeated without addition of NaOH. However, this did not affect the percentage yield of alumina obtained. The supernatant solution after the resin treatment was poured off and the sodium aluminum oxide treatment was repeated with fresh solution. After stirring for 12 hours, the resin was isolated by filtration, washed extensively with distilled water, and air-dried. Nanocrystalline alumina was obtained by firing the resulting resin (15.0 g) in the presence of air at 560^oC for 8 hours using a ramp rate of 4^oC per

minute to raise the temperature from room temperature to 560^{o}C. Alumina (0.84 g) was obtained with a ceramic yield of 5.6 %. The resultant material was flaky, white aggregates, which were mostly pieces from broken spherical aggregates. The spherical aggregates, were mechanically not strong enough to retain the inherent spherical resin shape and turned into a fine powder. The synthesis scheme for the synthesis is shown below in Scheme 3-2.

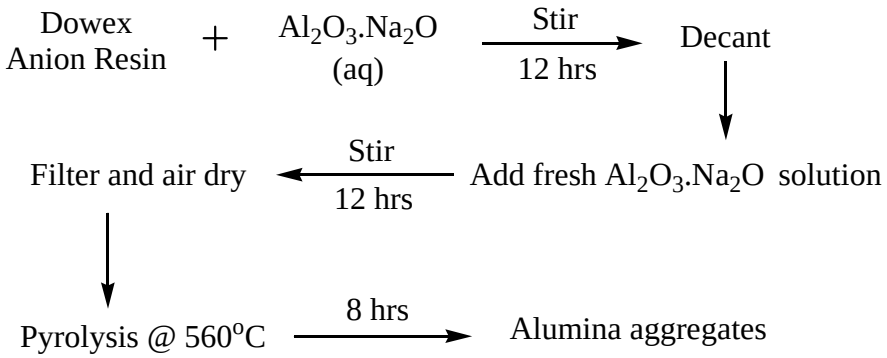

Scheme 3-2: Synthesis of alumina agglomerates from Dowex 550 OH form anion exchange resins

The aluminum loaded anion exchange resin was subjected to thermogravimetric analysis in order to obtain suitable pyrolysis temperature for the material. The plot of percentage loss of mass versus temperature is shown in Figure 3-19.

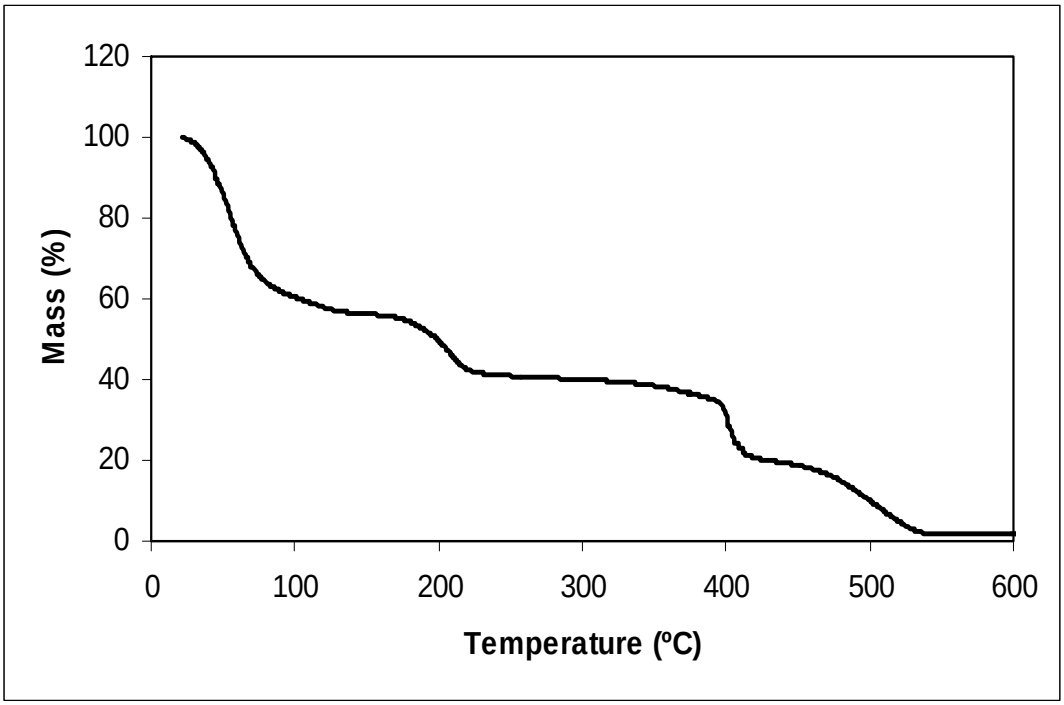

Figure 3-19: Thermogravimetric analysis of aluminum loaded Dowex 550 OH form anion exchange resin

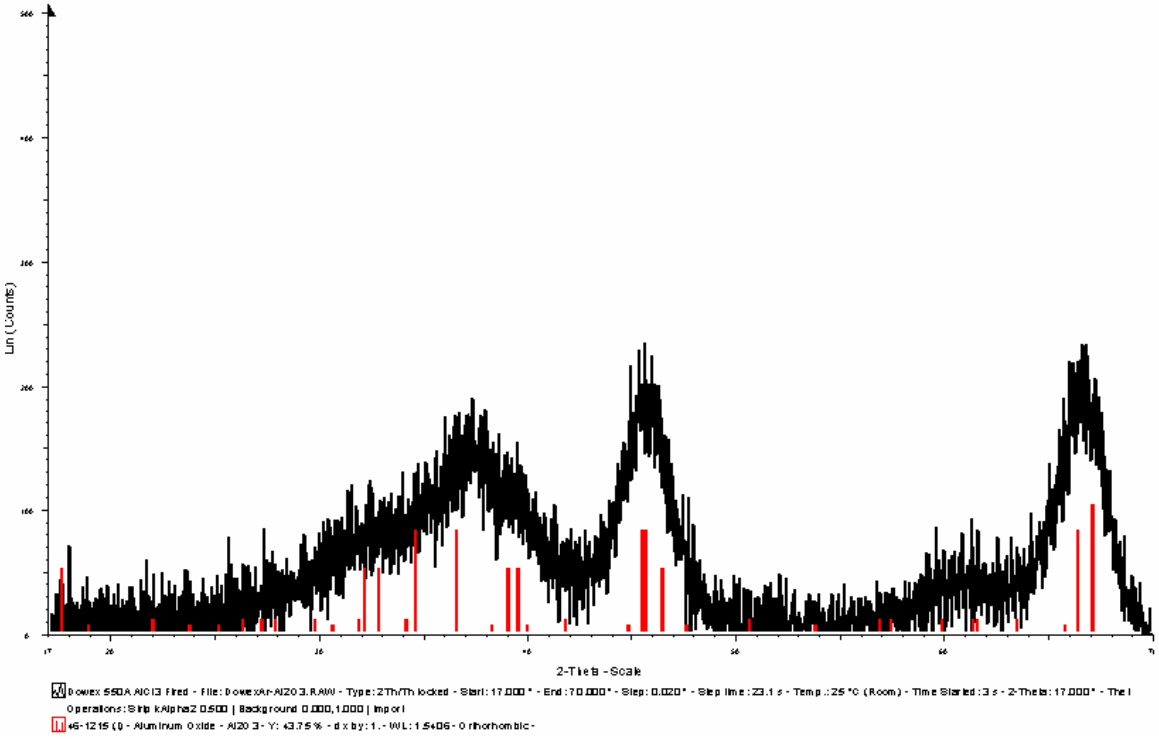

Figure 3-20: X-ray diffraction pattern of nanometric aluminum oxide aggregates

The X-ray diffraction pattern for the alumina showed material to be crystalline as shown in Figure 3-20. The diffraction pattern was run on a search database, which matched it to orthorhombic aluminum oxide (Al_2O_3) (a transition alumina). The surface area for alumina aggregates heated to 560 ºC was found to be 334 m^2/g. Scanning electron microscope images of alumina agglomerates are shown in Figure 3-21.

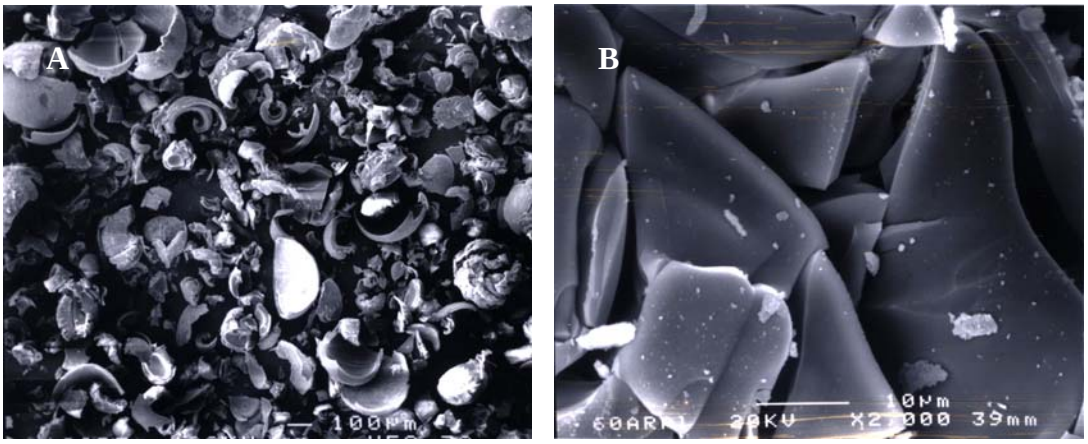

Figure 3-21: Scanning electron microscope images of alumina aggregates A)50x B) 2000x

An interesting fact in these two cases is that although the synthesis procedure is same except the type of resin used, they gave different types of morphology of the same product. On pyrolysis of the aluminum loaded materials the one with the cation exchange resin gave an amorphous material whereas the anion exchange resin yielded crystalline material. Even the surface areas were different. The amorphous material had a surface area of 110 m^2/g and the crystalline alumina has a very high surface area of 334 m^2/g.

Conclusions

Pyrolysis of the transition metal ion (Fe, Ni, and Zn) loaded resins at 560°C yielded nanometric spherical agglomerates of respective metal oxides. Water, carbon dioxide, and sulfur dioxide were the main by-products of pyrolysis. The observed X-ray reflections were broadened as compared to a highly crystalline sample of sintered bulk materials, which indicated the presence of small particles. The average crystallite size of the particles ranged from 12-15 nm with a somewhat broad distribution. Interestingly, their surface area values were also quite similar. The average crystallite size and surface area of the metal oxide agglomerates are shown in Table 3-2.

Table 3-2: Parameter comparison of synthesized nanometric metal oxide agglomerates

No.	Compound	Ceramic Yield (%)	Average Crystallite Size (nm)	Surface Area (m^2/g)
1	Iron oxide	14.9	12.0	30
2	Zinc oxide	16.0	12.3	37
3	Nickel oxide	14.1	15.3	28

These results suggest that domains within the ion-exchange resin exert a strong control over the size and morphology of the particles generated upon pyrolysis. If true, then the size of the oxide particles might be controllable by variation of the cross-linking of the polymer by changing of the divinylbenzene content. The degree of sulfonation might also be a parameter that controls particle size. This could be very helpful in tailoring the crystallite size of materials derived from pyrolysis of ion exchange resins. The biggest advantage of synthesizing such aggregates of nanomaterials is the controlled shape and high surface area obtained by pyrolysis as compared to the sintered bulk

material. This gives an edge over the conventional uses of the bulk materials in catalysis, environmental remediation, and biomedical and engineering applications. The practical use of these synthesized aggregates in environmental remediation is discussed in Chapter IV.

References

1. Gupta, A.K.; Gupta, M. *Biomaterials* **2005**, *26*, 3995-4021.
2. Thrall, J.H. *Radiology* **2004**, *230*, 315-318.
3. Lee, H.; Lee, E.; Kim, D.K.; Jang, N.K.; Jeong, Y.Y.; Jon, S. *J. Am. Chem. Soc*. **2006**, *128*, 7383-7389.
4. Nanotechnology. Researchers use nanoscale zinc oxide structures to detec anthrax. http://www.nanotechnology.com/news/?id=8450.
5. Foley, T.J.; Johnson, C.E.; Higa, K.T. *Chem. Mater*. **2005**, *17*, 4086-4091.
6. Yu, D.; Cai, R.; Liu, Z. *Spectrochim. Acta A Molecular and Biomolecular Spectroscopy* **2004**, *60A*, 1617-1624.
7. Nanotechwire. Nanophase announces doped zinc oxide nanomaterials. http://www.nanotechwire.com/news.asp?nid=468.
8. Air Products. Nano-ZnO dispersion. http://www.airproducts.com/AdvancedMaterials/Nano_Zinc.htm.
9. Obare, S.; Meyer, G. J. *J. Environ. Sci. Health A Tox. Hazard. Subst. Environ. Eng.* **2004**, *39*, 2549-2582.
10. Kuriyavar, S.; Apblett, A. Modified ion exchange resins for environmental remediation of heavy metal ions. Abstracts of the 60th Southwest Regional Meeting of the American Chemical Society, Fort Worth, TX, United States, Sept 29-Oct 4, 2004.
11. Kuriyavar, S. I.; Apblett, A. W. Spherical nanocrystaline aggregates of metal and metal oxides for heavy metal ion remediation. Abstracts of papers of the 229th

American Chemical Society National Meeting, Division of Industrial and Engineering Chemistry, San Diego, CA, United States, Mar 13-17, 2005.

12. Apblett, A.W.; Kuriyavar, S. I.; Bagabas, A.; Piquette, A.P. Nanotechnology for removal of arsenic from water. Preprints of Extended Abstracts of the American Chemical Society National Meeting, Division of Environmental Chemistry, Atlanta, GA, United States, Mar 26-30, **2006**, *46*, 752-760.
13. Apblett, A.W.; Kuriyavar, S.I.; Kiran, B.P. *J. Mater. Chem.* **2003**, *13*, 983-985.

CHAPTER IV

SPHERICAL AGGREGATES OF NANOPARTICULATE IRON AND ZINC OXIDE FOR ARSENIC REMEDIATION

Introduction

Arsenic poisoning is a major health problem worldwide, and of the two forms of arsenic, arsenic(III) and arsenic(V), the latter is more toxic. The Comprehensive Environmental Response, Compensation, and Liability Act (CERCLA) Priority List of Hazardous Substances prepared by the Agency for Toxic Substances and Disease Registry (ATSDT) and Environmental Protection Agency (EPA) lists substances that pose the most significant potential threats to the human health and arsenic(V) ranks first on this list [1]. The major contributor to this public health issue is consumption of water containing high amounts of arsenic. Several epidemiological studies indicate that arsenic exposure from drinking water contributes to skin lesions, neurological problems, high blood pressure, cardiovascular disease, respiratory disease, diabetes, and malignancies.[2] According to the National Research Council's Subcommittee on Arsenic in Drinking Water, there is sufficient evidence that chronic consumption of arsenic causes birth defects, reproductive problems, and bladder, lung, and skin cancers.[3]

The major sources of arsenic entry into water supplies are natural earth deposits, agricultural pollution, and industry. Arsenic occurs naturally in volcanic glass, sulfide minerals, metal oxides, and clay minerals. [4] Other natural sources of arsenic are mineral weathering and volcanic eruptions.[5] Several compounds containing arsenic are used in

agriculture as pesticides (e.g. lead arsenate, sodium arsenate, and calcium arsenate), herbicides (e.g. methyl arsenic acid and dimethyl arsenic acid), wood preservatives (chromated copper arsenite, sodium arsenate, zinc arsenate), and cattle feed additive (e.g. arsanilic acid) [6,7]. In industry, arsenic compounds are used in manufacturing of glass and glass products, ceramic, metal alloys (smelting of copper, lead, zinc, and nickel), pharmaceuticals, dyes, textiles, and paper.[7] Arsenic is also a byproduct of mining, fuel burning, and petroleum refining. Mining of ores containing arsenic, e.g. silver, gold, and uranium ores, and burning of fuels that contain arsenic, such as coal, release this toxic element into atmosphere[5,6]. Arsenic from all the mentioned sources leaches into ground water and causes its contamination.

Beginning in January 2006, the U. S. Environmental Protection Agency lowered the level for arsenic in drinking water from 50 ppb to 10 ppb in order to protect public from chronic arsenic exposure.[8] The U.S. Environmental Protection Agency estimates that the new limit for arsenic in drinking water will increase the cost of arsenic removal to about $327 per household per year in small municipal water systems and about $32 per household per year in larger community water systems.[9] Based on the U. S. Geological Survey, arsenic concentrations in ground water are the highest in the Western United States and also several areas in the Midwest and Northeast have arsenic concentrations that exceed 10 ppb.[10] The concentrations of arsenic in ground water samples in different areas of the United States are shown in Figure 4-1.

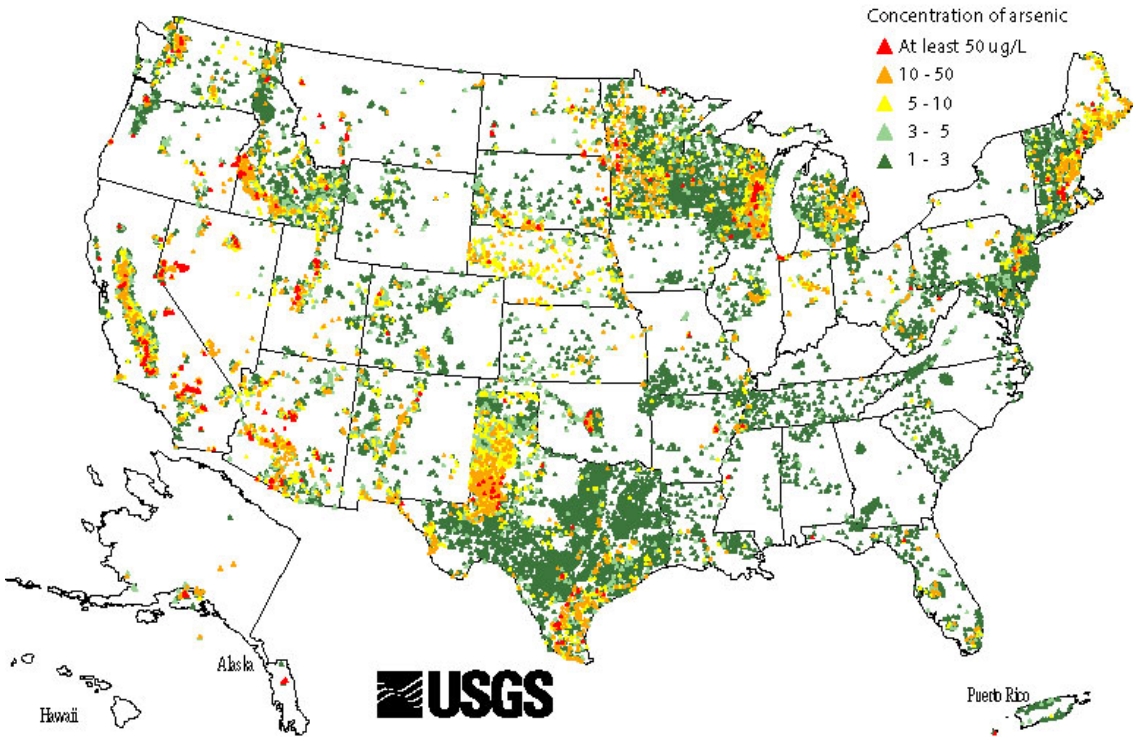

Figure 4-1: Mapping of arsenic in ground water in the U.S.[11]

The U.S. Geological Survey also revealed that Oklahoma, especially its central region, has areas with high arsenic concentrations. The levels of arsenic in the main water source in central Oklahoma, the Central Oklahoma Aquifer, commonly surpass the Environmental Protection Agency standard of 10 ppb. In some areas, the measured concentrations reached 62 ppb.[12] To solve this problem, the Central Oklahoma Water Resource Authority decided to build an 88-mile, $200 million water pipeline from southern Oklahoma to supply water to Canadian County which has the highest arsenic concentration in drinking water[13, 14] in the state.

Water contamination with arsenic is not limited to the United States. According to the World Health Organization, arsenic in drinking water has also been detected at concentrations greater than 10 ppb in Argentina, Australia, Bangladesh, Chile, China,

Hungary, India, Mexico, Peru, and Thailand. Adverse health effects due to arsenic exposure have been documented extensively in Bangladesh, China, and India. Figure 4-2. shows number of people that are at risk from arsenic contamination in the affected countries. The situation is especially alarming in Bangladesh where 28-35 million people are exposed to water with arsenic concentrations above 50 ppb and 46-57 million people consume water containing more than 10 ppb of arsenic.[15] The World Bank provided a $32.4 million, zero interest loan to Bangladesh to help alleviate this serious problem. [16]

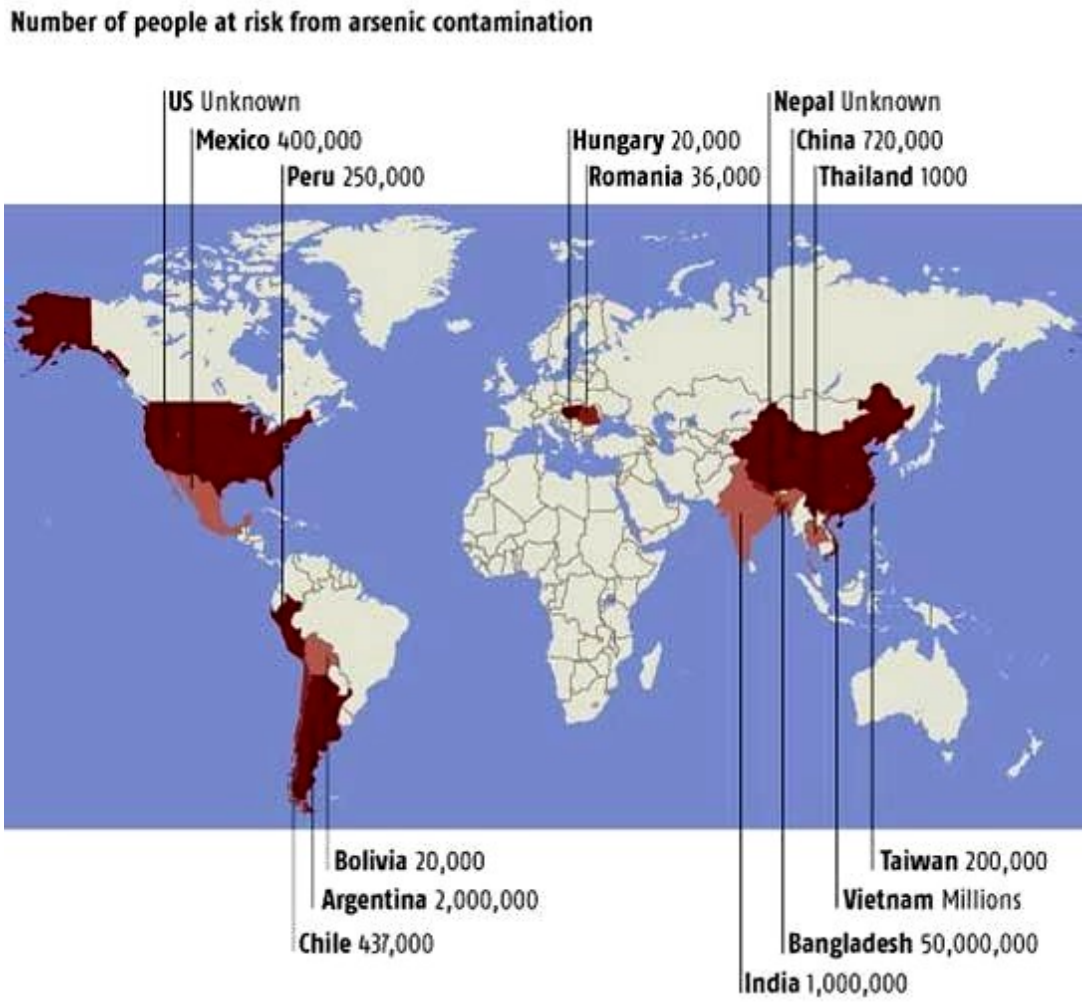

Figure 4-2: Number of people at risk from arsenic contamination worldwide[17]

Arsenic belongs to group VB of the periodic table along with nitrogen, phosphorous, antimony, and bismuth. Therefore, there is considerable amount of chemical similarity between As(V) and P(V) oxyacids, making the removal of arsenic(V) species in the presence of P(V) species quite difficult. Arsenic's occurrence and mobility in the natural environment depends on redox conditions, pH, and presence of any other interfering ions. Arsenic is present predominantely as arsenate ($H_2AsO_4^{-1}$ and $HAsO_4^{2-}$) under oxidized conditions whereas it is present as arsenite ($H_2AsO_3^{-1}$) under reducing conditions [18]. At near neutral pH and natural conditions, As(V) is the most predominant species, however, in ground water As(III) and As(V) are present due to prevailing pH and redox conditions [19,20]. The dissociation constants for As (V) are shown in Figure 4-3.

$$H_3AsO_4 \rightleftharpoons H_2AsO_4^- + H^+ \qquad pK_1 = 2.2$$

$$H_2AsO_4^- \rightleftharpoons HAsO_4^{-2} + H^+ \qquad pK_1 = 7.0$$

$$HAsO_4^{-2} \rightleftharpoons AsO_4^{-3} + H^+ \qquad pK_1 = 11.5$$

Figure 4-3: Dissociation constants for As(V) [21,22,23].

Remediation techniques

A variety of approaches have been investigated in order to remove arsenic from water. The most common treatment techniques employed to date are: ion exchange; sorption onto alumina [24]; iron oxide coated sand (IOCS) and manganese dioxide coated sand [25,26]; reverse osmosis [27,28]; coagulation with alum, iron(III) salts [29,30,31], and granular

ferric hydroxide particles [32]; and zero-valent iron on sand [33]. Even though there are so many developments achieved in this area, they still have some drawbacks associated with them. The sorption technique using activated alumina suffered due to poor As(III) removal, slower kinetics, and requirement for pH adjustments. Also, there was a problem in regenerating of the spent sorbent. The ion exchange approach is a well defined process that showed promising results in As(V) removal capabilities, although there were some inherent problems associated with it, such as interference due to competing ions, regeneration difficulties, and high maintenance and operational costs. Iron oxide coated sand (IOCS) showed fast kinetics for As(V) removal and was inexpensive but its inability to remove As(III) and low capacity for arsenic uptake outweighed its advantages. The co-precipitation method using aluminum salt, lime, and ferric oxide is the most commonly employed technique but it requires proper maintenance and a tight pH control. This technique worked well for removal of both As(III) and As(V) species and the process was developed for large water treatment facilities. The drawback of this technique was its inability to be used economically for small scale treatment facilities. In sharp contrast to this technique are techniques such as reverse osmosis and nano-filtration because they can be used for small scale water treatment facilities but lack the ability to be used for large scale water treatment plants.

Several metal oxides can be used to remove arsenic species from water bodies, among which hydrated ferric oxides (HFO)[34,35,36,37,38,39,40], Mn(IV) oxides, magnetite (Fe_3O_4) [41,42,43], goethite [44], titanium oxide [45], and zirconium oxide [46,47] are the most effective. Manganese and titanium oxides were especially useful since they oxidized As(III) to As(V) and were able to remediate both the species at the same time. Recently

some polymeric-inorganic hybrid types of sorbents have been developed that attempt to combine mechanical and hydraulic properties of spherical polymeric beads with sorption properties of hydrated ferric oxide (HFO) particles. Such systems consist of a spherical macroporous cation exchanger bead, within which agglomerates of nanoscale hydrated ferric oxide (HFO) particles have been uniformly and irreversibly dispersed. However, the removal process was hampered by slow intra-particle diffusion of the arsenate and arsenite species [26]. Arsenic contamination still continues to affect millions of people around the globe despite the advancement of arsenic remediation technology.

Nanoparticulate materials display unusual reactivity as compared to bulk materials due to their very high surface area to volume ratio, which offers favorable kinetics and uptake capacity. This approach cannot be applied in order to achieve arsenic remediation due to several practical difficulties. However, these nanoparticles cannot be used in water treatment plants in the form of fixed bed columns, reactive permeable barriers, or any type of plug-flow type systems due to excessive back pressure problems. Also, nanoparticles tend to suspend and clog the filtering media requiring excessive pressures for smooth operation. This is not only unfeasible but also impractical considering the large volume of water to be treated for day-to-day consumption of communities in a short period of time. A different approach has been investigated for this purpose. The idea is to use nanometric agglomerates of spherical iron and zinc oxides for arsenic remediation. Their spherical shape derived from the ion exchange resin precursors makes them ideal candidates for treatment columns. Due to their shape, the flow of water would be uninhibited through the gaps in between them. Also, these micron sized spheres

were shown to be highly porous in nature, which helps to maximize their interaction with the flowing aqueous media resulting in efficient removal of arsenic from drinking water.

Materials and methods

Sodium arsenate heptahydrate ($Na_2HAsO_4 \cdot 7H_2O$) was obtained from GFS chemicals, Inc. Bulk zinc oxide used for comparison was a dry process zinc oxide from Fisher Chemicals and was sintered at 1200^oC. All the reagents were commercial products (ACS reagent grade or higher) and were used without further purification. Water was purified by reverse osmosis and deionized before use. Nanometric hematite spheres were prepared by pyrolysing iron loaded Dowex cation resins at 550 ^oC. Similarly, zincite spheres were synthesized by pyrolysing zinc loaded Dowex cation exchange resins at 560^oC as described in Chapter III. Arsenic detection and quantification was done using a commercially available colorimetric test kit from EM Science. A series of arsenic(V) standards were prepared using 10,000 ppb stock solution ranging from 100 ppb to 3,000 ppb in concentration.

The various zinc and iron oxides (1.10 g) were stirred with 110 ml of standard arsenic solution for one hour in a sealed glass bottle. At this point, the solution was separated from the adsorbant by filtration through a fine sintered glass filter. The pH of the solutions was recorded before and after treatment with zinc and iron oxides. The treated and filtered solution was then analyzed using the colorimetric test kit to determine equilibrium concentration of arsenic.

Results and discussion

The spherical zinc oxide particles were used to treat increasing concentrations of arsenic from 300 up to 10,000 ppb until significant arsenic remained in solution. For comparison, a commercial sintered zinc oxide was also used to treat a 300 ppb solution. The results are given in Table 4-1. The current United States Environmental Protection Agency's limit for arsenic in drinking is 10 ppb and the level of arsenic in contaminated ground water in the US is around 100 ppb. When challenged with 110 ml of 300 ppb solution of arsenate, 1.1 g of the nanoparticulate zinc oxide reduced the arsenic concentration to the Environmental Protection Agency limit. Even at concentrations of arsenic as high as 3000 ppb (3 ppm), the spherical zinc oxide reduced the concentration to 40 ppb, less than the previous drinking water standard of 50 ppb. By contrast, sintered microcrystalline zinc oxide did not remove a detectable amount of arsenic from solution. The success of the spherical iron oxide powders is likely due to their composition of nanocrystaline primary particles. The capacity of the zincite spheres for arsenate adsorption was 985 µg As/g adsorbant, exceeding the adsorption capacity of iron-oxide-coated sand, ferrihydrite, and spherical nanoparticles that are established as 18.3, 285, and 303 µg/g, respectively[48,49,50].

Table 4-1: Results of arsenic adsorption studies

ZnO Sample	**Surface Area (m^2/g)**	**Initial [As] (ppb)**	**Final As (ppb)**
Commercial	0.13	300	300
Spherical	30.7	300	10
Spherical	30.7	3,000	40
Spherical	30.7	10,000	150

Arsenic uptake experiments were performed using nanometric hematite aggregates. For the purpose of comparison commercially available iron oxide was also tested but did not show any activity towards arsenic uptake. The adsorption properties of hematite spheres are presented in Table 4-2.

Table 4-2: Comparison of characteristics of nanometric zinc and iron oxide spheres

Agglomerate	Surface Area (m^2/g)	Average Crystallite Size (nm)	As Uptake Capacity (µg/g)	As Uptake Capacity (µg/m^2)
Zinc oxide	30.7	12.3	985	32.1
Iron oxide	30.0	12.0	992	33.1

The results show that the arsenic uptake trend is similar to that of nanometric spheres of zinc oxide. Therefore, the arsenic uptake capacities of iron oxide and zinc oxide aggregates are made by plotting Langmuir isotherm for these experiments (shown in Figure 4-4). The shape of the curves almost overlapped each other, which suggested that their uptake pattern is the same and both have almost same uptake capacity. This fact also falls in line with already established similarities and patterns in their physical properties as shown in Table 4-2. The uptake capacity for zincite and hematite spheres were calculated and found to be 985 and 992 µg/g of material. These values are very similar and reconfirm the fact that ion exchange resin matrix has control over the crystallite size of the nanometric oxide spheres and can be tailored according to size requirements.

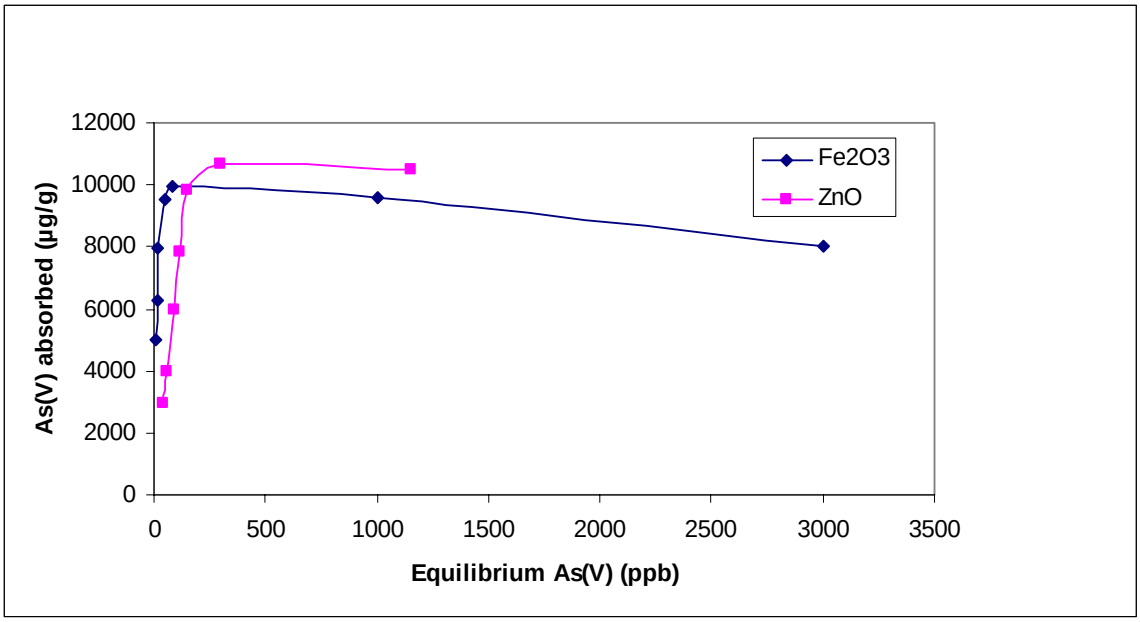

Figure 4-4: Langmuir isotherm for arsenic uptake experiments

Conclusion

This chapter gives another example of the ability of nanoparticulate materials to display unusual reactivity towards environmental contaminants as compared to bulk materials. The spherical nature of the ion-exchanger derived zincite particles are well suited for "at-the-tap" remediation of arsenic because they could not only pack together efficiently but also allow a decent flow of water as opposed to loose, fine powders. They could also be readily combined with ion-exchange resins typically used in water treatment.

References

1. Agency for Toxic Substances & Disease Registry. 2005 CERCLA priority list of hazardous substances. http://www.atsdr.cdc.gov/cercla/05list.html.
2. Yoshida, T.; Yamauchi, H.; Fan Sun G. *Toxicol. Appl. Pharmacol*, **2004**, *198*, 243-252.
3. Subcomitte on Arsenic in Drinking Water, National Research Council. *Arsenic in drinking water;* National Academies of Press: Washington DC, 1999.
4. U. S. Geological Survey. Geochemistry of arsenic. http://or.water.usgs.gov/pubs_dir/Online/Html/WRIR98-4205/as_report6.html.
5. Bissen, M.; Frimmel, F.H. *Acta Hydrochim. Hydrobiol.* **2003**, *31*, 9-18.
6. Natural Resources Defence Council. Arsenic in drinking water. http://www.nrdc.org/water/drinking/qarsenic.asp.
7. BangladeshNet. Arsenic: king of poison. http://bangladesh.net/article_bangladesh/health/hlt_03_arsenic_king_of_poison.htm.
8. U. S. Environmental Protection Agency. Arsenic in drinking water. http://www.epa.gov/safewater/arsenic/index.html.
9. U. S. Environmental protection Agency. Arsenic in drinking water – funding sources. http://www.epa.gov/safewater/arsenic/funding.html.
10. U. S. Geological Survey. Arsenic in ground-water resources of the United States. http://water.usgs.gov/nawqa/trace/pubs/fs-063-00/.
11. Ryker, S.J. *Geotimes* **2001**, *46*, 34-36.

12. Schlottmann, J.L. Naturally occurring arsenic in the central Oklahoma aquifer. http://wwwbrr.cr.usgs.gov/Arsenic/FinalAbsPDF/schlottmann.pdf.
13. U. S. Water News Online. Company pitching water pipeline to west Oklahoma City towns. http://www.uswaternews.com/archives/arcsupply/2compit5.html.
14. Oklahoma House of Representatives. Southern Oklahomans want aquifer studied before central Oklahomans start pumping water. http://www.lsb.state.ok.us/house/news5650.htm.
15. World Health Organization. Arsenic in drinking water. http://www.who.int/mediacentre/factsheets/fs210/en/index.html.
16. World Health Organization. *Guidelines for drinking water quality;* WHO: Geneva, Switzerland, 1993.
17. New Scientist. www.newscientist.com/news/news.gsp?id=ns99994024_7_august_2003.
18. Apblett, A.W.; Kuriyavar, S. I.; Bagabas, A.; Piquette, A.P. Nanotechnology for removal of arsenic from water. Preprints of Extended Abstracts of the American Chemical Society National Meeting, Division of Environmental Chemistry, Atlanta, GA, United States, Mar 26-30, **2006**, *46*, 752-760.
19. SenGupta, A.K. *Environmental separation of heavy metals engineered processes; 1st edition;* Lewis Publishers: Boca Raton, FL, 2001.
20. Cumbal, L. Ph.D. thesis, Lehigh University, Bethlehem, PA, 2004.
21. Drever, J. I. *The geochemistry of natural water;* Prentice Hall: Englewood Cliffs, NJ, 1998.
22. Ferguson, J.F.; Gavis, J. *Water Res.* **1972**, *6*, 1259-1274.

23. Morel, F.M.; Hering, J.G. *Principles and application of aquatic chemistry;* Wiley-Interscience: New York, NY, 1993.

24. Chwirka, J. D.; Thomson, B.M.; Stomp, J.M. *J. Am. Water Works Assoc.* **2000,** *93*, 79-88.

25. Benjamin, M.M.; Sletten, R.S.; Bailey, R.P.; Bennett, T. *Water Res.* **1996**, *30*, 2609-2620.

26. DeMarco, M.J.; SenGupta, A.K.; Greenleaf, J.E. *Water Res.* **2003**, *37*, 164-176.

27. Kang, M.; Kawasaki, M.; Tamada, S., Kamei, T.; Magara, Y. *Desalination* **2001**, *133*, 93.

28. Viraraghavan, T.; Subramanian, K.S.; Aruldoss, J.A. *Water Sci. Technol.* **1999**, *40*, 69-76.

29. Cheng, R.C.; Liang, S.; Wang, H.C.; Beuhler, M.D. *J. Am. Water Works Assoc.* **1994**, *86*, 79-90.

30. Hering, J.G.; Elimelech, M. *J. Am. Water Works Assoc*. **1996**, *88*, 155-167.

31. Hering, J.; Chen, P-Y.; Wilkie, J.A.; Elimelech, M. *J. Envir. Eng. ASCE* **1997**, *123*, 801-807.

32. Driehaus, M.; Jekel, M.; Hildebrandt, U. *J. Water SRT-Aqua* **1998**, *47*, 30-35.

33. Nikolaidis, N.P.; Dobbs, G M.; Lackovic, J.A. *Water Res.* **2003**, *37*, 1417-1425.

34. Laxen, D. P.H. *Heavy Met. Environ., 4th Int. Conf.* **1983**, *2*,1082-5.

35. Slavek, J.; Pickering, W.F. Water Air Soil Pollut. **1986**, *28*, 151-62.

36. Music, S.; Ristic, M. *J. Radioanal. Nucl. Chem.* **1992**, *162*, 351-62.

37. Tochiyama, O.; Endo, S.; Inoue, E. *Radiochim. Acta* **1995**, *68*, 105-11.

38. Pierce, M.L.; Moore, C.B. *Water Res.* **1982**, *16*, 1247-1253.

39. Manning, B.A.; Fendorf, S.E.; Goldberg, S. *Environ. Sci. Technol*. **1998**, *32*, 2383-2388.

40. Roberts, L.C.; Hug, S.J.; Ruettimann, T.; Billah, M.; Khan, A.W.; Rahman, M.T. *Environ. Sci. Technol*. **2004**, *38*, 307-315.

41. Surinenaite, B.; Simaityte, V.; Bendikiene, V.; Juodka, B. *Biologia* **1997**, *1*, 65-70.

42. Liu, C.; Honda, H.; Ohshima, A.; Shinkai, M.; Kobayashi, T. *J. Biosci. Bioeng.* **2000**, *89*, 420-425.

43. Leun, D.; SenGupta, A.K. *Environ. Sci. Technol*. **2000**, *34*, 3276-3282.

44. Dixit, S.; Hering, J.G. *Environ. Sci. Ttechnol*. **2003**, *37*, 4182-4189.

45. Dutta, P.K.; Ray, A.K.; Sharma, V.K.; Millero, F. *J. Colloid Interface Sci.* **2004**, *278*, 270-275.

46. Suzuki, T.M.; Bomani, J.O.; Matsunaga, H.; Yokohama, T. *React. Funct. Polym.* **2000**, *43*, 165-172.

47. Yuchi, A.; Ogiso, A.; Muranaka, S.; Niwa, T. *Anal. Chim. Acta* **2003**, *494*, 81-86.

48. Singh, D.B.; Prasad, G.; Rupainwar, D.C.; Singh, V.N. *Water Air Soil Pollut*. **1988**, *42*, 373-386.

49. Raven, K.P.; Jain, A.; Loeppert, R.H. *Environ. Sci. Technol.* **1998**, *32*, 344-349.

50. Apblett, A.W.; Kuriyavar, S.I.; Kiran, B.P. *J. Mater. Chem.* **2003**, *13*, 983-985.

CHAPTER V

SYNTHESIS OF MAGNETIC ION EXCHANGE BEADS FOR URANIUM AND DYE REMOVAL FROM WATER

Introduction

This chapter will concentrate on synthesis of magnetic spheres with nanometric nickel and magnetite on the surface. They will be used in radionuclide remediation and dye removal from water, respectively. The main advantages of using such magnetic resin beads is extremely rapid separations and the ability to make the process automated, which minimizes the exposure to the operators at nuclear power plants.

For the purpose of making magnetic ion exchange resins, the reduction of metal ions within the resin was explored as a means to make nanometric metals or metal oxides. There have been numerous approaches for the synthesis of such nanoparticles including the sol-gel method [1], hydrothermal process [2], and molten salt process [3]. There has also been some work done, in which reducing agents have been used to synthesize nanometric metals or metal oxides. Manithiram et al. have used alkali borohydrides as reducing agents to synthesize binary oxides such as VO_2, MoO_2, MnO_2, Cr_2O_3, and ternary oxides [4, 5,6,7,8]. Goodenough et al. used hydroxylamine hydrochloride ($NH_2OH.HCl$) to produce reduced transition metal oxides such as Fe_3O_4, VO_2, and MoO_2 at lower temperatures [9, 10]. Reduction of Fe^{+2}, $Co^{+2,}$ and Ni^{+2} in aqueous media using alkali borohydrides produced ultra fine particles of Fe, Co, and Ni, respectively [11]. Recently, there have been several

reports, which mention hydrazine being used as a reducing agent to prepare II and VI group semiconductor nano rods [12]. Cobalt nanoclusters were obtained by sonicating an aqueous solution containing Co^{+2} and hydrazine [13]. Gui et al. have reported synthesizing nanometric oxides of VO_2, Cr_2O_3, and γ-Mn_2O_3, nanoparticles of Co, Cu, and one-dimensional single crystal Ni nano-whiskers [14].

Materials and methods

The resin used was Dowex 650C (H) form resin, a cross-linked sulfonated polystyrene-divinylbenzene polymer that was purchased directly from Aldrich in the form of monodisperse spherical beads. These resin beads were used to exchange Ni^{+2} with exchangeable H^+ in order to get nickel loaded resin beads as described previously in Chapter 3 demonstrated in Scheme 3-1. The dried, nickel loaded resin was then treated with ~12 wt. % sodium tetrahydroborate (4.4 M) in aqueous sodium hydroxide (14.0 M) in a 2:1 mole ratio to that of the Ni^{+2} moles. This reduction process was carried out in a sealed glass bottle with stirring using a bar magnet. Sodium tetrahydroborate was added drop-wise and carefully making sure the glass bottle did not heat up too much. The cap was opened occasionally in order to vent off the released hydrogen gas. The nickel loaded ion exchange resins, which were originally light green in color turned dark, almost black in color. The mixture was stirred until the gas bubbles ceased to generate. The resulting material was washed with deionized water and air dried. This material was characterized using various techniques. The scheme for the preparation of magnetic resin beads loaded with metallic nickel is shown in scheme 5-1.

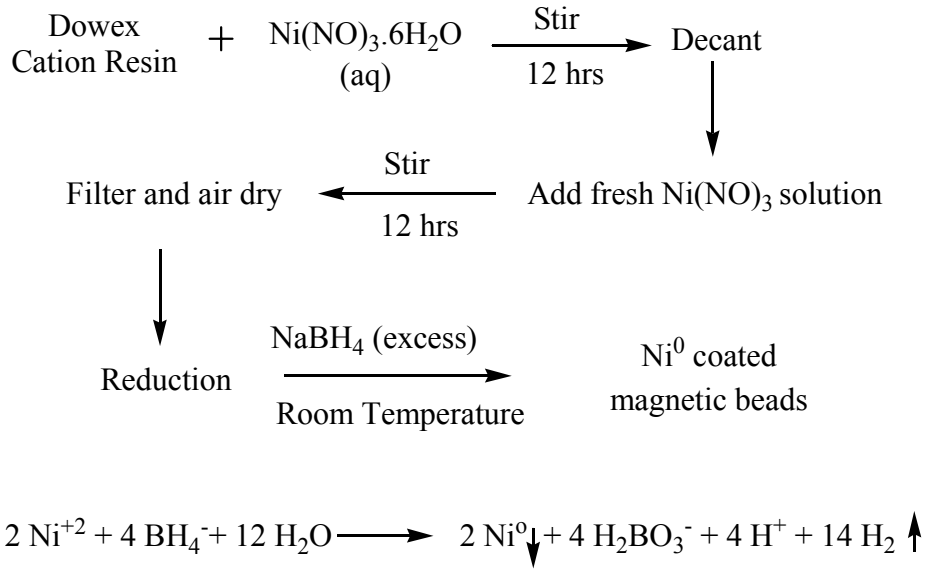

$$2\ Ni^{+2} + 4\ BH_4^- + 12\ H_2O \longrightarrow 2\ Ni^0\downarrow + 4\ H_2BO_3^- + 4\ H^+ + 14\ H_2\uparrow$$

Scheme 5-1: Synthesis scheme for nanometric nickel metal coated magnetic resin beads

Characterization

X-Ray diffraction:

X-ray powder diffraction (XRD) patterns were recorded on a Bruker AXS D-8 Advance X-ray powder diffractometer using copper K_α radiation. The X-ray diffraction pattern (Figure 5-1) was matched to that of synthetic nickel pattern in the International Center for Diffraction Database (ICDD).

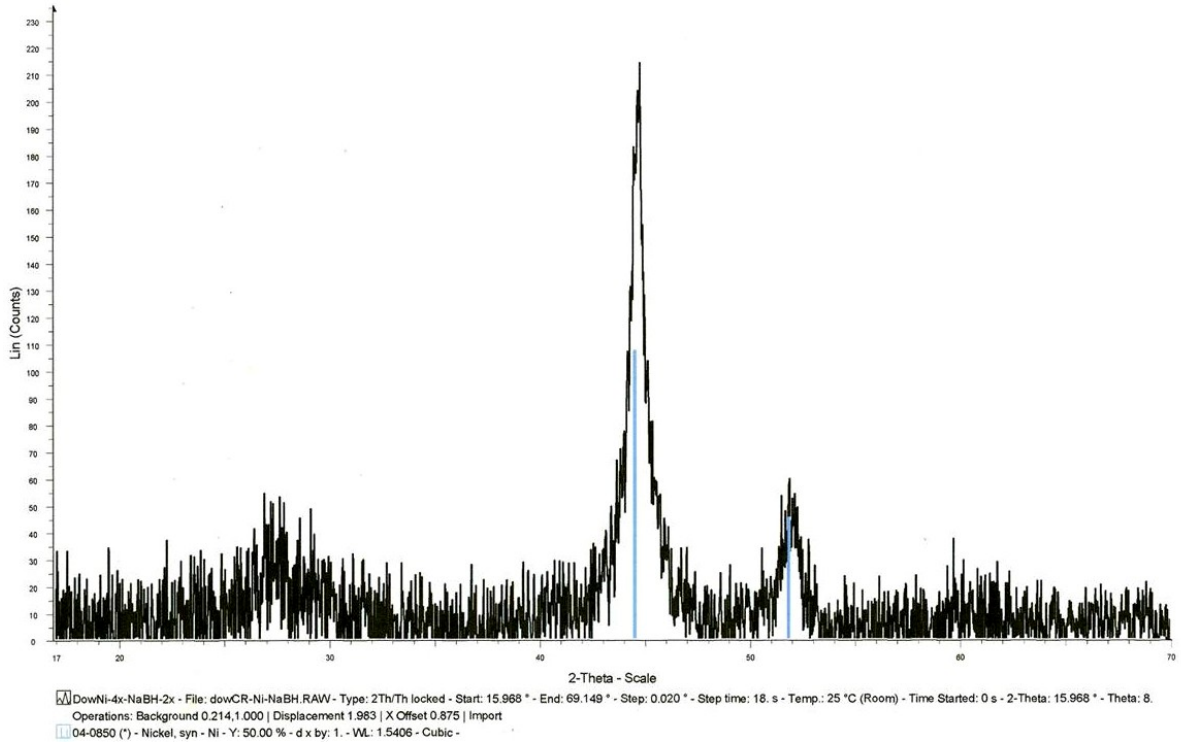

Figure 5-1: X-Ray diffraction pattern of nanometric nickel metal coated magnetic resin beads

Crystallite size analysis:

The observed X-Ray reflections were broadened as compared to a highly crystalline sample of Ni metal, so the crystalite size of the particles was analyzed. The result of this analysis, shown in Figure 5-2, revealed an average crystallite size of 1.7 nm, with a distribution of 2.6 nm full width at half-height. The maximum in relative frequency of crystallite size occurs at 1.1 nm. This confirmed that the material contains nanometric crystallites of metallic Ni in the sample.

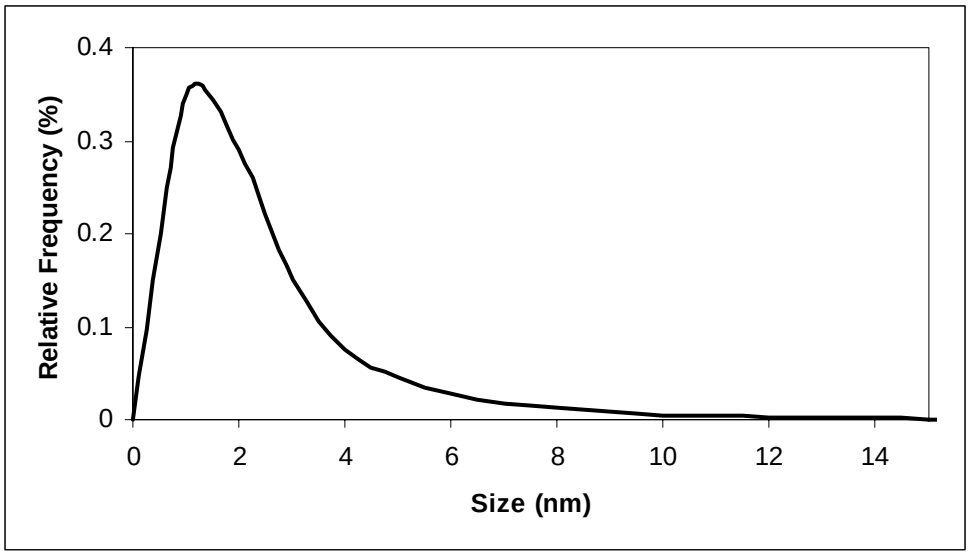

Figure 5-2: Crystallite size analysis of magnetic resin beads with nanometric nickel

Scanning electron microscopy:

Scanning electron microscope images were taken using a JEOL JXM 6400 Scanning Electron Microscope at Oklahoma State University Microscopy Lab. The spheres were dark black lustrous spheres with a very smooth surface. The images are shown below. Also some of the particles were cut into half after they were embedded in a polymer matrix in order to determine the distribution of nickel metal in the resin beads. Backscattered images of the cross section of the magnetic resin beads are shown in Figure 5-3 below. The image clearly indicated that nickel is located at the boundaries of the resin bead. The reduced nickel metal can be seen as a fine layer on the top of the resin beads and as a ring of nickel/resin composite at the outside of the resin. Also, in some cases peeling of the outside nickel film off of the resin bead is observed.

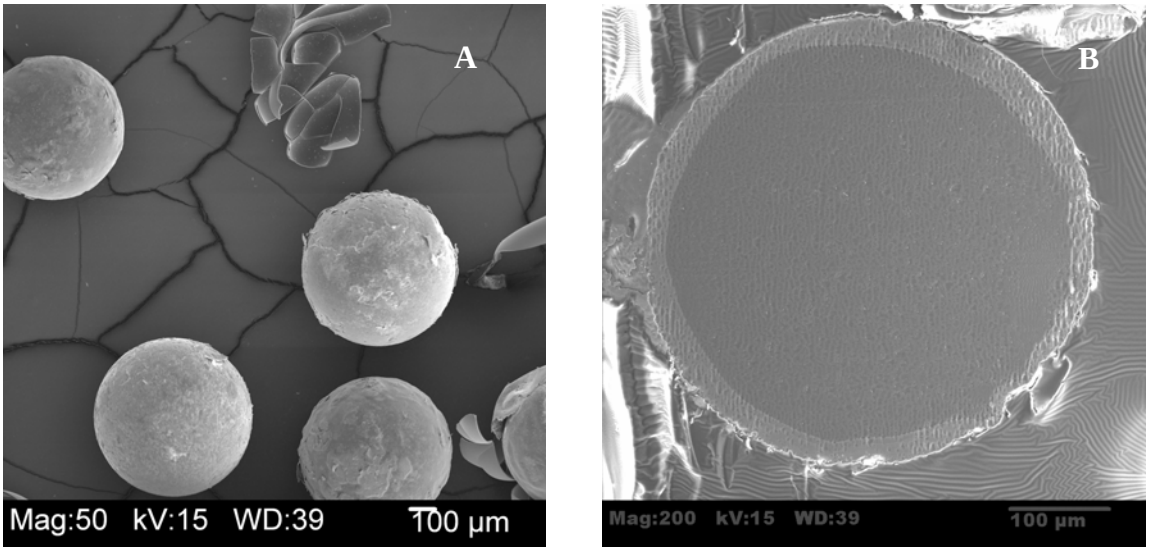

Figure 5-3: Scanning electron microscopy images of magnetic resin beads with reduced nickel on the surface showing A) intact beads B) cross section of single bead

Uranium remediation

Experimental:

All reagents were commercial products (ACS reagent grade or higher) and were used without further purification. Uranium(VI) concentration was determined using Spectronic 200 digital spectrophotometer using quartz cuvettes of 1 cm path length. Batch tests were performed using 10 ml solution of 0.1 M uranium(VI) solution, which was prepared in 0.1M glacial acetic acid. The solution was treated with varying amounts nickel coated magnetic spheres (0.25, 0.5, 1, 1.5 and 2.0 g). The mixture was shaken for an hour and then magnetically filtered to separate the spent magnetic resin. It was easily removed using a bar magnet to which they were attracted. The concentration of uranium(VI) in the treated solutions was analyzed using UV-visible spectroscopy by observing the absorption of the solution at wavelength of 415 nm.

Results and discussions:

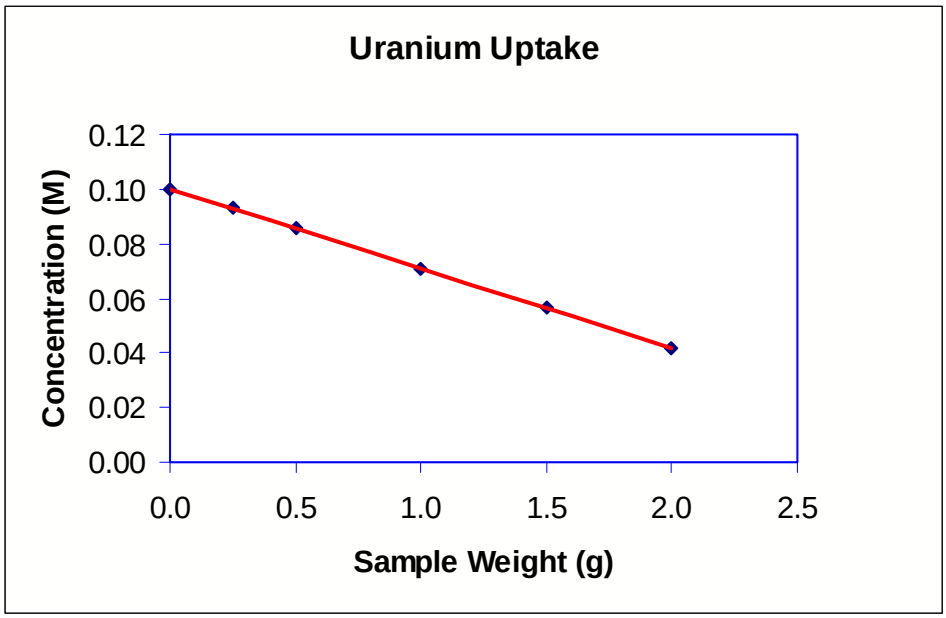

Figure 5-4: Uranium uptake using nickel coated magnetic ion exchange resin beads

The uranium uptake from the experiment is shown in Figure 5-4. The plot shows a linear relationship between the concentration of uranyl ions removed and the weight of the extractant used. The process seems to be mostly ion exchange resin. In order to investigate the distribution of uranium in the treated sample, Energy Dispersive X-ray analysis was performed in the scanning electron microscope. The analysis was used to pin point the location where the uranyl ions were situated inside the resin matrix, i.e. either on the surface or near the surface or concentrated more to the interiors of the resin. The image is shown in Figure 5-5.

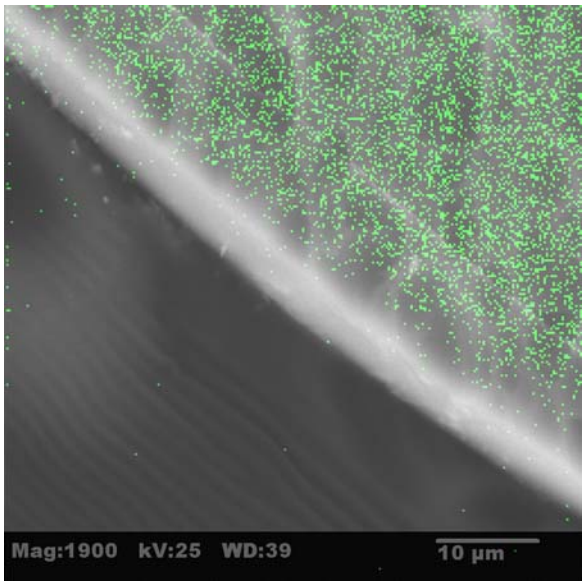

Figure 5-5: Distribution of uranium inside magnetic nickel coated resin beads

The image shows all the dots that are representatives of uranium species are distributed throughout the resin matrix inside the resin. This clearly suggested that the process was ion exchange process wherein the uranyl ions are diffusing inside the resin matrix. This has unique set of advantages for separation of uranium from water. This material, being ion exchange resin with magnetic nickel metal particle, can be manipulated remotely by magnetic fields without exposing any personnel to the harmful radiation. Also being spherical and mechanically robust, it can be left in the pipeline or internal structure along with the flow of water or effluent to be treated. Then it can be easily aggregated using a strong electromagnet and separated. This way it becomes totally automated process without the requirement of any human contact throughout the entire process. The uptake capacity of the material was found to be 0.29 mmol/g.

Synthesis of magnetite coated ion exchange resins

Experimental:

The resin used was Dowex 650C (H) form resin, a cross-linked sulfonated polystyrene-divinylbenzene polymer that was purchased directly from Aldrich in the form of monodisperse spherical beads. These resin beads were used to exchange Fe^{+3} with exchangeable H^{+} in order to get iron loaded resin beads. Iron loaded resins were obtained by using Dowex 650 cation exchange resin (20.0 g, 58.0 mmol of ion-exchange sites), which was stirred for 12 hours with a solution of iron(III) chloride hexahydrate (32.44 g, 120 mmol) in water (100 ml). The supernatant solution was poured off and the iron chloride treatment was repeated with fresh solution. After stirring for 12 hours, the resin was isolated by filtration, washed extensively with distilled water, and air-dried. This dried, iron loaded resin was treated with ~12 wt. % sodium tetrahydroborate in aqueous 14 M sodium hydroxide in a 2:1 mole ratio to that of the Fe^{+3} moles. The reduction process was carried out in a sealed glass bottle with stirring using a bar magnet. Sodium tetrahydroborate was added drop-wise and carefully making sure the glass bottle did not heat up too much. The cap was opened occasionally in order to vent off the released hydrogen gas. The iron loaded ion exchange resins which were originally red in color turned into shiny black beads. The mixture was stirred until the gas bubbles ceased to evolve. The resulting material was washed with deionized water and air dried. This material was characterized using various techniques. The scheme for the synthesis is shown in Scheme 5-2.

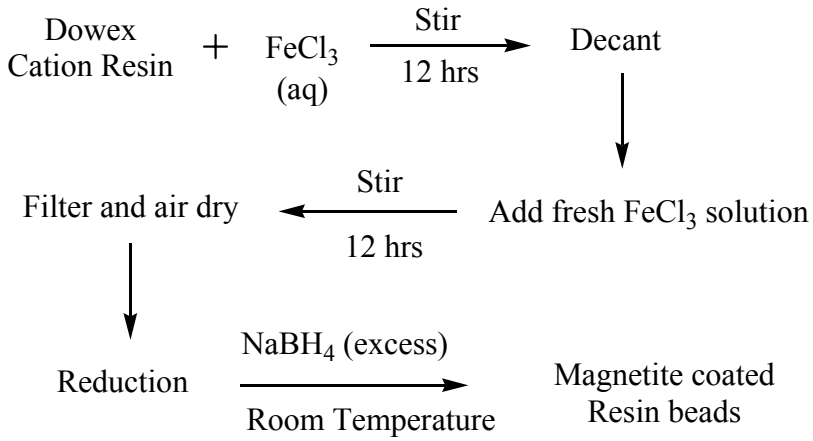

$$4\,Fe^{+3} + 3\,BH_4^- + 9H_2O \longrightarrow 4\,Fe^{o}\downarrow + 3\,H_2BO_3^- + 12\,H^+ + 6\,H_2\uparrow$$

$$3\,Fe^{o} + 2\,O_2 \longrightarrow Fe_3O_4$$

Scheme 5-2: Scheme for synthesis of nanometric magnetite coated resin beads

X-ray diffraction:

The X-ray diffraction pattern was matched to the magnetite (Fe_3O_4) pattern in the International Center for Diffraction Database (ICDD) as shown in Figure 5-6**.**

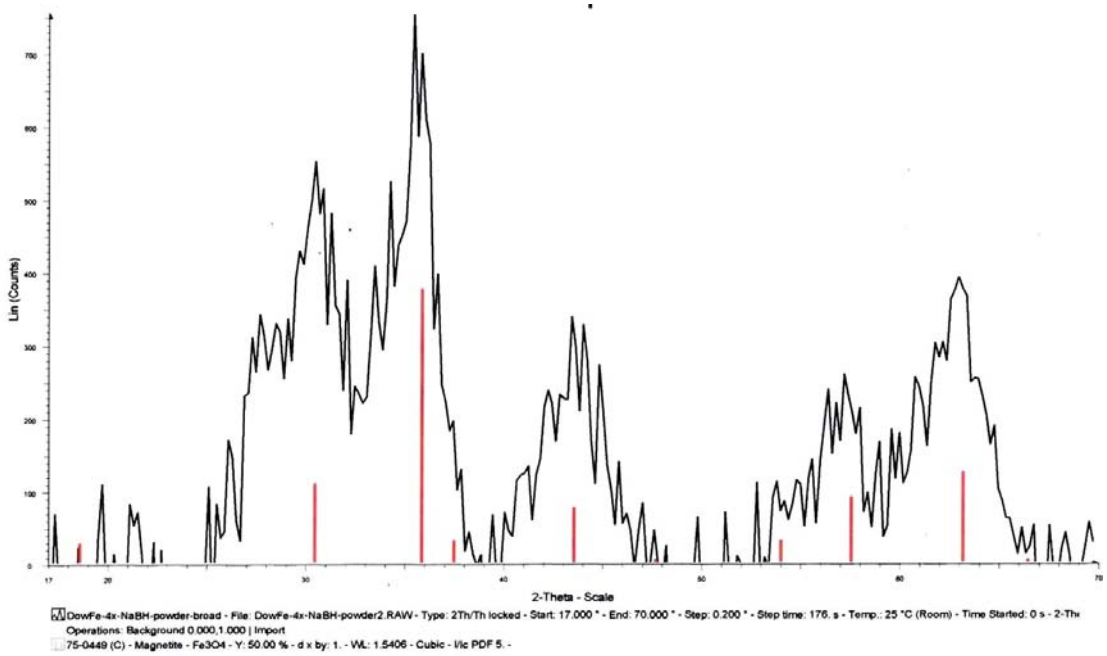

Figure 5-6: X-Ray diffraction pattern for magnetite coated resin beads

Dye remediation using nanometric magnetite coated resin beads

The magnetic beads were used to test their application in dye remediation from effluents from textile industries. The dye chosen was crystal violet (Fisher Scientific) since it is one of the top ten dyes found in water and is also a major dye used world wide. A very dilute solution (less than 0.01%) was used for batch tests. The samples were put in a 10 ml vial with 0.1-0.5 g magnetite coated resin beads were added and shaken for 30 minutes. The resultant solution became almost colorless as shown in Figure 5-7. This clearly shows potential applications of the material in dye remediation purposes. It can be clearly seen that magnetite coated resin beads are still strongly magnetic enough to segregate the beads using a strong bar magnet. This becomes highly useful when rapid and efficient separation is required.

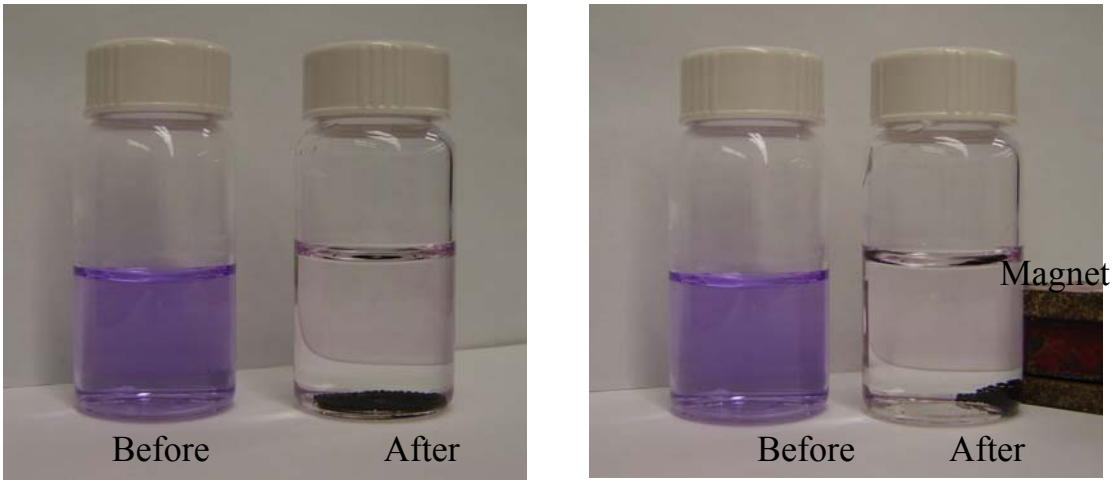

Figure 5-7: Remediation of crystal violet dye with magnetite coated resin beads

Magnetic susceptibility

Magnetic susceptibility of the material was carried out using a JM Magnetic Susceptibility Balance, which uses Guoy's method to determine the values. The values are in Table 5-1.

Table 5-1: Magnetic susceptibility of magnetic resins

MAGNETIC BEAD	(Xg) MASS SUSCEPTIBILITY (cc/g)	AV. CRYSTALLITE SIZE (nm)
Magnetite coated resin	0.734×10^{-6}	3.9
Metallic nickel coated resin	0.721×10^{-6}	1.7

The magnetic susceptibility values are quite low as compared to pure magnetite which might be due to the fact that these materials are nanometric and the fact that they are not pure magnetite. There is also a resin matrix in the material which might be responsible to certain extent. However, the main reason will be their nanometric crystallite size contributing to the lower values. The material has become super-paramagnetic due to their small size and hence the lower values.

Conclusion

Reducing the iron and nickel load cation exchange resin at room temperature using sodium tetrahydroborate gives nanometric magnetic resin beads coated with magnetite and metallic nickel, respectively. These find potential applications in remediation of uranium from water in nuclear power plant as well as removal of dyes from textile effluent streams rapidly with great efficiency.

References

1. Nozaki, C.; Tabata, K.; Suzuki, E. *J. Solid State Chem.* **2000**, *154*, 579-583.
2. Eda, K.; Chin, K.; Whittingham, M.S. *Chem. Lett.* **1999**, *7*, 811-812.
3. Oishi, S.; Nagai, Y.; Chiba, K.; Ishizawa, N. *Chem. Lett.* **1998**, *27*, 439-440.
4. Tsang, C.; Dananjay, A.; Kim, J.; Manthiram, A. *Inorg. Chem.* **1996**, *35*, 504-509.
5. Tsang, C.; Kim, J.; Manthiram, A. *J. Mater. Chem.* **1998**, *8*, 425-428.
6. Tsang, C.; Kim, J.; Manthiram, A. *J. Solid State. Chem.* **1998**, *137*, 28-32.
7. Tsang, C.; Lai, S.Y.; Manthiram, A. *Inorg. Chem.* **1997**, *36*, 2206-2210.
8. Zhu, Y.T.; Manthiram, A. *J. Solid State Chem.* **1994**, *110*, 187-189.
9. Manivannan, V.; Tichy, R.; Goodenough, J.B. *J. Solid State. Chem.* **1999**, *147*, 269-273.
10. Manivannan, V.; Goodenough, J.B. *Inorg. Chem.* **1998**, *37*, 3448-3449.
11. Wonterghem, J.; Morup, S.; Koch, C.J.; Charles, S.W.; Wells, S. *Nature* **1986**, *322*, 622-623.
12. Li, Y.D.; Ding, Y.; Wang, Z.Y. *Adv. Mater.* **1999**, *11*, 847-850.
13. Gibson, C.P.; Putzer, K.J. *Science* **1995**, *267*, 1338-1340.
14. Gui, Z.; Fan, R.; Mo, W.; Chen, X.; Yang, L.; Hu, Y. *Mater. Res. Bull.* **2003**, *38*, 169-176.

CHAPTER VI

CONCLUSIONS

Ion exchange resin degradation at nuclear power plants using batch and column experiments were studied, the results of which are presented in this dissertation. These experiments, it can be concluded that there are several mechanisms that can lead to resin degradation. Amines, in which the reactive functional groups of ethanolamine are blocked by methyl groups, were tested. This investigation helped in identifying key issues of resin degradation. Nitrogen terminal is determined to be the main culprit in resin degradation. These experiments led to the identification of 2-dimethylaminoethanol as a potential candidate to that could replace ethanolamine and ammonia. Future work can be aimed at complete analysis of strong and weak base sites on resins exposed to ethanolamine and other pH control agents, which will determine the magnitude of contribution of the degradation mechanisms revealed in this investigation. Further evaluation of the resin degradation mechanisms is possible in two ways. First, additional column and batch experiments can be performed in order to focus on the role of oxygen in the reactions. Specifically, it would also be helpful to run batch tests under nitrogen so that oxidation reactions could be decoupled from other thermally-activated reactions alongside experiments with defined oxygen concentrations. Secondly, the application of other analysis methods including X-ray fluorescence, functional group analysis and measurement of ion-exchange capacity, high performance liquid chromatography and

particle size analysis of aqueous solutions from the resin reactions would be very beneficial for elucidating the mechanism of resin degradation.

The first step in evaluating 2-dimethylaminoethanol as an alternative amine is to generate extensive thermodynamic data for steam cycle water chemistry applications. These data can be approximated computationally with current state-of-the-art simulation tools. After simulations are completed a limited number of confirmation experiments would be required prior to testing the amine in a steam cycle application.

Another problem with ion exchange resins addressed was the need to develop means of rapidly separating them from a flowing water stream or separating radioactive resins by remote operations. This was achieved by synthesizing magnetic ion exchange resin beads that could be used for rapid feed-through separation by magnetic filtration. This material showed promising results in dye remediation from waste water originating from textile industry. This method can also be utilized to prepare various hybrid materials wherein inorganic magnetic adsorbents will be immobilized in ion exchange resin matrix for variety of applications.

A Synthesis method was developed for converting ion exchange materials to spherical aggregates of metal oxide nanoparticles. Cation exchange resins loaded with transition metal ions, such as iron, zinc, and nickel on firing at higher temperatures (~ 550 ^{o}C) yielded high surface area oxides capable of removing As(V) from drinking water. These agglomerates of metal oxides exhibit extremely good adsorption capacities when compared to the bulk metal oxides and, since they are replicas of ion exchange beads, they have appropriate hydrodynamic properties for flow-through water treatment. Water treated with these aggregates is in compliance with the new stringent US

Environmental Protection Agency standard for arsenic for drinking water. In a similar fashion other transition metal oxides can also be prepared and characterized. These materials could find applications in various areas such as environmental remediation of heavy metal ions, catalysis, bio-medical, anti-terrorism, ceramics and other applications.

VITA

SATISH I. KURIYAVAR

Candidate for the Degree of

Doctor of Philosophy

Thesis: INVESTIGATION OF ION EXCHANGE RESINS: UNDERSTANDING FOULING MECHANISMS AND DEVELOPMENT OF NOVEL APPLICATIONS

Major Field: Inorganic Chemistry

Biographical:

Personal Data: Born in Ramdurg, Karnataka state in India on 5th August 1975, son of Renuka and Ishwarappa Kuriyavar.

Education: Received Bachelor of Science degree in Chemistry at Bombay University in June 1995. Received Master of Science degree in Analytical Chemistry at Pune University in June 1997. Completed the requirements for the Doctor of Philosophy in Chemistry at Oklahoma State University, Stillwater, Oklahoma in July 2006.

Experience: Quality Control Officer, CIPLA Pharmaceuticals, India (June 1997-December 1997). Research Project Assistant Level II, Catalysis Division, National Chemical Laboratory, India (February 1998 - March 1999). Research Staff, Catalysis Division, J. Heyrovsky Institute of Physical Chemistry, Prague, Czech Republic (April 1999-August 2000) Teaching Assistant, Chemistry Department, Oklahoma State University, Oklahoma (August 2000-May 2005)

Professional Memberships: Inorganic Division of American Chemical Society, Oklahoma Microscopy Society, Phi Lambda Upsilon Honorary Chemical Society, Graduate and Professional Student Government Association

Name: SATISH I. KURIYAVAR **Date of Degree:** 14th July, 2006

Institution: Oklahoma State University **Location:** Stillwater, Oklahoma

Title of Study: INVESTIGATION OF ION EXCHANGE RESINS: UNDERSTANDING FOULING MECHANISMS AND DEVELOPMENT OF NOVEL APPLICATIONS

Pages in Study: 177 Candidate for the Degree of Doctor of Philosophy

Major Field: Inorganic Chemistry

Scope and Method of Study:

Ion exchange resins play an important role in purifying water and a variety of industrial processes. One application, maintaining water purity in secondary steam cycle of nuclear power plants, has recently suffered from fouling of the resins due to the amine pH control agents that are added to reduce corrosion. This occurred after reactors switched from ammonia to ethanolamine (ETA) due to its superior corrosion protection. However the performance of the mixed bed ion exchange resins columns was found to occasionally degrade rapidly when ETA was present. Therefore, we adopted an approach of testing amines, in which the reactive functional groups of ETA are blocked by methyl groups. Another problem with ion exchange resins that was addressed was the need to develop means of rapidly separating them from a flowing water stream or separating radioactive resins by remote operations.

Findings and Conclusions:

The performed experiments led to the identification of 2-dimethylaminoethanol as a potential candidate to replace ETA and ammonia. Also, magnetic ion exchange resin beads that can be used for rapid feed-through separation by magnetic filtration were prepared. In other research, a method for converting ion exchange materials to spherical aggregates of metal oxide nanoparticles was developed. Cation exchange resins loaded with transition metal ions, such as iron and zinc on firing at 550^{o}C yielded high surface area oxides capable of removing As(V). These agglomerates of metal oxides exhibit extremely good adsorption capacities when compared to the bulk metal oxides and, since they are replicas of ion exchange beads, they have appropriate hydrodynamic properties for flow-through water treatment. Water treated with these aggregates is in compliance with the new stringent US Environmental Protection Agency standard for arsenic for drinking water.

ADVISER'S APPROVAL: _____